PB84-234384

REPORT NO.
UCB/EERC-84/03
APRIL 1984

EARTHQUAKE ENGINEERING RESEARCH CENTER

REFINED MODELLING OF REINFORCED CONCRETE COLUMNS FOR SEISMIC ANALYSIS

by

S. A. KABA
S. A. MAHIN

Report to the National Science Foundation

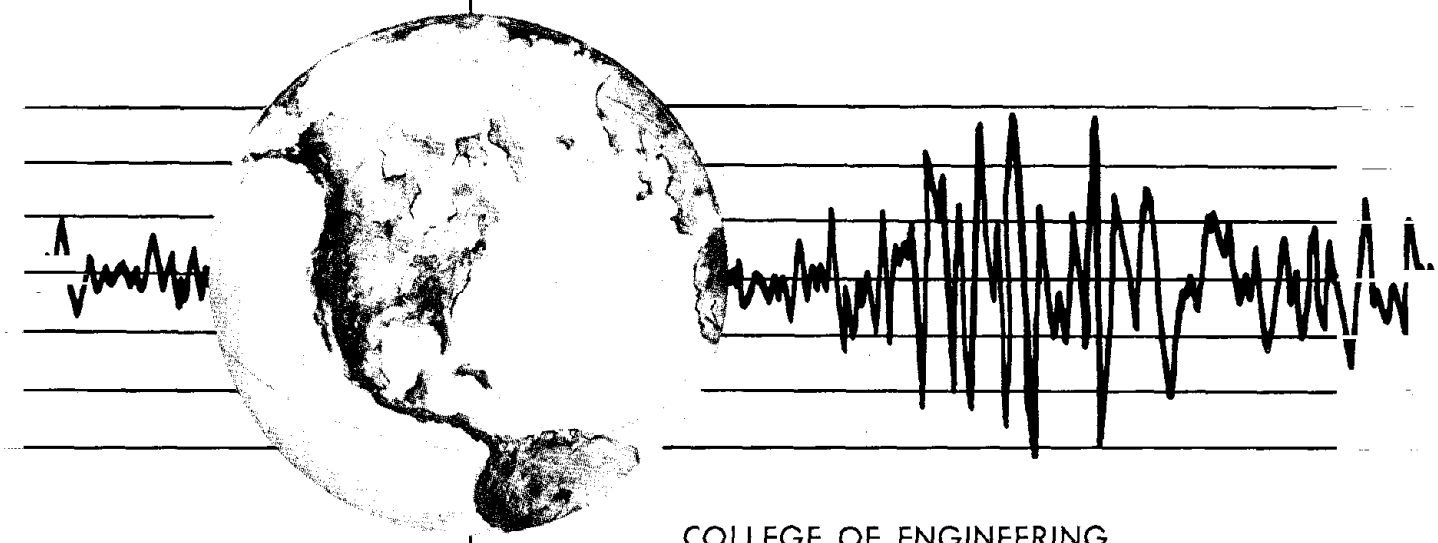

COLLEGE OF ENGINEERING

UNIVERSITY OF CALIFORNIA · Berkeley, California

For sale by the National Technical Information Service, U.S. Department of Commerce, Springfield, Virginia 22161.

See back of report for up to date listing of EERC reports.

DISCLAIMER

REFINED MODELLING OF REINFORCED CONCRETE COLUMNS FOR SEISMIC ANALYSIS

by

Said A. Kaba

and

Stephen A. Mahin

A report on research sponsored by

the National Science Foundation

Report No. UCB/EERC-84/3

Earthquake Engineering Research Center

College of Engineering

University of California

Berkeley, California

APRIL 1984

ABSTRACT

The report extends the fiber representation of a section to make possible the analysis of reinforced concrete or steel members independently or as part of two-dimensional frames. Hence, slice locations are specified along the length of the element. Each slice is further discretized into steel and/or concrete fibers. The state of the fiber is monitored and updated assuming plane sections remain plane. Slice stiffness is calculated from the fiber stiffness and the element stiffness is arrived at by integration over the length of the element assuming linear flexibility between slices. Shape functions which relate slice deformations to element displacements are also calculated and updated.

By monitoring the various fibers and slices, it is possible to obtain the local response at critical sections including moment-curvature and shear histories. Bond slip and shear effects are not considered however. Hence the multi-slice fiber element is suitable for modeling beams and columns in a steel or reinforced concrete frame especially when the effects of axial loads on strength and stiffness are significant. Furthermore, the element can account for axial load-bending moment interaction and the pinching of hysteresis loops due to compressive loads acting on the element.

The functioning of the element is tested separately and as part of a general dynamic two-dimensional frame analysis program (DRAIN-2D2). The results of analyses are compared with theoretical, experimental, and other analytical results and show the element to be a useful additional tool for the analysis of reinforced concrete frame behaviour. The limitations and advantages over some other conventional discrete models are also illustrated through analysis results.

ACKNOWLEDGEMENTS

The work described in this report was done under the sponsorship of the National Science Foundation. This financial support is gratefully acknowledged.

The assistance of graduate student Finley Charney with the *DRAIN-2D* runs is particularly appreciated. Thanks are also due to the University of California's Department of Civil Engineering for making available the facilities of the Microcomputer Research Laboratory of the Structural Engineering and Structural Mechanics Division as well as to the Earthquake Engineering Research Center for the use of their VAX 750 computer.

The report and many of the figures were prepared using the facilities of the Berkeley Campus Computer Center. The fine efforts of the technical illustrators, especially Miss Gail Feazell, are appreciated.

TABLE OF CONTENTS

I INTRODUCTION

1.1 Introductory Remarks

Recent research into the behaviour of reinforced concrete structures subjected to seismic loads has been extensive. Yet due to the many phenomena that have to be considered, there are still many aspects of the behaviour which are not fully understood and which result in wide variations in response predictions. The phenomena which affect the response include cracking and crushing of concrete as well as yielding , strain hardening, slipping, and buckling of the reinforcing steel. Furthermore, when load and displacement reversals are taken into consideration such phenomena as pinching of hysteresis loops due to shear, bond deterioration, and the Bauschinger effect become important. In addition, the effect of a varying axial load on the behaviour of structural elements can be significant, especially in the case of reinforced concrete columns in frames subjected to seismic loading.

Despite significant advances in numerical methods and computational techniques for solving these types of problems [1,2,3,4,5,6,7], there has been only limited improvement with regard to models for analytically predicting the nonlinear dynamic response of complete reinforced concrete frames. Although finite element programs have been developed to treat many of these phenomena individually, little emphasis has so far been placed on practical methods for predicting overall structural behaviour. There is a definite need for models which can provide a reliable indication of the complex inelastic behaviour exhibited by members, but which are simple and flexible enough to be implemented in general purpose computer programs for studying the seismic response of reinforced concrete frames. Such models would ideally provide information on the local behaviour of critical regions which can aid in checking the adequacy of a design, the collapse mechanism, and local detailing requirements.

Because of the many different phenomena involved, it is desirable to use different approaches to model different components of a reinforced concrete structure, e.g. slabs, joints,

beams, walls, and columns. While considerable research has been devoted to many of these components, relatively little analytical research has been directed recently to the problem of modelling columns. Axial loads acting on a reinforced concrete section affect the section's stiffness and strength characteristics as shown in Fig. 1.1. Furthermore, if the section is subjected to a cyclic curvature variation, the existence of a compressive axial load results in the pinching of hysteresis loops as shown in Fig. 1.2. Because of this, the member's capacity for energy dissipation is also reduced, an important consideration for seismic resistant design. The multi-slice fiber element, which is the object of this study, is especially suited to model the behaviour of reinforced concrete columns since it can take into consideration many of the controlling phenomena, including the effect of a varying axial load.

1.2 Available Models

This study is mainly concerned with modelling elements where flexure and axial load dominate the behaviour. Hence the emphasis is on column (and beam) modelling, while joints, slabs, and shear walls subjected to significant shear forces are not treated. Even with this restriction in scope, the relevant past research is extensive.

Different approaches have been suggested for modelling reinforced concrete frames. These include simple or lumped models which reduce a frame to a single degree of freedom or to a system consisting of a few degrees of freedom with lumped (and often simplified) mass and stiffness properties. Discrete models are more complex in that they represent each structural element separately. Even more complex fiber and finite element models, whereby each structural element is further discretized into a number of subelements, have been developed for special applications.

The following four sections briefly describe these simple, discrete, fiber, and finite element models, review recent studies conducted using these models, and outline their uses and limitations.

1.3 Simple Models

Due to the increasing availability of fast computers with large memories, emphasis has been shifting towards complex models. Yet simple modelling approaches have not been completely abandoned. Simple structure models include the shear beam model and various procedures for reducing a frame to a single degree of freedom. In addition to their low computational cost, simple models are relatively easy to apply and are very useful in preliminary design stages.

1.3(a) Multi-Degree of Freedom Systems

The shear beam is the simplest representation of a frame subjected to lateral forces. Such models have been used extensively to study the response of multi-story frames subjected to earthquake motions [7,8,9,10]. The nonlinearity is taken into account in the shear springs which model the story stiffness. For example, the envelope curve relating the story shear to lateral drift could be trilinear to account for cracking and yielding at the story level. A hysteresis rule must also be included to account for unloading and load reversal. Aziz [7] in his study of the dynamic inelastic analysis of frames includes an investigation of a ten-story frame using the shear beam model. Aoyama [10] has developed a slightly more complex model that incorporates flexural as well as shearing types of structural deformations.

1.3(b) Equivalent Single Degree of Freedom Systems

By assuming that the structure deforms according to its first mode or some other predetermined deflected shape, a multi-degree of freedom system can be reduced to an even simpler single degree of freedom representation. This was implemented by Pique [11] in his study of the use of simple models in nonlinear dynamic analysis. A second alternative called the Q-

model was developed by Saiidi and Sozen [12]. It consists of a massless rigid bar with a hinge and a rotational nonlinear spring at its base and a concentrated mass and damper at the top as shown in Fig. 1.3. A similar approach, used by Pique [11], superimposes a set of springs having different yield levels in parallel. In this model, the combined stiffness changes continuously, although the hysteresis function for each spring may be a simple relationship.

1.3(c) Uses and Limitations of Simple Models

Most studies using simple models arrived at the conclusion that the maximum response values predicted by the simple models are satisfactory when compared with results from complex models or tests carried out on scaled down frames. Since the input information required is quite simple, these methods are well suited for preliminary design and for performing parametric studies regarding overall performance characteristics.

One must keep in mind, however, the assumptions on which such simple models are based. For example, in the case of the single degree-of-freedom representation, the higher mode components of displacement are assumed to remain essentially unexcited by earthquake motions. In the case of the shear beam model it is implicitly assumed that the girders are significantly more rigid and stronger than the columns. This is true to a certain extent in the case of weak column-strong girder design. However, this is not the typical case in reinforced concrete construction and determination of appropriate modelling parameters may be difficult. The information obtained using simple models is also usually insufficient for final designs, detailing evaluations and reliability studies. For such purposes as well as for the analysis of general structures which cannot be adequately represented by simple models, more sophisticated modelling techniques are necessary.

1.4 Discrete Element Models

Discrete element models include a one-to-one correspondence between elements of the actual frame and the idealized system. However, they generally simplify the behaviour of the member by idealizing its hysteretic behaviour in terms of a set of predefined phenomenological rules. Discrete models can be further divided into single component elements, multi-component elements, elements which depend on interpolation functions, and plasticity based models. This section briefly reviews these various types of discrete models, their uses, their limitations, and recent studies which dealt with these models.

1.4(a) Single Component Models

Such models consist of a single element, usually elastic, flanked on either end by concentrated, nonlinear, rotational springs as shown in Fig. 1.4. Giberson [13] used this single element model with the two concentrated flexural springs at the ends which modelled the inelastic deformation of the member. Otani [14] used a similar approach to study the response of a reinforced concrete frame subjected to base acceleration. In Otani's model the point of inflection was assumed to be stationary at the member's mid-length, though this is not a necessary restriction in general.

As the effects of inelastic deformations on response become more significant, it becomes important to use as realistic a hysteresis model as possible. Hence the simpler bilinear model for reinforced concrete member behaviour was superseded by a model proposed by Clough and Johnston [15] which included overall stiffness degradation of a structure. Takeda, et al [16] then proposed a hysteresis model which better conforms with results of cyclic loading tests of reinforced concrete connections.

To account for the various loading and unloading stages, such models can be quite complex - see Fig. 1.5. Nevertheless, the pinching effects associated with shear, bond deterioration,

unequal top and bottom reinforcement in beams, and axial load effects in columns were not modelled in the original Takeda model. Hence, a somewhat modified model was developed by Takayanagi and Schnobrich [17]. In a study by Emori and Schnobrich [18] a further modification was introduced to describe the effect of bar slip.

A thorough study using three of the formulations mentioned above as well as two others was carried out by Saiidi and Sozen [12]. The structural members were idealized as indicated in Fig. 1.4. Shear deformations were ignored, infinitely rigid joints were assumed but the gravity load induced P-Δ effects were taken into account. The member moment-rotation (M-θ) relation was arrived at by simple numerical integration assuming a linear moment variation along the length of the element and a trilinear moment-curvature (M-ϕ) relation (with break points at cracking and yielding) as shown in Fig. 1.6. Using additional simplifying assumptions, rotations due to bond slip were calculated resulting in a modified M-θ curve.

Studies using five different hysteresis models for the concentrated flexural springs were compared with results of a shaking table test of small scale, 3-bay, 10-story frames subjected to the N-S component of the 1940 El Centro earthquake. The results of the comparison are summarized below.

The Takeda model [16] consists of sixteen rules applied to a trilinear primary curve. The rules give the stiffness characteristics for cyclic loading and unloading at various stages of cracking and yielding. The model results in energy dissipation for loads cycling below the yield point since cracking is a breakpoint; such energy dissipation is observed in tests and is consequently desirable to include in the model. Pinching, however, is not considered which resulted in an overestimation of structural stiffness during low-amplitude response. Nonetheless, the results were very good: relative story displacement, deformed shape, and maximum response values were in close agreement with experimental values. A refined version of the Takeda model has been implemented in the DRAIN-2D program [2,4].

The Sina [12] model which is simpler than the Takeda model in that there are only nine rules, has the additional advantage of including pinching which results in better prediction of low-amplitude response than the Takeda model. To use this model the user has to specify

certain parameters which define the shape of the hysteresis loops including the extent of pinching. This presupposes the availability of appropriate analytical or experimental results. Nonetheless, the response relative displacements as well as the absolute maxima were overestimated by up to 20 %. The normalized deflected shape, however, was found to be quite close to the experimental results.

The simple bilinear model, shown in Fig. 1.7, is used in the analysis of steel structures and because of its simplicity is relatively economical to use. The stiffness characteristics during unloading and load reversal are quite different from the observed cyclic behaviour of reinforced concrete members. The bilinear model overestimates the energy dissipation for high amplitude deformations and ignores dissipation for low amplitude deformations. Hence, the results were found to be vastly different from actual tests and the bilinear model is believed to be inadequate for modelling reinforced concrete members.

The Otani model [14] as shown in Fig. 1.8 has a bilinear primary curve and therefore ignores cracking altogether. This simplification was attempted to reduce the complexity and computational effort of the Takeda model. Nonetheless it remains relatively complex (there are 11 rules involved). In spite of this its performance was deemed unsatisfactory: for low amplitude response the predicted displacements deviated considerably from experimental results; and for high amplitude response, errors of up to 33 % were calculated.

Finally the Q-hyst model, developed for Saiidi's study [12], also has a bilinear primary curve as shown in Fig. 1.9. It differs from Otani's model mainly by using softened unloading and load reversal stages and reducing the number of rules to four. Its performance was very good in regions of low amplitude response. The peak values were overestimated by up to 17 %.

The results using the Takeda and the Q-hyst models were found to be satisfactory, but the latter has the additional advantages of simplicity and better reliability in low amplitude response regions. None of these models explicitly accounts for axial load effects. An attempt has been

made by Fintel and Ghosh [19] to devise a single component model in which axial load influences the plastic yield moment. The model is based on a modified Q-hyst model, but neither pinching nor change in elastic stiffness due to axial load is taken into account.

The most recent and possibly the most flexible concentrated spring model is the one proposed by Chen and Powell [20] for the dynamic analysis of reinforced concrete frames. The model is capable of representing three dimensional behaviour since it takes into account biaxial bending, torsion, and axial load effects. This is accomplished by application of plasticity theory to a four dimensional yield surface. As in other lumped plasticity models, zero-length plastic hinges are assumed at the members' ends with an elastic portion in between. The hinges are initially rigid, hence the initial stiffness of the member is identical to the stiffness of the elastic portion. Furthermore, by having two subhinges at each hinge location, cracking and yielding can be modelled. The model can represent stiffness degradation. However, it is unclear how well a model based on plasticity interpretations of yield surfaces can account for the behaviour of concrete columns where cracking and crushing of concrete may have a crucial role.

1.4(b) Multi-Component Parallel Models

Another type of model is the parallel two-component formulation proposed by Clough and Benuska [21,22,23]. The model consists of an elastic element in parallel with an elasto-perfectly plastic element; hence it results in a conventional bilinear hysteresis rule. The elastic portion is assigned a fraction of the member's assumed stiffness equal to the proposed post-yield hardening stiffness. The elasto-perfectly plastic element has an initial stiffness calculated such that the combined stiffness of the two components in the elastic range is equal to the initial elastic stiffness of the actual member.

The parallel two-component model was used in many early studies of reinforced concrete structures [24] and incorporated into several computer programs [2,4,24,25,26,27]. The basic bilinear hysteretic formulation would not be expected to result in reliable response prediction

for a particular structure and ground motion [12,24]. However, Powell and Row [26] found that the average response values obtained for bilinear and stiffness degrading models using many different ground motions are nearly identical. Takizawa [28] modified the two-component bilinear model to better reflect the softening observed on unloading from the yield range and used the modified model to analyze a three-story reinforced concrete frame. Aoyama [10] extended the model into a nondegrading trilinear hysteresis formulation by modifying it into a three -component element consisting of an elastic element in parallel with two elastoplastic elements. Klingner [27] uses two or three two-component elements in parallel to achieve the same effect. Nonetheless, the axial load effects are simplified using this approach.

1.4(c) Multi-Spring Serial Models

In the single and parallel component models plastic hinges are assumed to form only at the ends of a member. However, at large deformations or as the result of transverse loads the length of the plastic hinge regions can no longer be neglected. In addition, the stiffness characteristics of elements vary along their length even in the elastic range. To account for this a number of simple alternatives is possible. For example, as a simple extension of the single component model, Hsu [29], and Takayanagi and Schnobrich [17] proposed a multiple spring model for analyzing wall members. The member is divided into several sub-elements along its axis each connected by nonlinear springs, see Fig. 1.10. Emori and Schnobrich [18] in their study of frame-wall structures used single component elements to model beams and columns, and multiple spring elements to model the shear wall. The flexural properties of each of the subelements is defined by a trilinear moment-rotation primary curve and a set of hysteresis rules is used to describe the unloading and load reversal stages. Although the multi-spring serial model can represent the behaviour of a frame element subjected to a relatively general moment distribution along its length, it still does not directly account for the effect of axial load on member behaviour.

1.4(d) Use of Interpolation Functions

Another way of achieving variable stiffness along the length of the member is through the use of interpolation functions. Umemura et al [8,30] suggest such a model. They assume a parabolic distribution of flexural flexibility (1/EI) along the member's axis. They account for shearing deformations by assuming shear stiffness to be proportional to the flexural stiffness. Using the parabolic interpolation function the member flexibility can be calculated for a known moment distribution given the section flexibility at the two ends and point of inflection. The section flexibilities are obtained using a moment-curvature relationship based on a modified Takeda model. The element flexibility matrix is inverted to obtain the required member stiffness matrix.

Meyer et al [31,32] proposed a nonlinear reinforced concrete beam element that accounts for the spread of plastic regions. The model is also based on a simplified Takeda moment-curvature relation which needs to be calibrated against experimental test results. ZAP [33] is a similar model that considers fixed end rotations due to bond slip in addition to plastic zones of finite length.

Umemura and Takizawa [30], use similar modelling techniques for shear walls. The shear deformations are treated independently from the flexural deformations and the corresponding shear and flexural flexibility matrices are added to obtain the element flexibility which is inverted to arrive at the element stiffness. Umemura et al [8] suggest that the axial load-bending interaction for a fluctuating axial load can be accounted for by modifying the model. However, this is not implemented in their studies.

1.4(e) Limitations of Discrete Models

Discrete models briefly described in this section can provide more detailed and accurate information about the behaviour of reinforced concrete members than the simple models

discussed in Section 1.3. Nonetheless, discrete models based on simplified hinge or other representations of inelastic behaviour are incapable of simulating the complex behaviour of reinforced concrete members under arbitrary loading conditions and histories.

As discussed in Section 1.4(a) the concentrated spring model can be refined by increasing the number and complexity of the rules that govern the nonlinear moment-rotation relationship for the springs. The fact that the hysteretic behaviour is predefined results in significantly reducing the potential of the concentrated spring model to adapt to general loading conditions. The properties of these concentrated springs are a function of the particular loading developed in the member which is not generally known a priori. In addition, the hysteretic models usually incorporated in most programs are not sufficiently elaborate to account for pinching due to shear stress, axial force, and unsymmetrical steel distribution. However, the model proposed by Thom [49] considers the effect of shear on the pinching and degradation of hysteresis loops.

The concentrated spring model may indeed be incompatible with some of these problems due to the fact that unlike flexural deformations inelastic axial and shearing deformations may not be concentrated at the ends of the member. In addition, it may be difficult to define an appropriate set of phenomenological rules that govern the interaction of flexural and axial deformations. The use of interpolation functions can account for the spread of plasticity and cracking. However, models using interpolation functions are also based on a multilinear moment-rotation relationship which needs to be predefined. In addition, the fact that the form of the interpolation function is constant (e.g. parabolic) may result in an inexact approximation of the member's stiffness. Meyer et al [31,32] proposed a nonlinear reinforced concrete beam element that takes into account plastic deformations over regions of finite length. However, it is based on a simplified Takeda moment-curvature model which does not include pinching due to shear and axial loads and which needs to be calibrated against experimental test results. The similar ZAP [33] model considers fixed end rotations due to slip as well as plastic zones of finite length. It was developed to model reinforced concrete beams only and therefore does not include axial load effects nor axial load-bending interaction.

1.5 Finite Element Models, Uses and Limitations

Unlike the discrete models described in Section 1.4, finite element models idealize each structural member as an assemblage of a large number of finite elements. These elements can be of various types such as truss or beam elements for steel and two dimensional plane stress, plane strain elements or even three dimensional elements for concrete.

Analyses of reinforced concrete structures using the plane stress inelastic type of finite elements have been performed [34,35,36]. Such analyses are particularly suited to studies of wall panels. Such studies include Yuzugullu and Schnobrich's [37] investigation of a shear wall frame system under monotonically increasing loading, Darwin's analysis of reinforced concrete shear panels subjected to cyclic loading, and Cervenka's [38] inelastic analysis of reinforced concrete panels loaded in their own plane. Although the correlation with experimental results was good, such studies can be extremely costly. This is due to the number of elements involved and the nonlinear behaviour, especially when loads reach significant levels. In addition to material nonlinearities, the need to monitor crack propagation and bond deterioration further complicates the analysis. The cost and time involved become prohibitive in the case of large structures and when a dynamic analysis is contemplated. Furthermore, there are uncertainties involved in the material and stiffness formulations of the finite elements resulting in approximate results in spite of the apparent refinement of these methods.

1.6 The Fiber Model

The fiber model is based on the finite element approach but simplifications are introduced to increase computational efficiency. It differs from the phenomenological approach to discrete element modelling in that a relatively detailed analytical description of the geometry and material properties is used to evaluate the behaviour of critical regions rather than a simplified and predefined set of hysteresis rules.

The fiber model is somewhat more sophisticated than discrete models and can take into consideration more of the phenomena involved in reinforced concrete behaviour. Typically, the only data necessary to define the fiber model are the geometry of the member and section, and the stress-strain relationships for the concrete and the reinforcing steel. Such data is generally available and is more reliable than moment-curvature sectional properties or moment-rotation relationships which are needed in the case of phenomenological discrete models. The fiber model, however, is less detailed than finite element models. Hence the computational and storage requirements are less and the fiber model can be used to analyze the dynamic response of reinforced concrete frames. However, the simplifying assumptions reduce the generality of the method.

1.6(a) Basis of the Fiber Model

An extensive study of the fiber model approach to structural dynamic analysis was performed by Mark and Roesset [39]. The purpose of their study was to investigate the applicability of the fiber model to the prediction of the nonlinear dynamic response of reinforced concrete frames. The procedure started by dividing each element into segments along the axis of the member. The slices at the ends of each segment were further divided into concrete and steel fibers. The strains in these fibers were calculated from the centroidal strain and section curvature by assuming that plane sections remain plane. From the assumed uniaxial stress-strain relationships, tangent stiffness moduli were calculated for the various fibers. From these fiber stiffness moduli the slice stiffness can be arrived at by proper summation. Assuming linear variation of stiffness between slices, the element tangent stiffness matrix was calculated by integrating the slice stiffness along the length of the member.

Thus, the important first step was the adoption of suitable hysteretic stress-strain relationships for the materials involved. The concrete model adopted by Mark [39] consists of a trilinear envelope with linear loading and unloading. Concrete is assumed incapable of carrying

tensile stresses and once cracked, a concrete fiber cannot supply compressive strength until the crack has closed. This simple concrete model was adopted because the details of the model were found not to affect the section properties significantly. Mark models the steel behaviour, however, with greater care. Six different analytical models based on three experimental studies were compared. For small to moderate strains the bilinear elasto-plastic steel model was found to perform reasonably well.

To solve the dynamic problem, the tangent stiffness corresponding to a current computed moment and curvature state is used to predict the new curvature state (and hence moment). This approach avoids iterating on the neutral axis position to achieve equilibrium at the section level. However, Mark did not impose equilibrium corrections due to nonlinearities occurring within a step so that small errors accumulated at every step.

While Mark [39] and in a similar fashion, FIRES-RC [40] used the assumptions of plane sections and uniaxial stresses, Bazant and Bhat [41] in their study of the hysteretic response of reinforced concrete members used triaxial material properties and the deep beam bending theory with transverse shear. To describe the steel stress-strain relationship Bazant and Bhat [41] adopted a simple analytic formulation that takes into consideration strain hardening and the Bauschinger effect. To describe the triaxial concrete behaviour, they used the Endochronic Theory [42]. Triaxial stress states exist in reinforced concrete members because of shear effects and the transverse confinement provided by the ties. Although deflections due to shear deformations were not significant in the case considered, inelastic shear strains caused volume dilatancy which resulted in significant forces in the stirrups. To include the effects of confinement due to the ties, Bazant and Bhat [41] included transverse normal strains as separate variables. Results for a cantilever beam were found to be in good agreement with experimental data.

As used in the studies by Mark [39], Bazant and Bhat [41] the fiber model was found to be a valuable tool for studying the hysteretic response of reinforced concrete members. Such phenomena as the "pinching effect" and the effect of axial load on stiffness and strength can be

reproduced automatically. Both studies included comparisons of analytic and experimental results that showed that the fiber model can provide results which are in general agreement with experiments and which are far more reliable than phenomenological models.

1.6(b) Limitations of the Fiber Model

Many of the limitations of the concentrated model that were described in Section 1.4(e) do not apply to the fiber model since the fiber model starts with material stress-strain relationships, the moment-rotation curve is not predefined and the model can represent the pinching of hysteresis loops due to the a constant or varying axial load [39]. However, other considerations are only treated approximately. For example, the common assumption of plane sections remaining plane may not be exactly true, especially when there are significant amounts of shearing deformations, shear cracks, or bond slip. Most fiber model analyses disregard these effects. Bazant and Bhat [41] include shear strains which mean that the section (though remaining plane) need not be normal to the axis of the element. Filippou et al [43] in a recent study of bond deterioration do not assume compatibility of strains between the reinforcement and the adjacent concrete, hence bond slip is explicitly considered.

Further simplifying assumptions are made when deducing element stiffness properties from section properties. For example, a finite number of sections are chosen at various points along the element and the stiffness is then arrived at by integrating over the length of the element. The integration is performed by using a predetermined variation (shape or interpolation function) which is completely defined once the stiffnesses of the sections being monitored are calculated. Mark [39] uses twenty such sections while Bazant and Bhat [41] use nine. Both, however, place those sections at equidistant intervals along the element. Such interpolation functions cannot reflect the exact stiffness variation along the element especially since this variation changes as the loading conditions evolve.

1.7 Objectives

The fiber model as described in the previous section is particularly suited for modelling the behaviour of reinforced concrete members and frames. The increasing availability of high speed computers with large storage capacity has made the use of fiber models a viable option for the dynamic analysis of reinforced concrete frames.

The objective of this study is to develop and evaluate a multi-slice fiber element for predicting the inelastic cyclic behaviour of reinforced concrete beam-columns. Inherent in this development is the need to incorporate automatically those features of reinforced concrete member behaviour (such as cracking, stiffness degradation and pinching of hysteretic loops, axial load-bending moment interaction, etc.) that can have an important influence on structural behaviour, while achieving reasonable computational efficiency. Thus, certain simplifications will be introduced in order to permit analysis of complete structural systems using modern computer capabilities. Primary assumptions will limit consideration to uniaxial bending, and shearing deformations and bond slip will be disregarded at this stage. To facilitate application of the model it will be implemented in a general purpose nonlinear dynamic analysis computer program. Comparisons with experimental and other analytical results will be made to assess the accuracy and practicability of this modelling approach.

1.8 Scope

The following chapters discuss the theory of the multi-slice fiber model and its use in the static and dynamic analysis of steel and reinforced concrete members and frames. Chapter 2 includes a description of the theory and operation of the multi-slice fiber model including the step by step procedure for calculating and updating element stiffness. Material models are described in this chapter. The implementation of the element in the DRAIN-2D2 [4] program is also presented. Chapter 3 is mainly concerned with the verification of the functioning of the

element. Simple analyses including the monotonic and cyclic loading of a steel beam as well as the dynamic analysis of a linear elastic column are carried out and the results compared with theoretical solutions.

Chapter 4 presents results of dynamic analyses of reinforced concrete columns and frames subjected to sinusoidal as well as earthquake base motions. The effect of various modelling and discretization assumptions is investigated in addition to the influence of analysis technique and size of time step. The use of the multi-slice fiber model in predicting the response of reinforced concrete members subjected to constant or varying axial loads is illustrated through various analyses and comparisons with results of analyses using other available models. Finally, conclusions and suggestions for further research are presented in Chapter 5.

II Description And Operation Of The Multi-Slice Fiber Model

2.1 Introduction

Many approaches have been suggested for improved modelling of reinforced concrete members for dynamic analyses of frames. One option is the use of many single component elements connected in series. While this procedure can take into account spreading of yielding and cracking, it results in additional degrees of freedom and hence computational expense. More importantly in the non-iterative, step-by-step integration procedures used in most dynamic analyses, these additional degrees of freedom can develop significant unbalanced loads that have to be eliminated which frequently results in numerical instabilities. Another option is to use interpolation functions to distribute the yielding along the member. Such functions, however, need to be predefined and while they may accurately represent the elastic behaviour of the element, they would be incapable of representing inelastic behaviour under general loading histories. Moreover, these and other modelling alternatives are usually based on idealized moment-rotation relationships for the plastic hinge and it would be difficult to include the effect of varying axial loads.

As adapted by Mahasuverachai and Powell [46] for the inelastic analysis of steel piping and tubular structures, the multi-slice fiber element combines the advantages of both of these approaches. Sections at various positions along the length of the member can be monitored and interpolation functions can be used so that no additional degrees of freedom need to be included or condensed out. Furthermore, the sections (or slices) are modelled by a fiber representation so that the limitations associated with predefined phenomenological type hysteresis rules are overcome.

The multi-slice fiber element requires as input only the section and member geometry, and the stress-strain relationships of the various 'fibers'. From these relationships, the slice properties and subsequently the element stiffness can be deduced for the current load conditions.

The interpolation (or more appropriately shape functions) need not be predefined. These are formulated as matrix transformations relating slice deformations to member end displacements. Such functions depend on the current state of the various slices and need to be updated whenever yielding or other changes occur. The derivation, use and updating of the shape functions and element stiffness is central to the simplicity of the method and will be described in some detail in the following sections.

Members to be modelled using the multi-slice reinforced concrete fiber element are assumed herein to be straight and the locations of the slices along the length of the member can be arbitrarily located by the user as described in the next section. Each slice must have an axis of symmetry and the axes of the various slices must be in the same plane. All applied loads must be in that plane; thus, only uniaxial bending and axial effects are considered. The detailed theory and workings of the model are described in Section 2.3.

Theoretically the multi-slice fiber model for reinforced concrete can be formulated so as to be suitable for three dimensional frame analyses. The model as proposed by this study, however, is intended for evaluation purposes and will be implemented for nonlinear dynamic, two-dimensional, frame analyses using the computer program DRAIN-2D2. For a detailed description of the workings of the program as well as input requirements refer to Golafshani [4]. As part of this program, the multi-slice fiber element can be used with other available elements such as beam-column, brace, truss and panel elements. Since it is intended for the analysis of two-dimensional structures of arbitrary configuration, there are three degrees of freedom per node which can be fixed or slaved. Masses are lumped at the nodes resulting in a diagonal mass matrix. Damping can be mass and/or stiffness proportional. Static loads may be applied prior to the start of the dynamic analysis, but currently such loads should not cause inelastic deformations. Geometric stiffness (otherwise known as the P-Δ effect) may be included, but is a function of the axial loads resulting from the static analysis; hence the geometric stiffness of an element does not change with variations in the axial load which occur as the dynamic analysis progresses. Finally, a major advantage of the program is the capacity of performing an event-

to-event analysis - i.e. the structural stiffness is modified whenever an element undergoes a change in stiffness due to a change in state. Depending on the element and the events considered such a procedure can reduce or eliminate the unbalanced forces which accumulate during a time step and have to be corrected, or balanced at the end of every step, a process which necessitates small time steps and may result in numerical instability.

2.2 Element and Slice Geometry

As shown in Fig. 2.1 the slice locations are specified at arbitrary points along the member. That is, the slices need not be equally spaced. Furthermore, the slices are completely independent which permits the modelling of a member with a variable cross section and/or material properties. Fig. 2.2 shows a slice broken down into its component fibers. The user needs to specify the fiber coordinates with respect to an arbitrary axis around which the moments are later calculated. Note that there are no internal degrees of freedom. Hence the slice deformations and therefore fiber strains are calculated from the three local degrees of freedom which in turn are calculated from the six global degrees freedom - see Fig. 2.3. Moreover, appropriate transformations are also included to consider two rigid end zones of arbitrary length. Note, however, that the member and the rigid end zones have to be on a straight line joining the two end nodes as shown in Fig. 2.3.

In the current implementation of the element up to 15 slices can be used and their positions, chosen by the user, remain fixed throughout the analysis. The element flexibility is assumed to vary linearly between the slices. With this in mind, slice locations should be chosen to represent as accurately as possible the expected flexibility variation along the member taking into account cracking, crushing, and yielding.

In the case of pure bending, for example, if the flexibility ($\frac{1}{EI}$) is constant, then only two slices at the ends of the member would be needed to accurately capture member behaviour. In the case of reinforced concrete members, however, even for a linearly varying moment

distribution the section flexibility varies along the member and changes dramatically when the reinforcement yields. Generally the moment and, therefore, the curvature variation is unknown a priori which makes the choice of optimum slice locations difficult. This is further complicated by the fact that the flexibility distribution changes due to loading, unloading and load reversal as well as moment-axial load interaction. In general, however, the model's accuracy increases with an increasing number of slices. In the case of a reinforced concrete column where the moment distribution is linear and the largest moments are expected to be near the ends of the member, it would be reasonable to concentrate the slices near the member's ends with additional slices near midspan. This is possible since the slices need not be located at regular intervals along the member's length. However, caution is required to insure that one captures an adequate picture of the flexibility variation along the member - see Fig. 2.4.

2.3 Theory and Workings of the Multi-Slice Fiber Model

This section describes the theory and the implementation of the multi-slice fiber model representing the behaviour of reinforced concrete members. The various sub-sections describe the assumptions and methods used for calculating fiber, slice, and element stiffnesses as well as determining the shape functions.

Beam theory is the basis of this model. Plane sections are assumed to remain plane, hence the strains in the various fibers can be easily calculated and the corresponding fiber stresses and stiffnesses deduced from the cyclic stress-strain material relationships. The element flexibility is arrived at by integrating slice flexibilities which are calculated by summation over the fibers. The tangent element stiffness is calculated by inverting the element flexibility and expanding from the three local degrees of freedom to the six global ones. The shape functions relating slice deformations to element displacements are derived from the current slice and element flexibilities.

2.3(a) Fiber Stiffness

Using the assumption of plane sections remaining plane, the strains in the various fibers can be calculated once the strain at some reference point has been determined along with the slice curvature. The equation giving the strain (ϵ_i) in the i'th layer is:

$$\epsilon_i = -\epsilon_p + \phi y_i \tag{1}$$

where,

ϵ_p	=	strain at reference point (usually plastic centroid or midheight)
ϕ	=	slice curvature
y_i	=	distance from centroid of i'th fiber to the reference point

The sign convention governing the various quantities appearing in Equation (1) is given in Fig. 2.2. Note that compressive strains and stresses in the fibers are assumed positive.

Once the strains in the various fibers are determined, the stresses are arrived at from the adopted cyclic stress-strain material relationships discussed later. The accuracy and generally the complexity of the fiber model are a direct function of the adopted stress-strain relationships. The tangent stiffness of the fiber is of course the slope of the stress-strain curve for the given strain. Note that, as in the case of stress calculations, the stiffness (or slope) must be derived giving due consideration to the previous strain history of the fiber and whether the fiber is loading or unloading.

In the special case when the stress-strain curves are approximated by multi-linear segments, the stiffness would simply be the slope of the segment corresponding to the given strain. Hence, the multi-linear stress-strain formulation reduces the amount of calculation involved since the fiber stiffness is readily available without the need for differentiation. The multi-

linear formulation also simplifies the definition of an 'event' i.e. a significant change of fiber stiffness. Such a change in any fiber's stiffness also leads to a change in the overall stiffness of the member. To obtain 'exact' results the element stiffness should therefore be updated whenever any event occurs. This, however, can be computationally unfeasible especially if highly complex material models are adopted and the element is part of a large reinforced concrete frame undergoing a dynamic analysis. Because of this, the material models should be as simple as possible while still retaining the significant physical properties.

The bilinear steel model described in Fig. 2.5 was found by Mark [39] to give sufficiently accurate results provided that the inelastic deformations remained relatively small. For this model there are only two possible stiffnesses, the initial (or elastic) and the post-yield (or strain hardening) stiffnesses. Any transition from one to the other is considered an event, i.e. yielding and unloading. More complex material behaviour can be modelled by superimposing several bilinear steel fibers at the same location. The complexity of the material models must be consistent with the other assumptions being made (i.e. no shear deformations, no bond slip etc.) and the computational effort. The bilinear model appears to be a reasonable compromise for this application. The concrete model shown in Fig. 2.6 consists of a monotonic envelope defined by five linear segments. The number of segments can be easily increased which would result in a slight increase of storage requirements. As shown in Fig. 2.6 concrete is assumed incapable of taking any tension. Unloading proceeds elastically and a crack opens once zero stress is reached. The fiber can carry compressive stresses only upon the closing of the crack, and reloading to the envelope curve again proceeds elastically.

It can be noted that there are many events (stiffness changes) associated with the concrete model. It has been observed [39,44,45] that the precise details of the concrete stress-strain diagram do not greatly affect the overall behaviour of a member, especially in the case of large cyclic deformations. Concrete properties can often be simplified without adversely affecting accuracy. Hence, to reduce computational effort this type of simplified concrete model may be appropriate. Furthermore, the user has the option of disregarding many of the events associated

with the concrete fibers that might occur during a loading increment. Unloading, however, can be retained as a 'significant' event. This reduction in the total number of events to be considered can be numerically advantageous, since every significant event requires the element's and therefore the structure's stiffness to be updated.

By disregarding certain events it is clear that an approximate stiffness is being used. This results in errors which can accumulate, such that the final results may be quite inaccurate. To avoid this, an exact state determination for the element is used which does not ignore any of the events. Once the state of the element is determined at the end of a step, the forces at the ends of the member are calculated based on (1) the significant events and (2) all events and any difference between them is corrected on the nodes at the ends of the member. This procedure is described in Section 2.3(e).

2.3(b) Slice Flexibility

Once the stiffness of the various fibers making up a given slice are determined, the slice stiffness and therefore flexibility can be easily calculated. Two degrees of freedom per slice along with the assumption of plane sections remaining plane are sufficient to define the state of the slice. As shown in Fig. 2.2, the two degrees of freedom can be chosen as the curvature and the strain at some reference axis, usually the plastic centroid (or simply the middepth of the section). Slice bending moment (M_s) around this reference axis and an axial load (P_s) are associated with these degrees of freedom. Incremental section forces are calculated using the following pair of equations which express summations over the fibers in a slice:

$$dP_s = \sum_i A_i \cdot E_i \cdot d\epsilon_i \tag{2}$$

$$dM_s = \sum_i A_i \cdot E_i \cdot d\epsilon_i \cdot y_i \tag{3}$$

where A_i = area of fiber i

E_i = current stiffness of fiber i

and ϵ_i, y_i as defined in Eq.(1)

Making use of Eq. (1) these equations can be rewritten as:

$$dP_s = \sum_i A_i \cdot E_i \cdot (-d\epsilon_p + d\phi \cdot y_i) \tag{4}$$

$$dM_s = \sum_i A_i \cdot E_i \cdot y_i \cdot (-d\epsilon_p + d\phi \cdot y_i) \tag{5}$$

Denoting the slice tangent stiffness by $\mathbf{k}_s$ we have:

$$\begin{Bmatrix} dM_s \\ dP_s \end{Bmatrix} = \mathbf{k}_s \begin{Bmatrix} d\phi \\ d\epsilon_p \end{Bmatrix} = \begin{bmatrix} a_{11} & a_{12} \\ a_{21} & a_{22} \end{bmatrix} \begin{Bmatrix} d\phi \\ d\epsilon_p \end{Bmatrix} \tag{6}$$

From Eqs. (4) and (5) it is clear that:

$$a_{11} = \sum_i A_i \cdot E_i \cdot y_i^2 \tag{7}$$

$$a_{21} = a_{12} = \sum_i A_i \cdot E_i \cdot y_i \tag{8}$$

$$a_{22} = \sum_i A_i \cdot E_i \tag{9}$$

Hence the (2 x 2) tangent slice stiffness matrix is completely defined and the corresponding slice flexibility matrix $\mathbf{f}_s$ is given by simply inverting the stiffness matrix:

$$\mathbf{f}_s = \mathbf{k}_s^{-1} \tag{10}$$

2.3(c) Element Stiffness

The two end rotations along with the axial displacement shown in Fig. 2.3 constitute the three local degrees of freedom for the element (θ_1, θ_2, and Δ). Associated with these degrees of freedom are the two end moments (M_1, M_2) and the axial load (P). Assuming linear variation of flexibility between slices, the element flexibility can be calculated by closed form integration of section flexibility along the length of the element. This procedure is described in this section.

The first step is to relate the slice forces $\vec{S}_s$ (M_s, P_s) to the forces at the end of the member $\vec{S}_m$ (M_1, M_2, P); in other words to determine the (2 x 3) matrix $\mathbf{b}$ in the equation:

$$\vec{S}_s = \mathbf{b}\vec{S}_m \tag{11}$$

This can be accomplished by straightforward application of the equations of equilibrium as shown in Fig. 2.7. One therefore arrives at:

$$\mathbf{b} = \begin{bmatrix} -1+\frac{x}{L} & \frac{x}{L} & 0 \\ 0 & 0 & 1 \end{bmatrix} \tag{12}$$

The slice flexibility was developed in Section 2.3(b) and by assuming linear variation of flexibility along the member, the flexibility $\mathbf{f}_s(x)$ of any section can be calculated by interpolation. This section flexibility relates incremental slice deformations $d\vec{v}_s$ ($d\phi$, $d\epsilon_p$) to the incremental slice forces: $d\vec{S}_s$ (dM_s, dP_s) as follows:

$$d\vec{v}_s(x) = \mathbf{f}_s(x)d\vec{S}_s(x) = \begin{bmatrix} f_{11} & f_{12} \\ f_{21} & f_{22} \end{bmatrix} d\vec{S}_s(x) \tag{13}$$

Equations (11) and (13) along with the virtual work principal lead to:

$$d\vec{v}_m = \mathbf{f}_m\, d\vec{S}_m \tag{14}$$

where $\mathbf{f}_m$ the (3 x 3) element flexibility matrix is given by:

$$\mathbf{f}_m = \int_0^L \mathbf{b}^T(x)\mathbf{f}_s(x)\mathbf{b}(x)dx \tag{15}$$

By breaking up the integral over the individual slices and using natural coordinates with the transformation defined in Fig. 2.8, Eq. (15) can be rewritten as:

$$\mathbf{f}_m = \sum_{i=1}^{ns-1} L_i \int_{\frac{-1}{2}}^{\frac{1}{2}} \mathbf{b}^T(\xi)\ \mathbf{f}_s(\xi)\ \mathbf{b}(\xi)d(\xi) \tag{16}$$

where: ns = number of slices used

L_i = length of member between slices 'i' and 'i + 1'

Hence the (3 x 3) element flexibility matrix relating end displacements to end forces can be calculated. The element stiffness matrix can be obtained by simple inversion of the flexibility matrix:

$$\mathbf{k}_m = \mathbf{f}_m^{-1} \tag{17}$$

Finally the element tangent stiffness can be expanded to the complete element (6 x 6) stiffness matrix which includes rigid body displacements and a transformation applied so that the final stiffness matrix relates global displacements to global forces. This transformation takes into consideration rigid end zones of arbitrary length.

2.3(d) Shape Functions and State Determination

One of the advantages of the multi-slice fiber model is the fact that there are no predefined interpolation or shape functions. The shape functions used to calculate slice deformations from member end displacements are a function of the slice flexibilities and are therefore continually updated as the state of the element evolves [46].

Combining Eqs. (11), (13), and (14) leads to

$$d\bar{v}_s = \mathbf{f}_s \mathbf{b} \mathbf{f}_m^{-1} \, d\bar{v}_m \tag{18}$$

Therefore the shape functions which give slice deformation increments in terms of element deformation increments are given by:

$$\mathbf{a} = \mathbf{f}_s \mathbf{b} \mathbf{f}_m^{-1} \tag{19}$$

These shape functions can be used to calculate the slice deformations and hence to update the state of the slices and consequently the element. For a differential increment in slice deformations the shape functions as derived are exact. For finite deformation increments, however, the shape functions would only be exact if the state determination and updating phase is divided into sufficiently small steps so that the shape functions are changed every time a material event occurs - e.g. the yielding of a steel fiber or the cracking of a concrete fiber, etc. Even if this procedure is implemented, one should keep in mind that the state determination phase would be exact only in so far as the adopted linearized material stress-strain relationships represent the actual material behaviour.

2.3(e) Unbalanced Forces

If a strict event-to-event approach is adhered to - i.e. if the structure's stiffness is modified whenever any of the elements and therefore fibers changes state - then equilibrium would always be satisfied. The axial load would be constant along the element and the bending moment would vary linearly. To save on computations, however, the user may ignore the stiffness changes during a time step and apply corrective forces at the end of the step. Consequently, equilibrium will not necessarily be satisfied at the end of the step. While iterative strategies exist to correct for this, they are incompatible with the desired computational efficiency. An alternative that may be acceptable if the size of the unbalance is relatively small is to add to

the next time step's load vector a set of self-equilibrating corrective forces. These corrective forces should equal the difference between the 'nonlinear' or actual element forces at the end of the step and the 'linear' forces that result from the assumption of constant element stiffness throughout the time step. The 'nonlinear' forces are obtained by going through a strict event-to-event element state determination given the state of the element at the beginning of the time step and the additional displacements imposed on the element during the time step in question. This is done in all cases and the 'nonlinear' forces become the starting point for the subsequent step. The 'linear' forces on the other hand are simply equal to the initial element forces plus the element stiffness at the beginning of the step multiplied by the additional displacements. Note that in the case of an analysis using 'significant' events, 'linear' forces are updated whenever a 'significant' event occurs and not merely at the end of a given time step. If no events occur for a given element during a certain time step then the be no need to apply corrective forces. If an event does occur a correction is required to prevent a divergence from the true solution.

III ELEMENT VERIFICATION

3.1 Introduction

This chapter deals mainly with the verification of the multi-slice fiber element's operation. The element can be used separately, in which case it is capable of tracing the slice (as well as the fiber) deformations and forces given the history of displacements at the ends of a single member. The model can also be used as part of DRAIN-2D2 [4] to analyze the dynamic response of two-dimensional frames. Several analyses will be carried out to illustrate these two uses of the element. The effect of various parameters, such as the number of fibers per slice, the number and location of slices, and the size of the time step used will be investigated. Simple analyses will be used and the results compared with theoretical, analytical, or experimental values. The analyses include static monotonic and cyclic loadings of a steel beam and dynamic sinusoidal linear elastic analyses of a column. Further verifications and analysis of reinforced concrete columns and frames will be included in later chapters.

3.2 Monotonic and Cyclic Loading of a Steel Beam

The steel beam used has a five inch by twelve inch rectangular section. As shown in Fig. 3.1(b) the beam analyzed is fixed at both ends and one end is moved vertically relative to the other. Hence, the load-deflection curve for a beam loaded as shown in Fig. 3.1(c) can be derived. These are then compared to theoretical results based on an elasto-perfectly plastic steel stress-strain formulation.

For the purpose of comparison, the yield moment for the given section is 7200 lb-in. and the plastic moment is 10,800 lb-in. The corresponding yield load is 288 lb. and the ultimate load is 432 lb. The theoretically derived load-deflection relation is given in Fig. 3.2 assuming the geometry and the material properties given in Fig. 3.1 and a steel strain hardening slope of

zero - i.e. elasto-perfectly plastic steel.

Results of a multi-slice fiber model analysis of this beam are given in Fig. 3.3 which show the effect of the assumed strain hardening slope. The value of this second branch of the stress-strain curve is alternately set at 10.0, 100.0, and 1000.0 Ksi. As expected, the pre-yield behaviour is not affected, but the load required to produce equal displacements beyond first yield is higher for higher strain hardening rates.

Because of possible numerical problems, it is advisable to use a small second slope instead of an elasto-perfectly plastic model. In this case a minimum second slope of 10.0 Ksi was used which amounts to 0.033% of the initial slope - 30,000 Ksi. As expected the results of the analysis using a 10.0 Ksi second slope are therefore essentially identical to the theoretically derived curve based on an elasto-perfectly plastic steel model and given in Fig. 3.2.

Fig. 3.4 shows the effect of varying the number of fibers per slice. These analyses all divide the member into equidistant slices along it's length and use a hardening slope of 1000.0 Ksi. The number of fibers per slice, however, is changed from 6 to 12 and 18. Note that there is a slight difference between the analyses using 6 and 12 fibers. Since the yield load is a function of the distance between the neutral axis and the centroid of the extreme fiber, the yield load drops from 336 lb. to 312 lb. Increasing the number of fibers further - from 12 to 18 per slice - again results in a decrease in the yield load - from 312 lb. to 304 lb. However, the shape of the curve does not change appreciably and the curves corresponding to 12 and 18 fibers per slice nearly coincide.

The number and positions of the slices were held constant in the previous comparisons. Fig 3.5 indicates the effect of varying the number and position of the slices along the length of the member while keeping the number of fibers per slice constant at 12. Using the analysis with eleven equidistant slices as a reference, note that the number of slices used does not make a difference as long as the beam is behaving elastically. As yielding starts to spread, the larger the number of slices, the better the results. Concentrating slices in the region of the anticipated hinging is highly advantageous. However, it is essential to have some slices in the elastic

portion of the beam to capture the elastic flexibility distribution.

Finally, Fig. 3.6 indicates the capacity of the model to consider cyclic behaviour. The displacement is cycled between extremes of -4.0 and 4.0, inches and the figure gives the corresponding $P - \Delta$ variation. Keeping the basic assumptions in mind, the figures presented so far are "exact" since the model takes into consideration the yielding and unloading of each fiber in every slice. The steel stress-strain relationship is bilinear. Consequently the Bauschinger effect is not in evidence. This absence can be detected in Fig. 3.6.

3.3 Dynamic Analysis of a Linear Elastic Column

A steel column fixed at the base and restrained from rotation at the top is subjected to the sinusoidal ground acceleration record shown in Fig. 3.7. The amplitude of the ground acceleration is scaled in such a way as to insure that the behaviour of the column throughout its length remains elastic. This simple analysis is performed, since theoretical results are available for easy comparison. Furthermore, a parametric study of the effect of the analysis time step can be performed.

The acceleration record is discretized into steps of 0.025 seconds. The time step used in the analysis, however, is varied between 0.005 and 0.015 seconds. Noting that the natural period of the system (T) is 0.15, the analysis time step is thus varied between $\frac{T}{30}$ and $\frac{T}{10}$. The results are given in Fig. 3.8 along with the theoretical curve. This indicates satisfactory correlation so long as the integration time step is sufficiently small.

IV ANALYSIS OF REINFORCED CONCRETE COLUMNS AND FRAMES

4.1 Introduction

Although the multi-slice fiber element can be used to model members of a steel frame, the main concern of this report is its capabilities for modelling reinforced concrete frames. The element appears especially well suited for modelling the behaviour of reinforced concrete columns when the axial load is appreciable or fluctuates significantly with time. Of course, shear considerations must not be dominant and other elements must be used to model deformations associated with bond slip in connections. The ability of the multi-slice fiber element to account for the influence of an axial load on a member's strength and stiffness characteristics as well as on the shape (pinching) of hysteresis loops will be illustrated in the following sections. Results of dynamic analyses of several reinforced concrete columns and frames are examined. Comparisons are made with results of other analytical studies to identify the capabilities of the method.

4.2 Dynamic Analyses of a Reinforced Concrete Column

To check the functioning of the multi-slice fiber model several parametric studies were run on a reinforced concrete cantilever column subjected to horizontal base excitation. Various modelling and analysis assumptions were considered to assess their effect on the accuracy of the element and to develop some insight into the dynamic response of simple reinforced concrete structures.

4.2(a) Example Column

The column selected, shown in Fig. 4.1, has been previously analyzed and tested [39,44]. The geometry and material properties of the column assumed in the analyses are given in Figs. 4.1 and 4.2. The bilinear steel model was used with a yield stress of 48.4 Ksi, an initial slope of 29000 Ksi and a strain hardening slope of 300 Ksi. The concrete stress-strain curve shown in Fig. 4.2 closely follows the suggested relationship for the confined portion of the column section [39]. Since spalling did not occur in previous analytical and experimental analyses, large concrete strains were not anticipated and the same concrete model was used to represent the behaviour of the unconfined portion. This observation was born out by the results of these analyses. For purposes of later comparisons, the maximum axial load capacity of the section P_{max} (given by $A_c \cdot f'_c + A_s \cdot f_y$) is equal to 301 Kips.

Unless otherwise specified, the section was discretized into eight equal concrete layers and six slices were considered along the length. Since the moment diagram expected for this column varies linearly from a maximum at the base to zero at the top, slice locations were concentrated in the vicinity of the base. Hence for this standard case the slices were spaced at 2.0-3.0-5.0-5.0-5.0 inches starting at the base.

The excitation used in most of the analyses consisted of a simple sinusoidal base acceleration record with a period of .075 seconds shown in Fig. 4.3. This was used to develop significant deformation reversals. Some analyses were performed using the N-S component of the 1940 El Centro acceleration record. The analysis time step used was 0.00125 seconds (or approximately 1/38 of the apparent period of the column).

4.2(b) Influence of Modelling and Discretization

The first parameter to be considered was the number of slices along the length of the member. Two runs were made, one using eleven slices uniformly spaced at 2.0 inches and

another using the standard six slices. To make sure the steel yielded, the acceleration record amplitude was set at 2.0g. In both cases the column was subjected to an axial load of 33.5 Kips or P_{max} / 9 in order to produce relatively complex hysteresis behaviour. The tip displacement histories are compared in Fig. 4.4(a), while Fig. 4.4(b) compares the moment-curvature histories developed at the base of the column. It is clear from Fig. 4.4(b) that the element is able to trace the very complex hysteretic loops developed by this column. The global displacement response and moment-curvature response obtained using only six slices are very close to the results obtained using eleven equally spaced slices. This is reasonable since the flexibility variation in regions of lower bending moments would be less dramatic (or even linear) and hence can be adequately captured by a relatively small number of slices. Slices should be located in regions where significant variations in flexibilities are likely to occur rather than arbitrarily or uniformly spaced along the member. Because of the satisfactory results provided by the six-slice model, the following analyses use this configuration as standard.

The second modelling parameter of interest is the number of concrete fibers considered across a slice. Fig. 4.5 shows a comparison of two analyses, one discretizing the section into eight and the other into sixteen layers of equal depth. Again, the axial load applied to the section was 33.5 Kips and the sinusoidal acceleration record with an amplitude of 2.0g was used. The tip displacement histories (given in Fig. 4.5(a)) corresponding to the two analyses are in close agreement. The moment-curvature histories for the base of the column (given in Fig. 4.5(b)) differ to a somewhat larger extent. As expected, the sixteen fiber discretization results in relatively smoother stiffness transitions. The tip displacement history, however, reflects the overall stiffness of the member and in regions of low bending moment - which remain essentially elastic - the number of fibers is not of great consequence. Hence, the variation of tip displacement is less sensitive to the number of fibers per slice than is the moment-curvature history at the base of the column. It appears that a relatively small number of fibers can be used to adequately represent the section behaviour.

4.2(c) Influence of Geometric Stiffness

As mentioned earlier DRAIN-2D2 [4] has the capacity of including simple geometric stiffness ($P - \Delta$ effect) based on the axial loads resulting from a static analysis. Fig. 4.6 shows results of two analyses, one ignoring and the other including geometric stiffness. The geometric stiffness in this case is a function of the applied axial load which is constant throughout the analysis and equal to 16.75 Kips or P_{max} / 18. Note that in the initial elastic phases the two curves show no significant difference. Later, however, the extent of inelastic behaviour increases as evidenced by the elongation of the period, and the effect of geometric stiffness correspondingly increases.

4.2(d) Influence of Acceleration Record Amplitude

Fig. 4.7 compares the tip displacement histories resulting from sinusoidal acceleration records scaled to 1.0g and 2.0g amplitudes. As expected the larger amplitude record results in larger displacements. Furthermore, while the lower amplitude record exhibits periodic motion, the higher amplitude record does not. This can be explained by the fact that the behaviour of the column subjected to the 1.0g record is essentially elastic, though nonlinear, as shown in Fig. 4.8(a). This figure shows the moment-curvature history at the base of the column - the location of the largest moments. A definite cracking load is observed, since the column is subjected to a compressive axial load. The steel, however, does not yield for this excitation. Upon reversal of a displacement excursion, open cracks on one side of the section close, while cracks start opening on the other side. This results in the nonlinear elastic moment-curvature behaviour indicated. Fig. 4.8(b) shows the moment-curvature history corresponding to the higher amplitude record. Clearly the steel yields in this case and the behaviour is no longer elastic. Because of the inelastic behaviour, the response is no longer periodic.

4.2(e) Influence of Applied Axial Load

The axial load applied to the column can also significantly change its behaviour. Using the 1.0g sinusoidal record three runs were made as the axial load varied from 0.0 to 16.75 Kips and finally to 33.5 Kips. The mass, however, was held constant. The tip displacement histories are given in Fig. 4.9(a) and indicate an increase in maximum displacement with a decrease in axial load. This is essentially due to the fact that for this range of loading the stiffness increases with the applied load. Furthermore, note that the displacement history corresponding to the 33.5 Kip load is periodic and the behaviour elastic as indicated by the moment-curvature plot given in Fig. 4.9(b). The moment-curvature plots corresponding to the lower loads, however, indicate steel yielding and hysteresis loops developing and growing as the axial load decreases - see Figs. 4.9(c) and 4.9(d). This can be explained by the fact that for this range of loading the yield moment increases with an increase in axial load.

4.2(f) Influence of Analysis Technique

In the preceding analyses the event-to-event procedures discussed in Chapter II were used. That is, all stiffness changes occurring during an integration time step are detected and accounted for in determining the response. Since the member is represented by several slices, each consisting of several fibers, the number of potential events during a single time step is very large and could result in excessive computational effort. DRAIN-2D2 [4] has the option of disregarding events during time steps - i.e., the structure's stiffnesses at the beginning of the time step is assumed constant throughout the step, irrespective of actual element stiffness changes. The stiffness is updated at the end of the step and equilibrium errors (unbalanced forces) are then corrected for at the beginning of the next step.

Two analyses were carried out to illustrate these procedures using a 2.0g amplitude sinusoidal acceleration record (shown in Fig. 4.3). An axial load of 33.5 Kips was applied to

the column. The first analysis proceeded strictly event-to-event, that is the column's stiffness was updated whenever any of the fibers changed stiffness. In the second analysis such midstep 'events' were disregarded until the end of the time step. The corresponding two tip displacement histories are given in Fig. 4.10(a). Note that the difference is not appreciable for the time step used and while the analysis disregarding midstep events took two minutes, the one considering all events took five minutes - these and the following analyses were made using a VAX 750 machine. Fig. 4.10(b) compares the corresponding moment-curvature histories at the base of the column. Note that updating the stiffness whenever a fiber changes state results in a smoother curve, but that the maximum values and the overall shape of the hysteresis loops is not appreciably affected.

As a means of cutting computation effort while still achieving satisfactory results, an additional option was incorporated into the multi-slice fiber model for use in conjunction with the event-to-event approach of DRAIN-2D2. This option disregards 'insignificant' events. For the purposes of this element the only significant event considered for the concrete is unloading. Any change in a steel fiber's stiffness is considered a significant event, since the behaviour of the reinforcing steel has a greater influence on section behaviour. Fig. 4.11(b) shows a comparison of the tip displacement histories corresponding to a strict event-by event analysis and an analysis which considers only significant events. The difference is not appreciable while the analysis times were five minutes and two and a half minutes, respectively. Fig. 4.11(a) shows the corresponding moment-curvature histories. Note that the maximum values and overall shapes are quite similar. It is also interesting to note that including 'significant' events results in a smoother curve than disregarding all midstep events - compare Figs. 4.10(b) and 4.11(a) - without an appreciable increase in computational effort.

4.2(g) Analysis Using El-Centro Record

To illustrate the capabilities of the element under earthquake type excitations, the example column was also subjected to 6 seconds of the 1940 N-S El-Centro record. A constant axial load of 16.75 Kips was assumed to act on the column throughout the duration of the excitation. The analysis time step used was 0.0025 seconds. The analysis was performed considering all events, only significant events and no midstep events. Figs. 4.12 and 4.13 compare results of the three analysis techniques. Note that for the small time step used, the tip displacement histories are very close.

Fig. 4.14 shows a typical moment-curvature hysteretic loop from the three analyses. Although ignoring midstep events results in some discrepancies, the envelope values and energy dissipation are not greatly affected. Compared to a complete event-to-event analysis, considering only significant events and ignoring all midstep events reduced the computation time by 50% and 75%, respectively.

The results of the analysis using the multi-slice fiber model will now be compared with results of a more conventional analysis. Since the column has a single lateral degree of freedom, the program NONSPEC [47] could be used to compute the response. This program considers single degree of freedom systems with a bilinear restoring force envelope. Both bilinear hysteretic and stiffness degrading [47] hysteretic characteristics may be considered.

The multi-slice fiber model was used to calculate the monotonic lateral load-displacement relation of the example column with an axial load of 16.75 Kips. A bilinear envelope curve was approximated as shown in Fig. 4.15 for use with NONSPEC. As shown in Fig. 4.16 for small displacements, the bilinear and stiffness degrading models give essentially identical results. Later, however, after significant yielding and reversals, the response histories diverge, although the number of zero crossings remains the same.

Fig. 4.17 compares the response of the multi-slice fiber model with those of the bilinear and the stiffness degrading models. Table 1 compares the maximum and minimum

displacements given by the three models.

Type of Model:	Multi-slice fiber	Bilinear	Stiffness Degrading
Max. Disp.	0.058	0.047	0.052
Min. Disp.	-0.075	-0.083	-0.067

Table 1. Extreme displacement values using various models

For the initial low acceleration input phase the bilinear and stiffness degrading models overestimate the response. This is due to the fact that the bilinear envelope curve on which these models are based does not account for cracking, and thus, as illustrated in Fig. 4.15, a lower initial stiffness results. Later, when significant yield excursions occur the stiffness degrading model better approximates the response given by the multi-slice fiber model. Nonetheless, the results are significantly different, most likely due to the highly pinched hysteretic loops exhibited by the column which are not accounted for in the standard stiffness degrading model incorporated in NONSPEC. The simple models, moreover, do not provide information on the local behaviour such as moment-curvature histories. Since the behaviour of concrete elements in even the 'elastic' range is complex due to cracking and axial load effects, simple models are not likely to produce reliable results.

4.3 Dynamic Analysis of a Reinforced Concrete Frame

Results of analyses performed on a one-bay, one-story, reinforced concrete frame will be given in this section. The effects of geometric and material modelling assumptions will be investigated as well as analysis technique and time step used.

4.3(a) Example Frame

The reinforced frame shown in Fig. 4.18 has been previously used for experimental [48] and analytical [39] studies. As shown in Fig. 4.18 the frame made up of two 5 in. square columns and a 10 in. by 5 in. beam. The reinforcement in columns and beam consists of 4 # 3 bars giving a reinforcement ratio of 1.76% in the columns (based on gross section area). Average values obtained in material tests [48] were used to idealize the primary steel and concrete stress-strain curves. The models used are given in Fig. 4.19.

For the experimental study conducted by Gulkan and Sozen [48], plates weighing 4.0 Kips were bolted to the beam at midspan. For the analyses to follow, this has been idealized as two 2.15 Kip loads (the additional weight accounts for beam weight, etc.) placed at the two joints. Hence, each column is assumed to be subjected to an initial static axial load of 2.15 Kips and a corresponding concentrated mass is lumped at the beam-column joints.

The sinusoidal base acceleration record used in the analyses is shown in Fig. 4.20. An attempt has been made to match as closely as possible the record used in Mark's study of the same frame [39] - thus, an amplitude of 1.21g was used. Unless otherwise stated, the analyses are carried out using a time step of 0.00125 seconds. For later comparisons, Fig. 4.21 shows the result of analyses carried out by Mark using time steps of 0.0005 and 0.001 seconds and 20 slices for each element. Mark ignores stiffness changes during a time step and does not apply equilibrium corrective forces at the end of the step. This explains the somewhat large difference between the calculated responses for the two time steps. The following two sections will use the frame described above to study the effects of modelling and analysis assumptions on the calculated response.

4.3(b) Effect of Some Modelling Assumptions

As discussed earlier, the multi-slice fiber model avoids the need to define moment-curvature relations, moment-rotation relations or yield surfaces. Nevertheless, various material and geometric modelling decisions need to be made. The sensitivity of the calculated response to variations in these modelling assumptions is investigated in this section. In particular the influence of the steel strain hardening stiffness, the number of slices used to discretize an element and the assumption of perfectly rigid joints are studied.

Fig. 4.22(a) compares the tip of column 1 displacement histories assuming strain hardening slopes of either 300 or 1000 ksi. Note that a higher strain hardening slope does not necessarily result in smaller displacements. In fact the analysis based on the higher value results in a half-cycle maximum sway of 0.4 in. compared to 0.36 in. for the lower value of strain hardening rate. This may be explained by the fact that changing the stiffness also changes the effective period which affects the dynamic response. The corresponding moment-curvature plots for the base of column 1 are compared in Fig. 4.22(b). Note that a higher strain hardening rate results in a stiffer second branch as expected. However, as illustrated in Fig. 4.22(b) a higher strain hardening rate also results in larger hysteretic loops in this case which explains the larger displacements - compare points C and C' in Figs. 4.22(a) and 4.22(b).

To assess the importance of the number of slices used along the length of the elements, two analyses were carried out : one using 5 slices per element and the other 9 slices per element. In both cases, however, the spacing was not uniform : the first two slices at each end of an element were placed closer together since that is were the greatest moments and flexibility variations are expected. In the case of the columns, the end slices were spaced at 3.75 and 0.875 inches apart for the 5-slice and 9-slice idealizations, respectively. Fig. 4.23(a) compares the two displacement histories and Fig. 4.23(b) the corresponding moment-curvature histories at the base of column 1. Again, note that considerable differences in moment-curvature histories do not necessarily result in correspondingly large differences in displacements. For

example, this can be seen by comparing the loops ABC and A'B'C' in Figs. 4.23(a) and 4.23(b). This is due to the fact that the slice spacings in the two analyses are not the same, hence comparing the moment-curvature histories of just one slice is not sufficient for comparing the overall element behaviour. The displacement histories are not greatly different, however. Furthermore, compared to the analysis reported by Mark using 20 equally spaced slices and a time step of 0.0005 seconds (see Fig.4.21(b)) the analysis using only 5 slices gives very good results. Finally, using 5 slices as opposed to 9 considerably reduces analysis time. Hence, the 5 slice configuration was adopted for the following analyses.

Another modelling decision to be made is whether to consider the joints rigid or not. In fact the joints are never perfectly rigid, but are considered such in certain analyses as a matter of convenience. Sources of flexibility - such as shear, bond slip etc. - can be partially accounted for by extending the elements to the center of the the corresponding joints. Fig. 4.24 compares the displacement histories based on the flexible and rigid joint assumptions. Note that assuming rigid joints results in an increased initial stiffness, reduced displacement and period. Later, however, after cycling and significant yielding the two histories come closer together in terms of displacements and periods. A precise analysis of joint deformations including bond slip would require development of a special element to be included in the model.

4.3(c) Influence of Analysis Technique and Time Step

As discussed and illustrated earlier, DRAIN-2D2 [4] has the capacity of carrying out event-to-event analyses which take into consideration every change of stiffness in any of the elements. In addition, the multi-slice element model was developed such that certain changes in fiber stiffness are considered 'significant', namely yielding and unloading of steel fibers, and the unloading of concrete fibers. Figs. 4.25 and 4.26 compare the results of analyses based on considering all events, 'significant' events, and ignoring events altogether during the time step. The sinusoidal record given in Fig. 4.20 along with an analysis time step of 0.00125 seconds are

used. Note that the displacement response histories (Fig. 4.25) almost coincide, although the analysis times were 40, 8 and 6 minutes for the strict event-to-event, 'significant' events, and no events analyses respectively. Figs. 4.26(a) and 4.26(b) compare the moment-curvature histories at the base of column 1. Clearly the variation is not very significant, although taking the 'significant' events into consideration (Fig. 4.26(a)) gives closer results and a smoother moment-curvature history than ignoring events altogether (Fig. 4.26(b)).

The preceding discussion of the influence of analysis technique illustrates the fact that significant computational effort may be saved by taking into account only significant stiffness changes or even ignoring all stiffness changes during the time step (and applying equilibrium corrective forces at the end of the step). As Fig. 4.25 illustrates this may not result in significant loss of accuracy. Care must be taken, however, to insure that the corrective forces do not grow to such an extent that their application leads to numerical instability. Usually,the larger the time step the larger the unbalance and the greater the risk of numerical instability. In addition, numerical inaccuracies result from the use of large time steps [4]. To illustrate this, the same analyses used to produce Fig. 4.25 were repeated using a time step of 0.00625 seconds (or T/7.6) as opposed to the time step of 0.00125 seconds used previously. The results considering all events, 'significant' events and no events are given in Fig. 4.27. Note that the analysis ignoring all events diverges, while the analysis considering 'significant' events remains stable although the accuracy diminishes with the increased time step size - compare Figs. 4.25 and 4.27. Thus, the size of the time step should be chosen to attain the required accuracy and insure numerical stability. The event-to-event techniques usually mean a larger computational effort than the no events technique for the same time step size. On the other hand, such techniques permit the use of a larger time step with acceptable accuracy and no numerical problems.

4.3(d) Effect of Axial Load

The action of an axial load significantly changes the behaviour of a reinforced concrete section. As discussed and illustrated previously, the stiffness, especially before yielding, and the yield moment are functions of the axial load acting on the section. Furthermore, a compressive axial load can result in pinched hysteresis loops. To illustrate these phenomena and their effect on the response of a reinforced concrete frame, the example frame of Section 4.3(a) was reanalyzed for the sinusoidal record given in Fig. 4.20 considering a different column axial load. The same time step (0.00125 seconds), material, and geometric idealizations were used for this analysis. For the previous runs, an axial load of 2.15 Kips due to gravity effects was assumed to act on each column. For the new run, the axial load was arbitrarily increased to 25.4 Kips, or $P_{max}/6$. Both of these gravity loads are below the balanced axial load which is about 55 Kips for this column. The mass of the structure was unchanged in the analysis.

The results of the two analyses are shown in Fig. 4.28 which gives the lateral displacement as well as column base moment-curvature histories. Note that, as expected, the higher axial load results in a larger initial stiffness and in this case a higher yield moment. These effects are illustrated in the first branch of the moment-curvature history. The higher initial stiffness and yield moment corresponding to the higher axial load case also mean that the displacements of the frame would tend to be lower than for the frame whose columns were subjected to the higher axial loads. This is apparent in Fig. 4.28(a) - compare the displacements up to point A. Later, however, the higher axial load results in appreciable pinching of the hysteresis loops as shown in Fig. 4.28(b) which in turn means reduced stiffness during significant portions of the response and larger displacements as shown in Fig. 4.28(a).

4.3(e) Comparison with Other Models

The two analyses presented in the previous section, corresponding to gravity axial loads of 2.15 and 25.4 Kips, were also carried out using a more conventional reinforced concrete member model available in DRAIN-2D [2]. This model is a one component element with concentrated end springs having rotational characteristics based on a simplified Takeda stiffness degrading model. The simplified Takeda model assumes a bilinear moment-rotation relation for the concentrated springs. It requires as input the axial stiffness (assumed constant), the yield moment, and the initial as well as strain hardening flexural stiffnesses. Member moment-curvature relations were computed using UNCOLA [44] and the two required flexural stiffnesses were established by ignoring the cracking transition. The displacement histories for an axial load of 2.15 Kips calculated using the multi-slice fiber element and the concentrated spring element based on the simplified Takeda stiffness degrading model [2] are compared in Fig. 4.29. As illustrated in this figure, ignoring the initial precracking stiffness does not significantly affect the response, since the axial load is very low. The stiffness degrading model gives satisfactory results except in the final phase of the response where, as shown in Fig. 4.28(b), the results from the multi-slice fiber model indicate a small but noticeable pinching of hysteresis loops.

For the higher axial load case, the required yield moment and stiffnesses were deduced from the moment-curvature relation corresponding to the specified axial load. The results of the analyses using the multi-slice fiber model and the concentrated spring model are given in Fig. 4.30. Note that for this higher axial load (25.4 Kips) ignoring cracking results in a larger initial discrepancy. The significant pinching of hysteresis loops observed in Fig. 4.28(b) results in greater difference between the responses than for the case with the lower axial load. The same analysis was carried out using the two-component parallel model incorporated in DRAIN-2D. This element represents members exhibiting bilinear hysteretic moment-rotation relations. The results obtained with this element are shown in Fig. 4.31. Comparing Figs. 4.30 and 4.31

indicates that the single component element based on the stiffness degrading model leads to better prediction of the response than the two-component parallel element based on the simpler bilinear model.

The response to 4 seconds of the N-S component of the El Centro record were also computed using the multi-slice fiber model and the simplified Takeda model. Since the frame is a scaled down model, the acceleration amplitudes were magnified by a factor of 4 to produce yielding. Fig. 4.32(a) compares the results of the analyses. Note that by ignoring the higher initial precracking stiffness, the concentrated spring model leads to higher calculated displacements in the initial low amplitude acceleration phase. Although the two response curves are similar in shape, they differ appreciably as far as extreme displacement values are concerned. It is interesting to note that at point A in Fig. 4.32(a) the responses start to diverge significantly and that the corresponding point on the moment-curvature history - point A Fig. 4.32(b) - is where the hysteresis loops are most severely pinched.

4.3(f) Effect of a Varying Axial Load

The previous two sections analyzed the dynamic response of the example frame when its columns were subjected to an essentially constant axial load. This section will demonstrate the capacity of the multi-slice fiber model to predict the behaviour of reinforced concrete members when subjected to a varying axial load.

The same example was used for the analysis except that a concentrated mass corresponding to five additional stories was introduced. The mass was placed at the center of gravity of the additional structure and was assumed to be rigidly connected to the tops of the columns - see Fig. 4.33. In addition, the static axial loads acting on the columns were increased to 12.75 Kips to account for the five additional stories. The model was subjected to the same sinusoidal record - see Fig. 4.20 - and the response was calculated using the multi-slice fiber model as well as the two-component parallel model and the modified Takeda models. The resulting

displacement histories are given in Fig. 4.34. Note that results from the two-component model deviate considerably from those of the fiber model, although the two-component model takes into account the variation of yield moment with applied axial load. The two-component model does not, however, account for changes of stiffness in the 'elastic' range that result from variations in axial load. The stiffness within the yield surface is fixed and was set equal to the initial cracked stiffness under a load equal to the static axial load. The modified Takeda model results in closer agreement as far as displacement history is concerned. The Takeda model does not account for variations of stiffness or yield moment with axial load. The superior results of the Takeda model when compared to the two-component parallel model are mainly due to the fact that the modified Takeda model accounts for stiffness degradation.

Figs. 4.35-4.37 give additional results of the analysis using the multi-slice fiber model and summarize the behaviour of the columns. Fig. 4.35 traces the history of the axial load variations in the two columns. As expected, the sum of the two axial loads is constant, as equilibrium would require. Hence, as the compressive load in one column increases the load in the other decreases which results in significant variations in the bending moments and shears to which the columns are subjected - see Fig. 4.36. Note that initially at least the column subjected to larger compressive loads receives a larger portion of the base shear. This would be a consequence of the effect of axial load on stiffness. Fig. 4.37 gives the moment-curvature histories at the bases of the two columns. Note that variations in axial load produce frequent and significant variations in stiffness. This results in complex moment-curvature relationships which the multi-slice fiber model can trace.

Fig. 4.38 summarizes the behaviour of the columns as given by the analysis based on the Takeda model. As Fig. 4.38(a) shows, the sum of the axial loads in the two columns remains constant. The history of axial load in the individual columns is similar to the history prediced by the multi-slice fiber model - compare Figs. 4.35 and 4.38(a). There are differences, however, which are mainly due to the fact that the Takeda model assumes constant axial stiffness while the multi-slice fiber model updates the axial stiffness to reflect the state of the element.

Furthermore, the multi-slice fiber model takes into consideration the axial load-bending moment interaction. This also explains the significant differences in the predicted shear history variation in the two columns - compare Figs. 4.36 and 4.38(b). Since the Takeda model assumes the flexural stiffness to be independent of the axial load and stiffness, the shears in the two columns are identical throughout the analysis. A more realistic shear distribution is given by the multi-slice fiber model as illustrated in Fig. 4.36. For example, when the maximum base shear is attained the column in compression carries 70% of it while the column in tension carries the remaining 30%. Finally, it might be worth mentioning that information concerning local behaviour cannot be obtained using discrete models. The multi-slice fiber model, however, can provide such information as illustrated by the various moment-curvature histories.

V CONCLUSIONS

Various models have been proposed for the analysis of reinforced concrete members and structures ranging from very simple single degree of freedom models to finite element discretizations. The multi-slice fiber model seems to be a satisfactory alternative for modelling elements of a reinforced concrete frame. The model requires as input material stress-strain relationships for the various fibers and provides as output detailed history of local and member behaviour including curvatures, rotations, axial deformations as well as member forces. The model can account for axial load-bending interaction, thus variations in yield moment and flexural stiffness due to the presence and change in axial load can be considered. As illustrated, the model can also trace complex hysteresis loops which show the effects of crack opening and closing as well as pinching due to a compressive axial load acting on the member. The various features of the multi-slice fiber model make it ideally suited for modelling reinforced concrete columns where axial load-bending interaction is important.

The limitations of the multi-slice fiber model arise from the assumptions on which it is based as well as the adopted concrete and steel stress-strain relations. Hence, the assumption of plane sections remaining plane ignores the effects of shear and bond slip on section geometry. The model, moreover, does not consider the shear-flexural interaction and is therefore not suitable for modelling members where shear considerations are dominant. The bilinear steel model implemented for this study has the virtue of simplicity, but does not realistically model strain hardening and does not account for the Bauschinger effect. Finally, due to the large number of fibers and the need to trace the history of each of the fibers, the required computational effort can be considerable especially in the case of dynamic event-to-event analyses.

This study has shown the multi-slice fiber model to be a flexible analysis tool. However, various improvements and uses can still be investigated. For example, the steel model can be modified to account for local buckling and the Bauschinger effect, the use of the model in static load-to-collapse analyses can be studied, and the extension of the model for three dimensional analyses can be investigated. To reduce computational effort, parametric studies can be

performed to establish guidelines for efficiently locating fibers and slices and for judiciously choosing an analysis time step. Finally, a simplified beam model can be adapted for use in cases where axial load-bending interaction does not significantly affect behaviour.

REFERENCES

(1) Otani, S., "SAKE - A computer program for inelastic response of R/C frames to earthquakes," Civil Engineering Studies, Structural Research Series No. 413, University of Illinois, Urbana, November 1975.

(2) Kanaan, A.E. and Powell, G.H., "DRAIN-2D - A General Purpose Computer Program for Dynamic Analysis of Inelastic Plane Structures - With User's Guide," EERC Reports No. 73/6 and 73/22, University of California, Berkeley, April 1973, Revised September 1973 and August 1975.

(3) Saiidi, M., "User's Manual for the LARZ Family - Computer Programs for Nonlinear Seismic Analysis of Reinforced Concrete Planar Structures," Civil Engineering Studies, Structural Research Series No. 466, University of Illinois, Urbana, November 1979.

(4) Golafshani, A.A., "DRAIN-2D2 - A Computer Program for Inelastic Seismic Response of Structures," Ph.D. Dissertation, Dept. of Civil Engineering, University of California, Berkeley, 1982.

(5) Mondkar, D.P. and Powell, G.H., "ANSR-II Analysis of Nonlinear Structural Response, User's Manual," EERC Report No. 79/17, University of California, Berkeley, July 1979.

(6) Bathe, K.J., "ADINA - A Finite Element Program for Automatic Dynamic Incremental Nonlinear Analysis," M.I.T. Report 82448-1 (Revised 1978).

(7) Aziz, T.S., "Inelastic Dynamic Analysis of Building Frames," Publication No. R76-37, Dept. of Civil Engineering, M.I.T., Cambridge, August 1976.

(8) Umemura, H., Aoyama, H., and Takizawa, "Analysis of the Behaviour of Reinforced Concrete Structures During Strong Earthquakes Based on Empirical Estimation of Inelastic Restoring Force Characteristics of Members," Proceedings of the Fifth World Conference on Earthquake Engineering, Rome, Italy, June 1973, Vol. 2, pp. 2201-2210.

(9) Takizawa, H., "Non-Linear Models for Simulating the Dynamic Damaging Process of Low-Rise Reinforced Concrete Buildings During Severe Earthquakes," *Earthquake Engineering and Structural Dynamics,* John Wiley & Sons, Chichester, Sussex, England, Vol. 4, No. 1, July 1975, pp. 73-94.

(10) Aoyama, H., "Simple Nonlinear Models for the Seismic Response of Reinforced Concrete Buildings," Proceedings of the Review Meeting of the U.S.-Japan Cooperative Research Program in Earthquake Engineering, Honolulu, Hawaii, August 1975, pp. 291-309.

(11) Pique, J.R., "On the Use of Simple Models in Nonlinear Dynamic Analysis," Publication No. R76-43, Dept. of Civil Engineering, M.I.T., Cambridge, September 1976.

(12) Saiidi, M. and Sozen, M.A., "Simple and Complex Models for Nonlinear Seismic Response of Reinforced Concrete Structures," Report to the National Science Foundation, Dept. of Civil Engineering, University of Illinois, Urbana, August 1979.

(13) Giberson, M.F., "The Response of Nonlinear Multistory Structures to Earthquake Excitation," Earthquake Engineering Research Laboratory, California Institute of Technology, Pasadena, May 1967.

(14) Otani, S. and Sozen, M.A., "Behavior of Multistory Reinforced Concrete Frames during Earthquakes," Civil Engineering Studies, Structural Research Series No. 392, University of Illinois, Urbana, November 1972.

(15) Clough, R.W. and Johnston, S.B., "Effect of Stiffness Degradation on Earthquake Ductility Requirements," Proceedings, Japan Earthquake Engineering Symposium, Tokyo, October 1966, pp. 195-198.

(16) Takeda, T., Sozen, M.A., and Nielsen, N.N., "Reinforced Concrete Response to Simulated Earthquake," Journal of the Structural Division, ASCE, Vol. 96, ST12, December 1970, pp. 2557-2573.

(17) Takayanagi, T. and Schnobrich, W.C., "Computed Behavior of Reinforced Concrete Coupled Shear Walls," Civil Engineering Studies, Structural Research Series No. 434, University of Illinois, Urbana, December 1976.

(18) Emori, K. and Schnobrich, W.C., "Analysis of Reinforced Concrete Frame-Wall Structures for Strong Motion Earthquakes," Civil Engineering Studies, Structural Research Series No.457, University of Illinois, Urbana, December 1978.

(19) Fintel, M. and Ghosh, S.K., "Case Study of Seismic Resistance of a 16-Story Coupled Wall Structure Using Inelastic Dynamic Analysis and an Energy Dissipation Approach," Portland Cement Association, Skokie, Illinois, April 1979, 67.

(20) Chen, P.F. and Powell, G.H., "Generalized Plastic Hinge Concepts for 3D Beam-Column Elements," EERC Report No. 82/20, University of California, Berkeley, November 1982.

(21) Clough, R.W., Benuska, K.L., and Wilson,E.L., "Inelastic Earthquake Response of Tall Buildings," Proceedings of the Third World Conference on Earthquake Engineering, Auckland and Wellington, New Zealand, January 1965, Vol. II, pp. 68-84.

(22) Clough, R.W., Benuska, K.L., and T.Y. Lin and Associates, "F.H.A. Study of Seismic Design Criteria for High-Rise Buildings," HUD TS-3, U.S. Housing and Urban Development, Federal Housing Administration, Washington D.C., August 1966.

(23) Clough, R.W. and Benuska, K.L., "Nonlinear Earthquake Behavior of Tall Buildings," Journal of the Engineering Mechanics Division, A.S.C.A., Vol. 93, No. EM3, June 1967, pp. 129-146.

(24) Mahin, S.A., "An Evaluation of the Seismic Response of Reinforced Concrete Buildings," Ph.D. Dissertation, Dept. of Civil Engineering, University of California, Berkeley 1974.

(25) Anderson, J.C. and Bertero, V.V., "Seismic Behavior of Multistory Frames by Different Philosophies," EERC Report No. 69/11, University of California, Berkeley, October 1969.

(26) Powell, G.H. and Row, D.G., "Influence of Analysis and Design Assumptions on Computed Inelastic Response of Moderately Tall Frames," EERC Report No. 76/11, University of California, Berkeley, April 1976.

(27) Klingner, R.E. and Bertero, V.V., "Infilled Frames in Earthquake-Resistant Construction," EERC Report No. 76/32, University of California, Berkeley, December 1976.

(28) Takizawa, H., "Notes on Some Basic Problems in Inelastic Analysis of Planar R/C Structures (Parts I and II)," Transactions of the Architectural Institute of Japan, No. 240, February 1976, pp. 51-62; No. 241, March 1976, pp. 65-77.

(29) Hsu, L.W., "Behavior of Multi-Story Reinforced Concrete Walls During Earthquakes," Ph.D. Thesis, Dept. of Civil Engineering, University of Illinois, Urbana 1974.

(30) Umemura, H. and Takizawa, H., "Strong Motion Response Analysis of R/C Frames," Transactions of the Architectural Institute of Japan, Extra, 1972.10.

(31) Meyer, C., Arzoumanidis, S.G., and Shinozuka, M., "Earthquake Reliability of Reinforced Concrete Buildings," Proceedings of the Symposium on Probabilistic Methods in Structural Engineering, Edited by Shinozuka, M. and Yao, J.T.P., ASCE, New York 1981, pp. 378-398.

(32) Arzoumanidis, S.G. and Meyer, C., "Modeling Reinforced Concrete Beams Subjected to Cyclic Loads," Dept. of Civil Engineering and Engineering Mechanics, Columbia University, New York, Report No. NSF-PFR-79-24695-CU-1, 1981.

(33) Soleimani, D., Popov, E.P., and Bertero, V.V., "Nonlinear Beam Model for R/C Frame Analysis," Seventh Conference on Electronic Computation, ASCE, St. Louis, Missouri, August 6-8, 1979.

(34) Agrawal, A.B., Jaeger, L.G., and Mufti, A.A., "Crack Propagation and Plasticity of Reinforced Concrete Shear Walls under Monotonic and Cyclic Loading," Conference on Finite Element Methods in Engineering, Adelaide, Australia, December 1976.

(35) Schnobrich, W.C., "Behavior of Reinforced Concrete Structures Predicted by the Finite Element Method," An International Journal, Computers and Structures, Vol. 7, No. 3, June 1977, pp.365-376.

(36) Suidan, M. and Schnobrich, W.C., "Finite Element Analysis of Reinforced Concrete," Journal of the Structural Division, ASCE, Vol. 99, No.ST10, Proc. Paper 10081, October 1973, pp. 2109-2122.

(37) Yuzugullu, O. and Schnobrich, W.C., "A Numerical Procedure for the Determination of the Behavior of a Shear Wall Frame System," Journal of the ACI, Proc., Vol. 70, No. 7, July 1973, pp. 474-479.

(38) Cervenka ,V., "Inelastic Finite Element Analysis of Reinforced Concrete Panels Under In-Plane Loads," Ph.D. Dissertation, Dept. of Civil Engineering, University of Colorado, Boulder, 1970.

(39) Mark, K.M.S., and Roesset, J.M., "Nonlinear Dynamic Response of Reinforced Concrete Frames," Publication R76-38, Department of Civil Engineering, M.I.T., August 1976.

(40) Iding, R., Bresler, B., and Nizamuddin, Z., "Fires-RC II, A Computer Program for the Fire Response of Structures-Reinforced Concrete Frames - Revised Edition," Fires Research Group, University of California, Berkeley, July 1977.

(41) Bazant, Z.P., and Bhat, P.D., "Prediction of Hysteresis of Reinforced Concrete Members," Journal of the Structural Division, ASCE, Vol. 103, No. ST1, January 1977, pp. 153-167.

(42) Bazant, Z.P. and Bhat, P.D., "Endochronic Theory of Inelasticity and Failure of Concrete," Journal of the Engineering Mechanics Division, ASCE, Vol. 102, No. EM4, Proc. Paper 12360, August 1976, pp. 701-722.

(43) Filippou, F.C., Popov, E.P., and Bertero, V.V., "Effects of Bond Deterioration on Hysteretic Behavior of Reinforced Concrete Joints," EERC Report No. 83/19, University of California, Berkeley, August 1983.

(44) Kaba, S.A. and Mahin S.A., "Interactive Computer Analysis Methods for Predicting the Inelastic Cyclic Behaviour of Structural Sections," EERC Report No. 83/18, University of California, Berkeley, July 1983.

(45) Ma, S.M., Bertero, V.V., and Popov, E.P., "Experimental and Analytical Studies of the Hysteretic Behavior of Reinforced Concrete Rectangular and T-Beams," EERC Report No. 76/2, University of California, Berkeley, May 1976.

(46) Mahasuverachai, M. and Powell, G.H., "Inelastic Analysis of Piping and Tubular Structures," EERC Report No. 82/27, University of California, Berkeley, November 1982.

(47) Mahin, S.A. and Lin, J. ,"Construction of Inelastic Response Spectra for Single-Degree-of-Freedom Systems," EERC Report No. 83/17, University of California, Berkeley, July 1983.

(48) Gulkan, P. and Sozen, M.A., "Response and Energy Dissipation of Reinforced Concrete Frames Subjected to Strong Base Motions," Civil Engineering Studies, Structural Research Series No. 377, University of Illinois, Urbana, May 1971.

(49) Thom, C.W., "The Effect of Inelastic shear on the Seismic Response of Structures," Ph.D. Dissertation, Dept. of Civil Engineering, University of Auckland, New Zealand, March 1983.

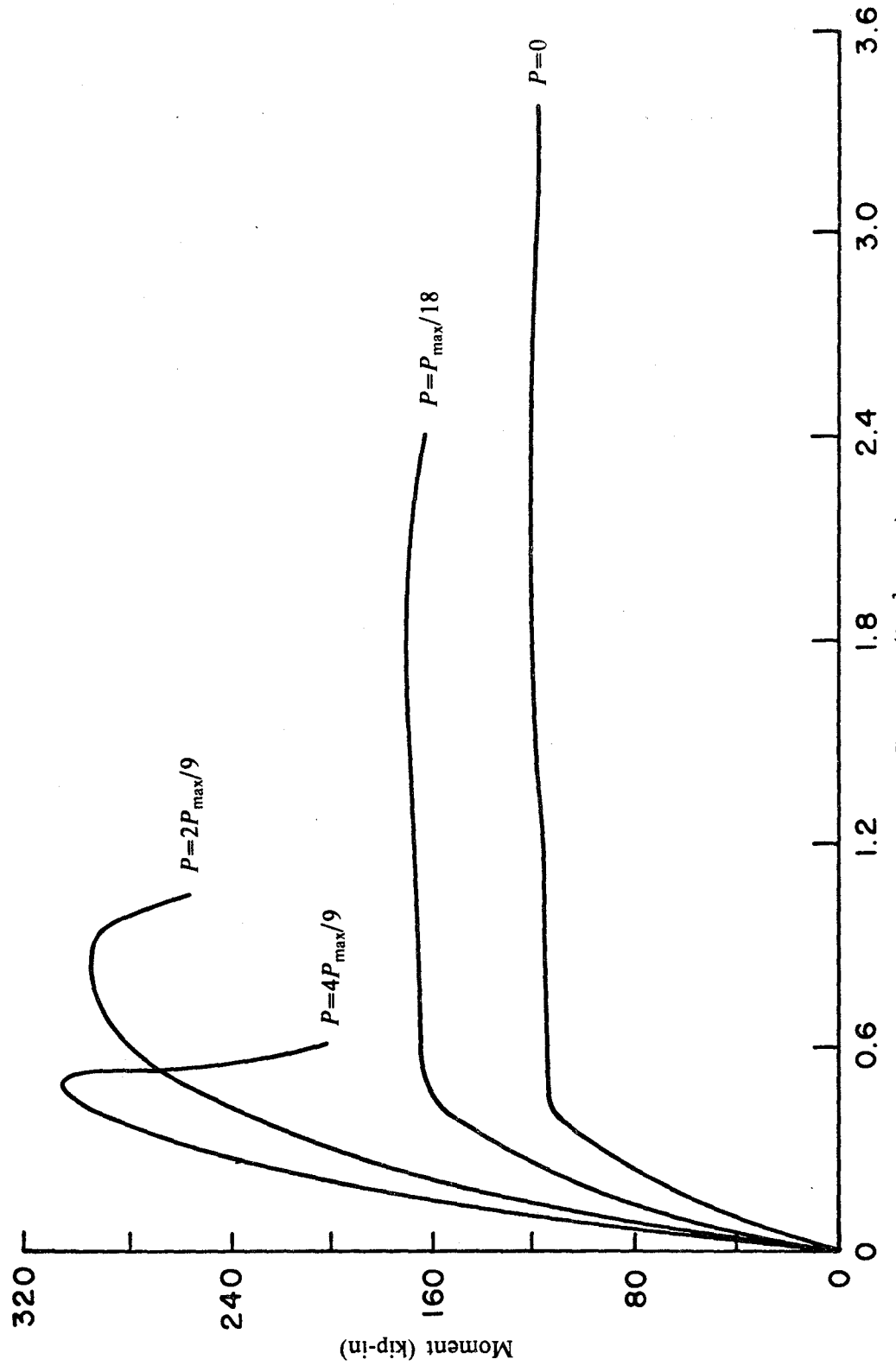

Fig. 1.1 Influence of axial load on section strength and stiffness

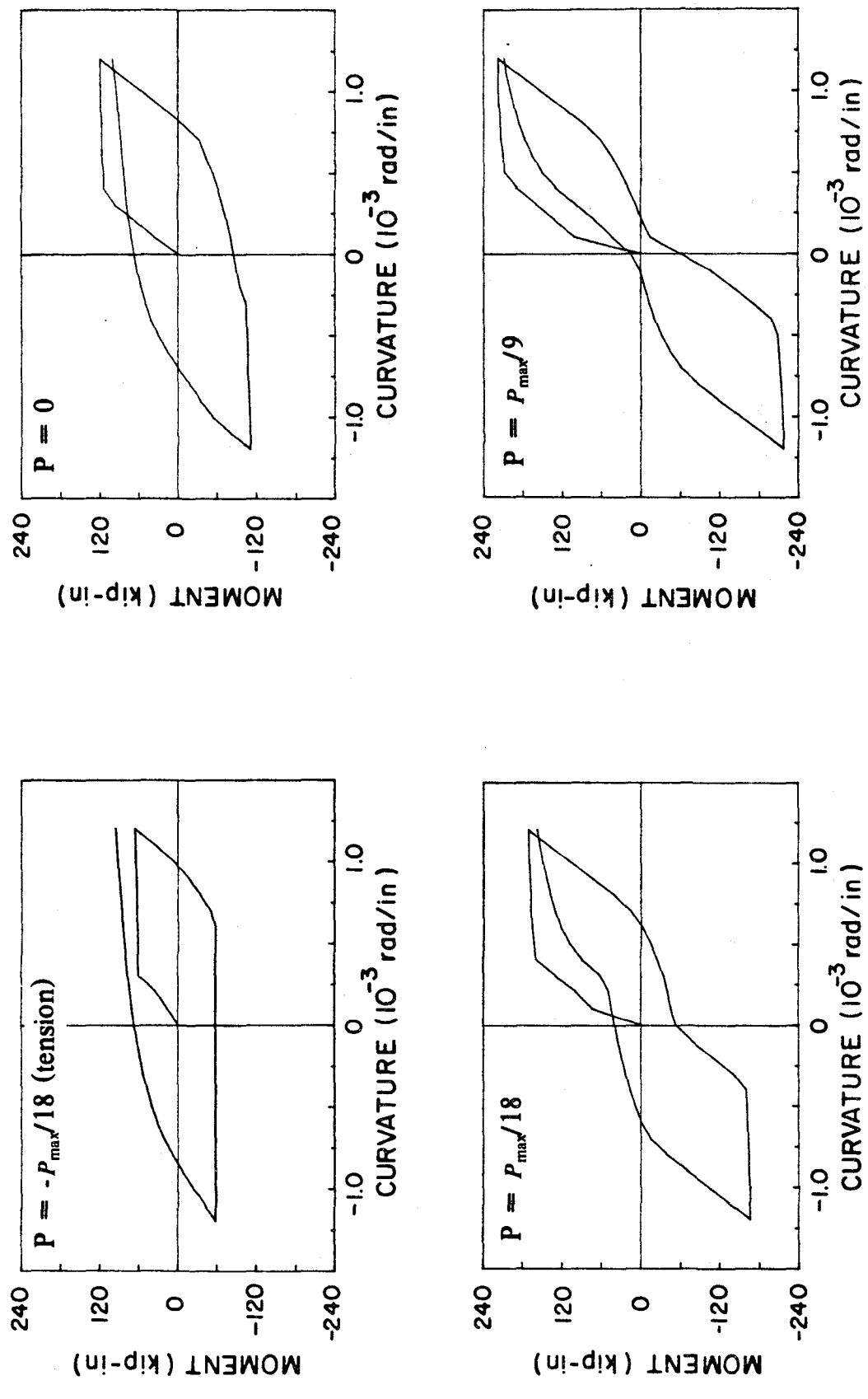

Fig. 1.2 Effect of axial load on cyclic moment-curvature behaviour

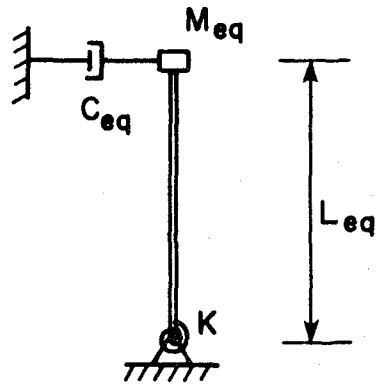

Fig. 1.3 The Q-Model

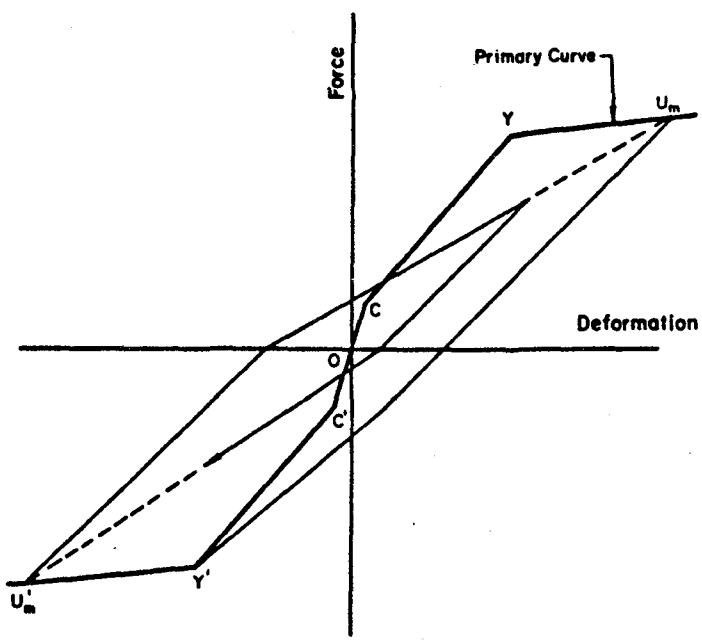

Fig. 1.5 Takeda hysteresis model

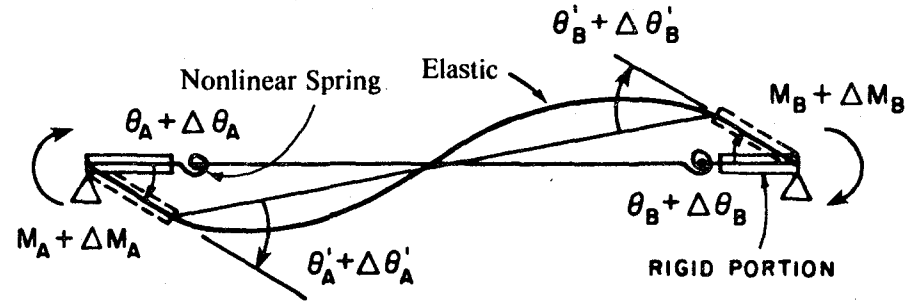

Fig. 1.4 Single component or concentrated spring model

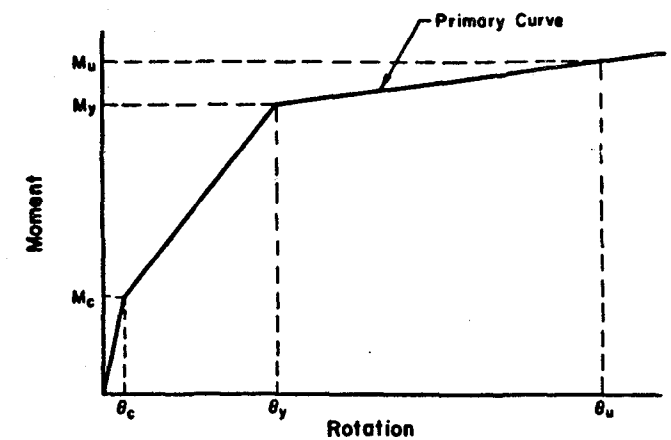

Fig. 1.6 Trilinear model - primary curve

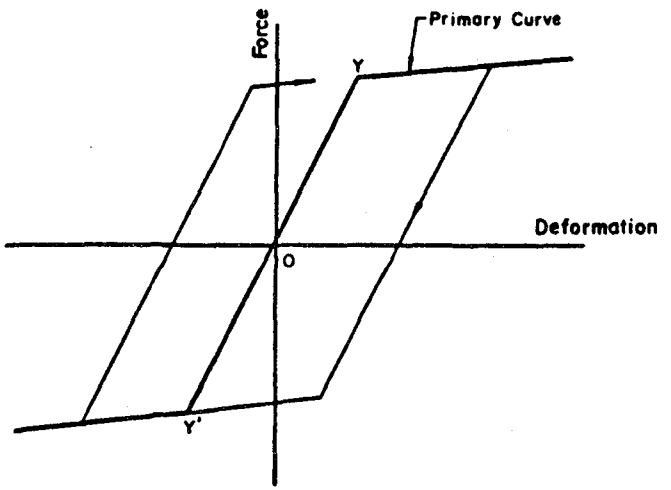

Fig. 1.7 Bilinear hysteresis model

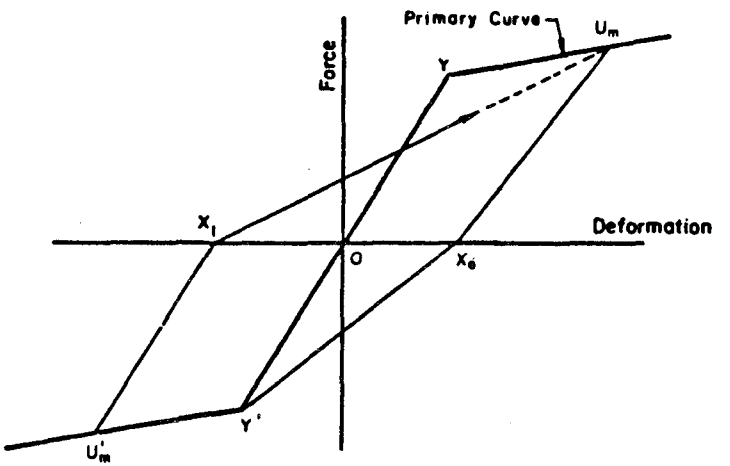

Fig. 1.8 Otani hysteresis model

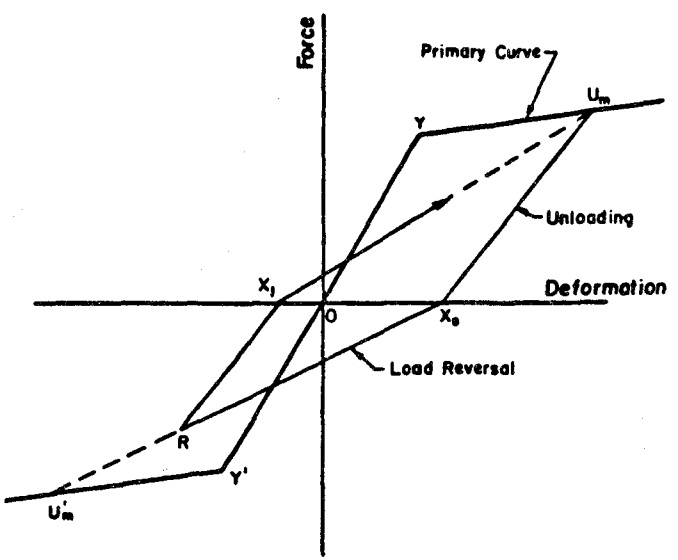

Fig. 1.9 Q-Hyst model

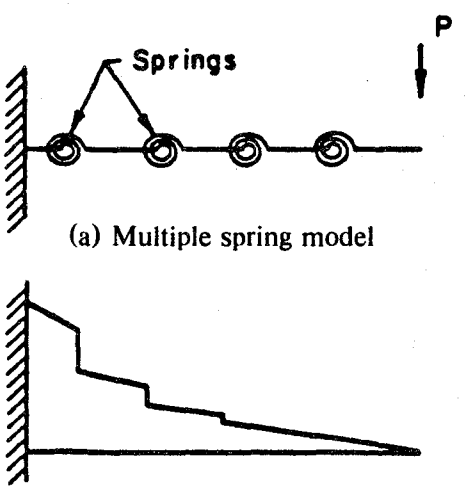

(a) Multiple spring model

(b) Idealized curvature distribution

Fig. 1.10 Multiple spring element for modelling wall members

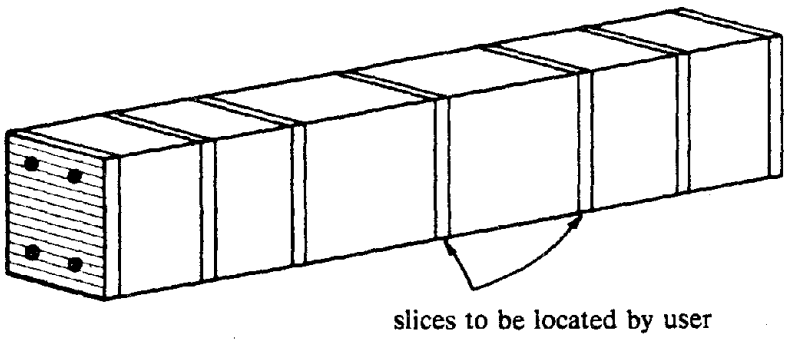

Fig. 2.1 Slice locations along the element length

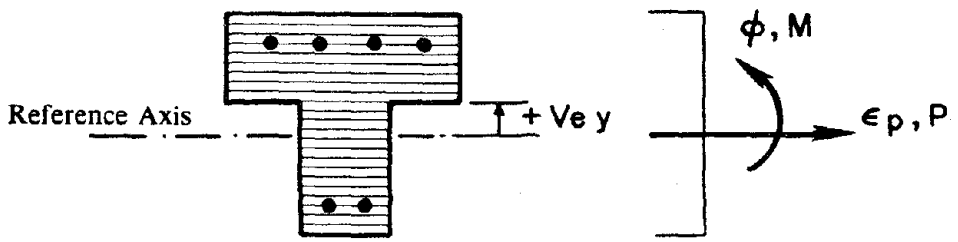

Fig. 2.2 Typical slice showing fibers and sign convention

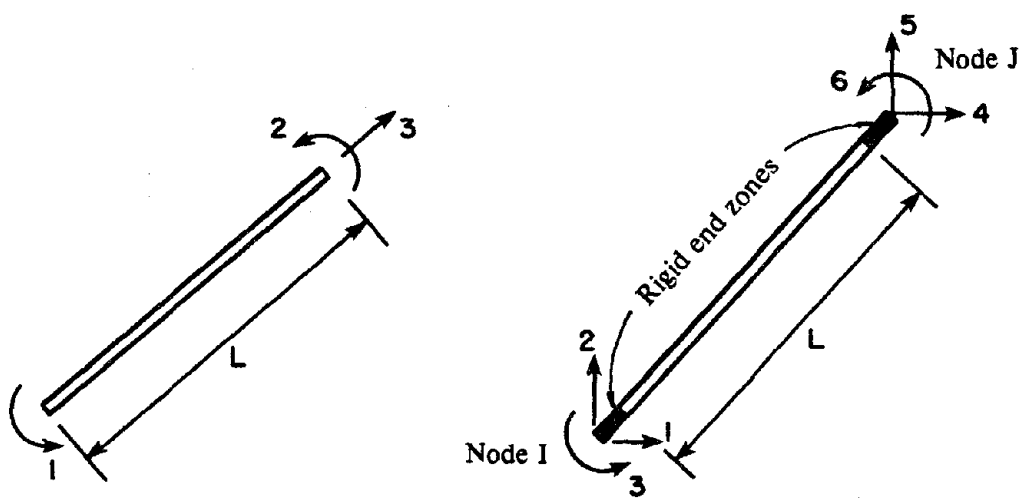

(a) Local D.O.F.'s (b) Global D.O.F.'s

Fig. 2.3 Local and global degrees of freedom

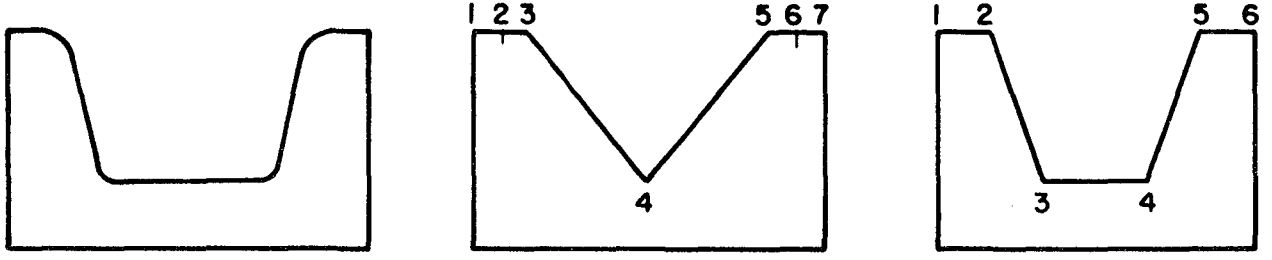

(a) Actual flexibility variation

(b) Flexibility variation using 7 slices

(c) Superior flexibility variation using only 6 slices

Fig. 2.4 The importance of a suitable selection of slice locations

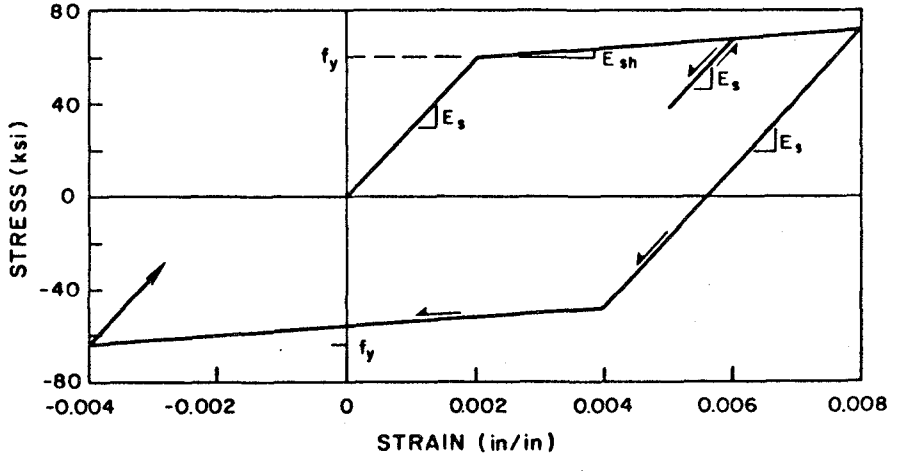

Fig. 2.5 Bilinear steel model

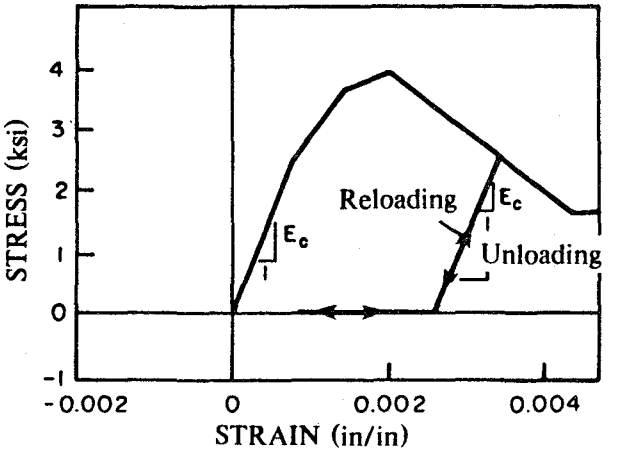

Fig. 2.6 Concrete model

$$P_S = P$$

$$M_S = (M_1 + M_2)\, x/L - M_1$$

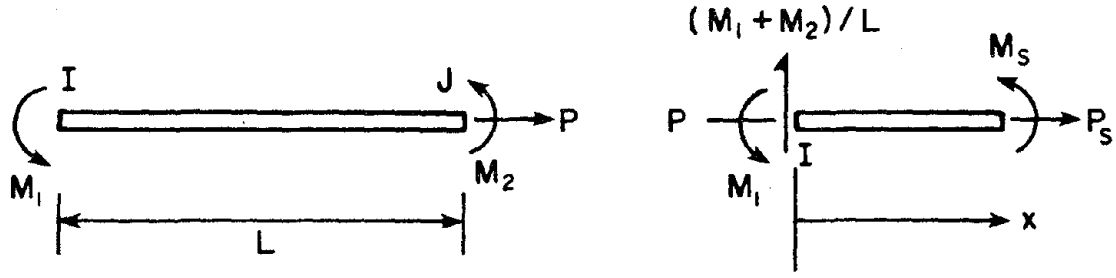

Fig. 2.7 Relating section forces to member forces

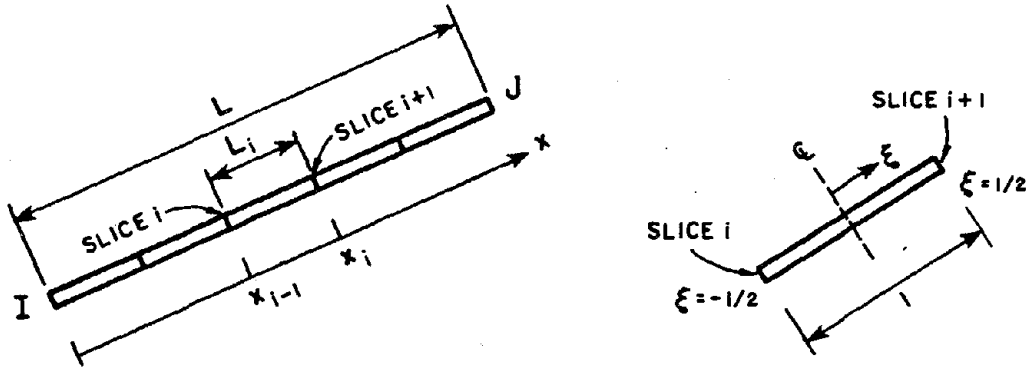

$$\xi = \frac{x - 0.5\,(x_{i-1} + x_i)}{L_i}$$

Fig. 2.8 Transformation to natural coordinates

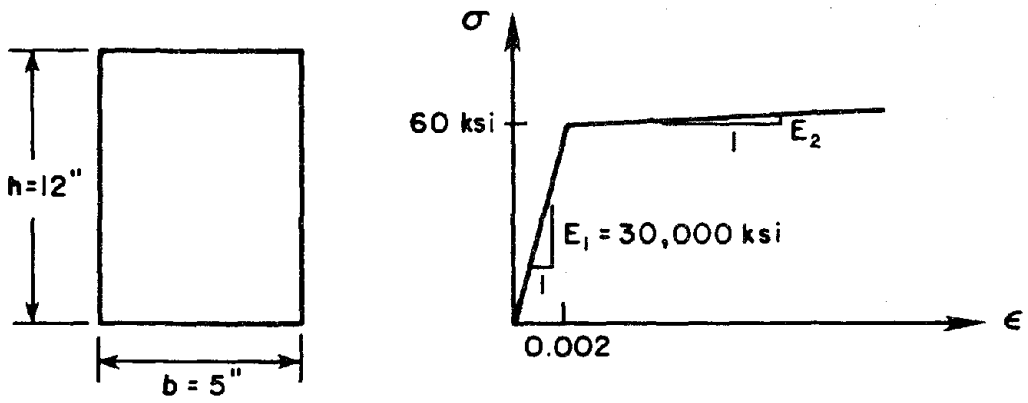

(a) Section geometry and assumed stress-strain relation

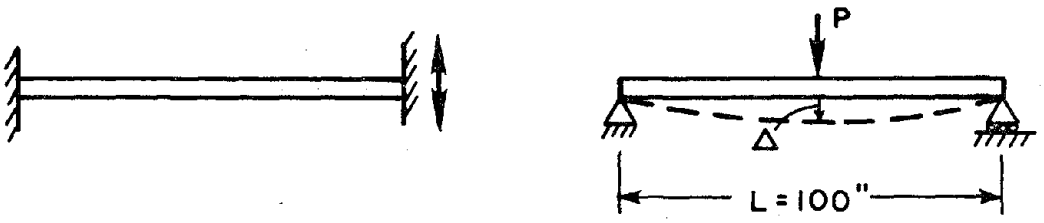

(b) Displacement controlled loading

(c) Equivalent loading

Fig. 3.1 Section geometry, material properties and loading configuration

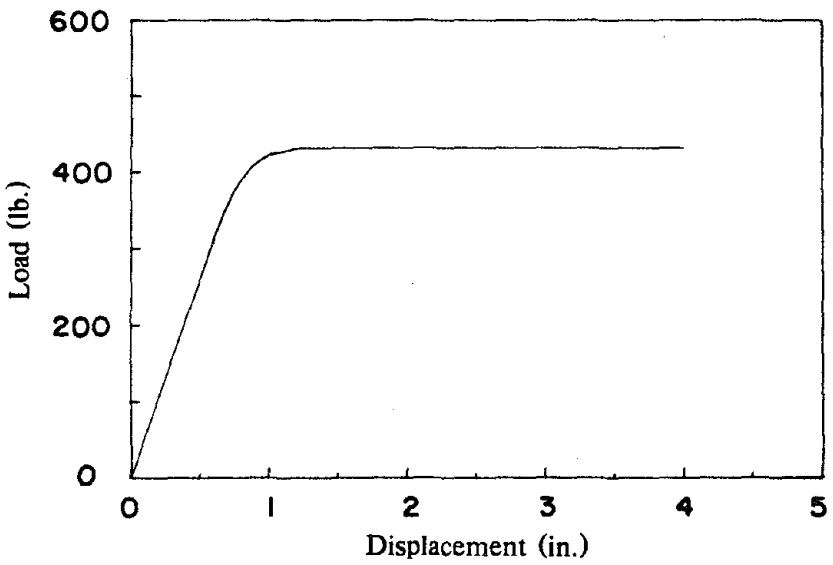

Fig. 3.2 Theoretical load-displacement curve assuming EPP steel

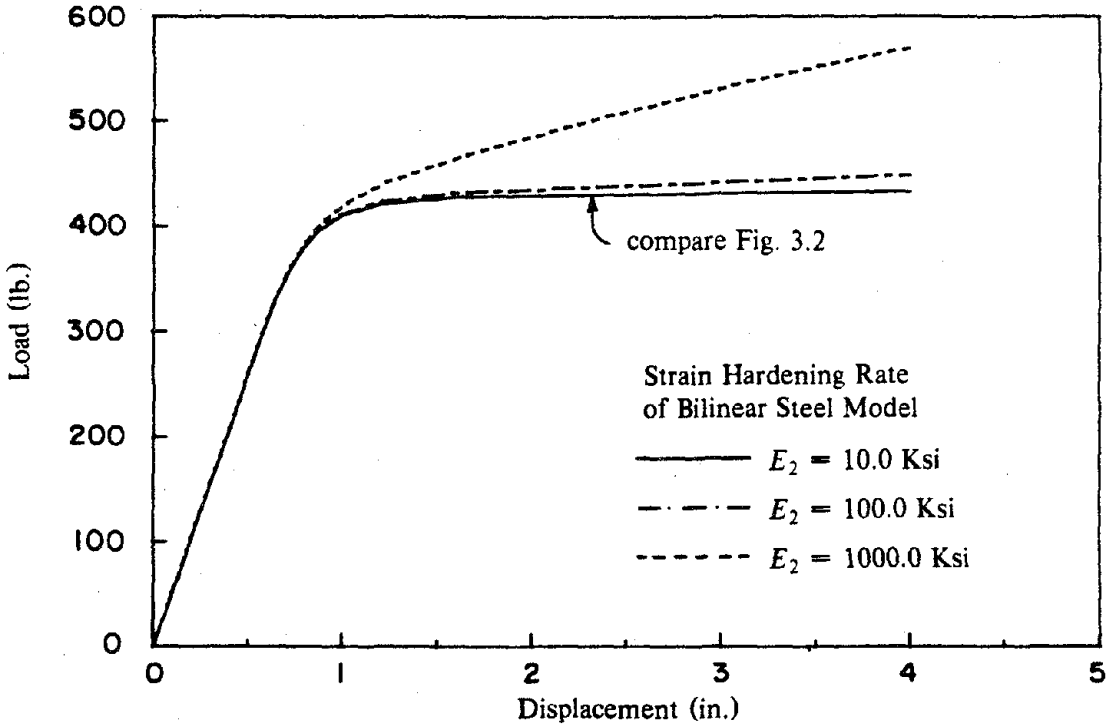

Fig. 3.3 Influence of rate of strain hardening (second slope of stress-strain curve)

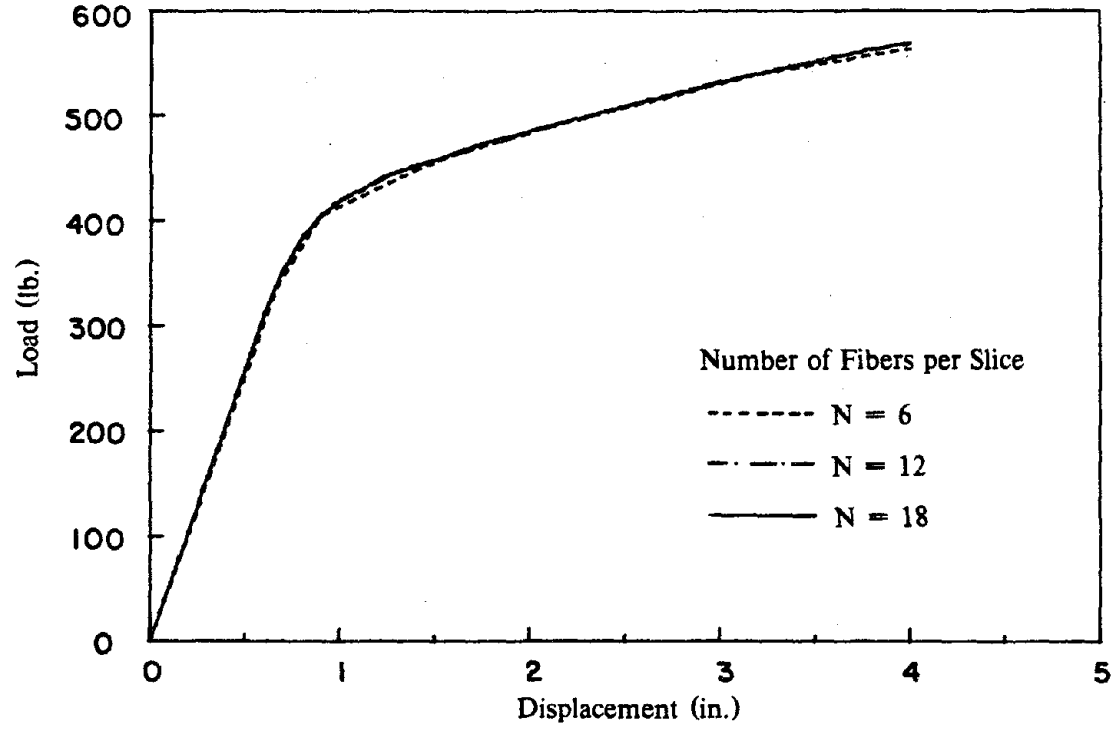

Fig. 3.4 Influence of number of fibers per slice used to discretize the section

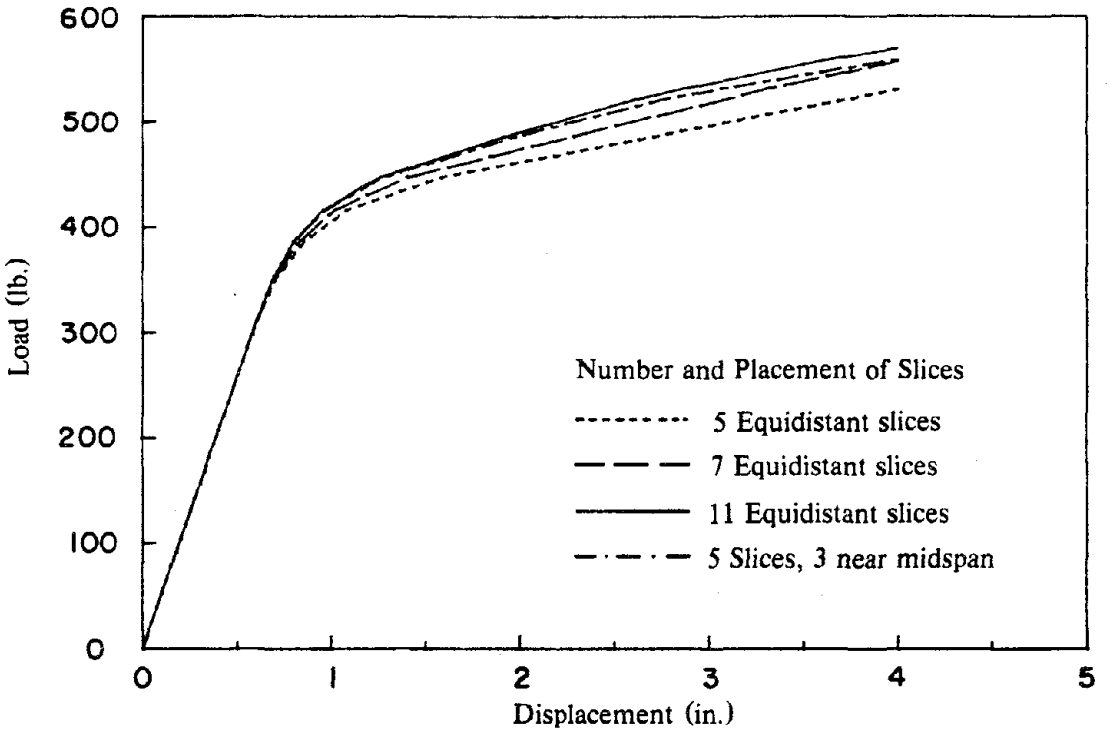

Fig. 3.5 Influence of number and position of slices along the member

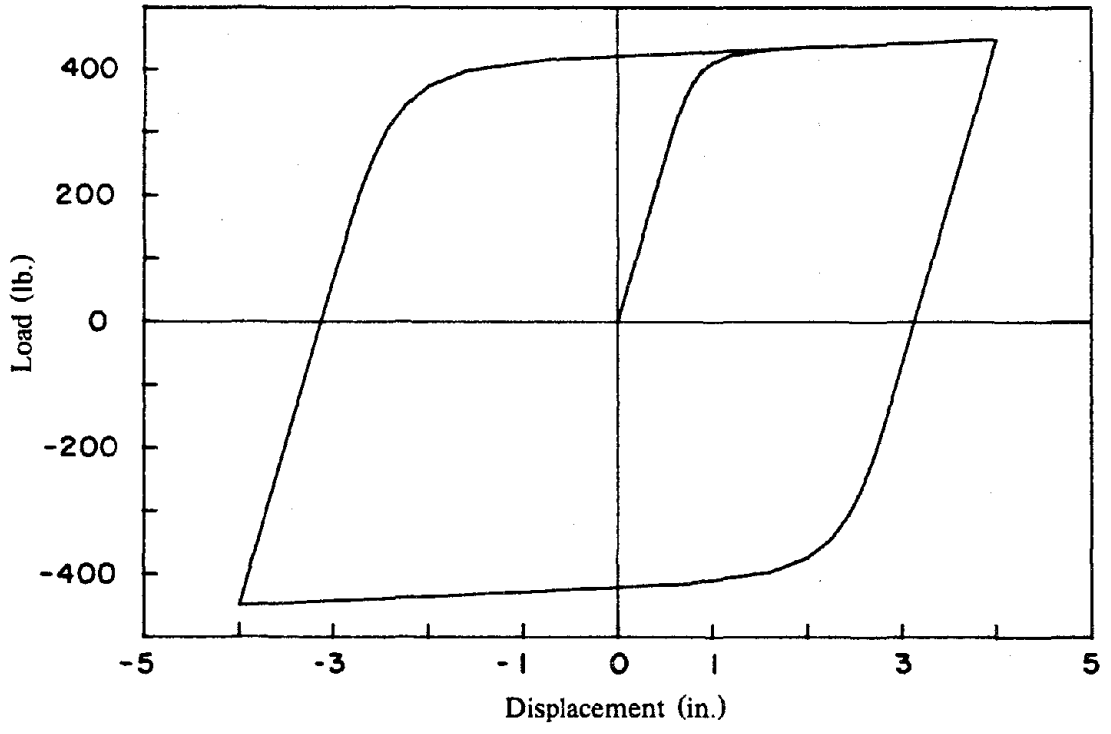

Fig. 3.6 Cyclic load-displacement curve using bilinear steel model

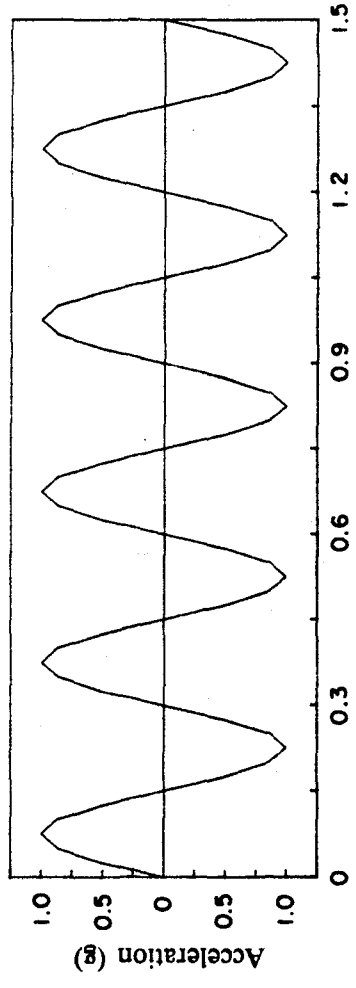

Fig. 3.7 Acceleration record used to analyze elastic column

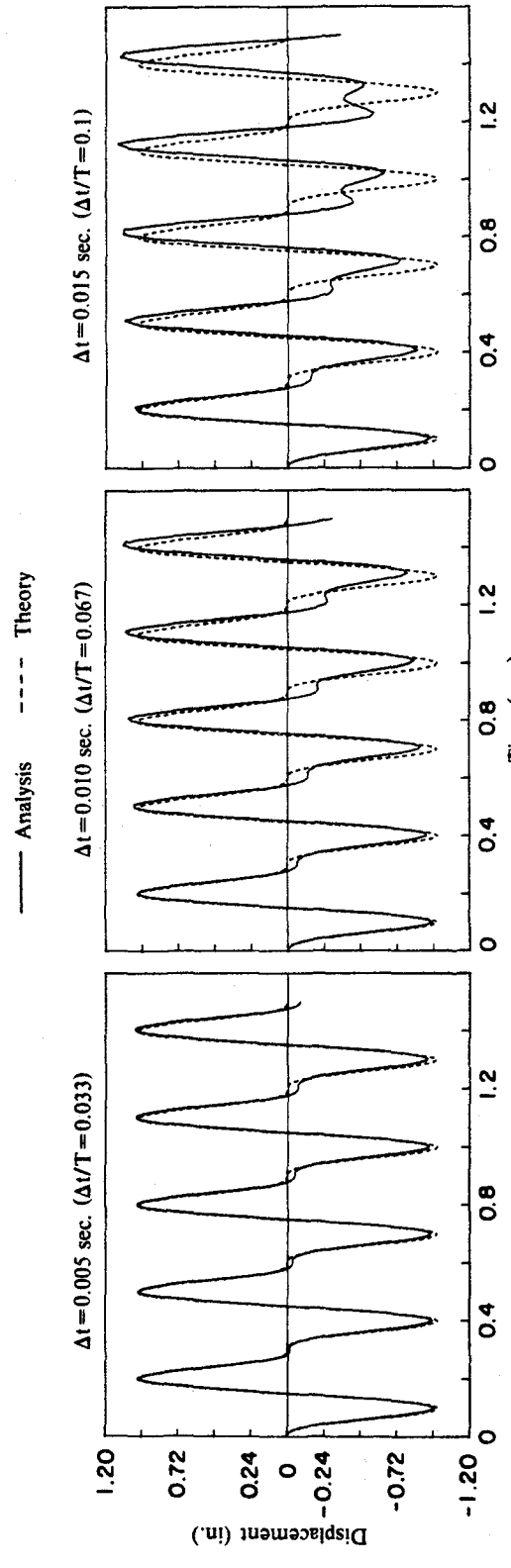

Fig. 3.8 Influence of the analysis time step used

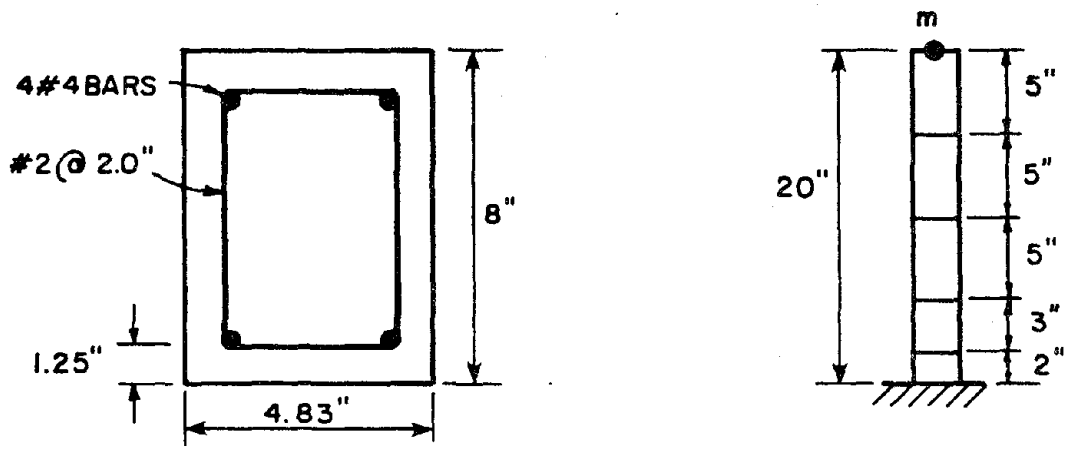

(a) Section Geometry

(b) Column Showing Standard Slice Spacing

Fig. 4.1 Example column

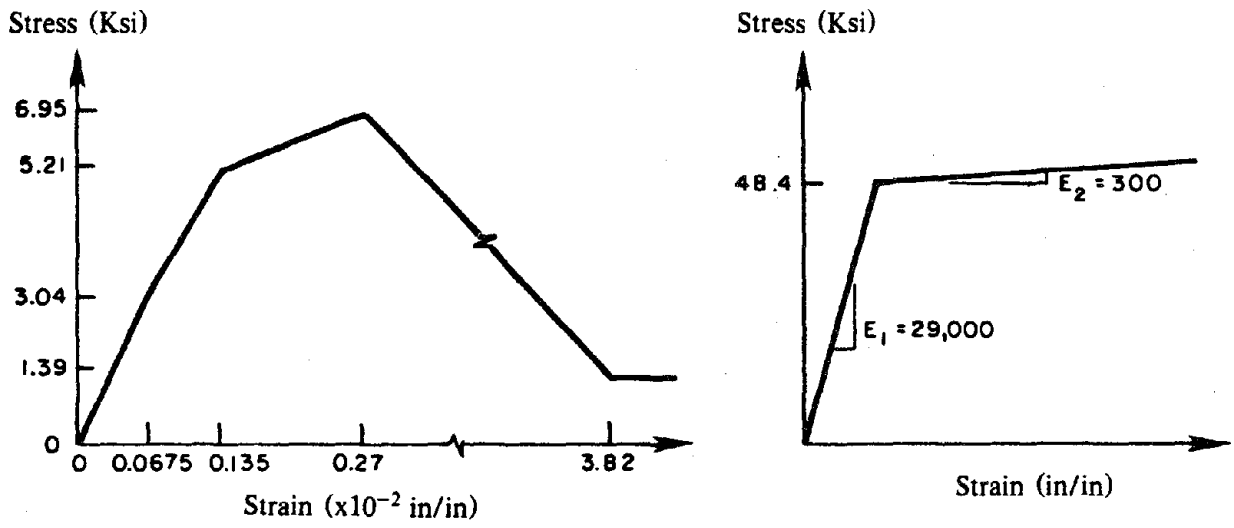

(a) Concrete

(b) Steel

Fig. 4.2 Idealized material properties of example column

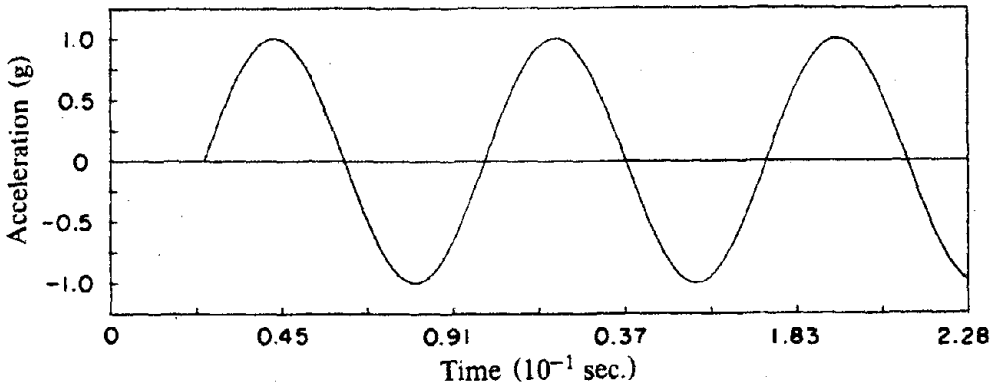

Fig. 4.3 Acceleration record used to analyze reinforced concrete column

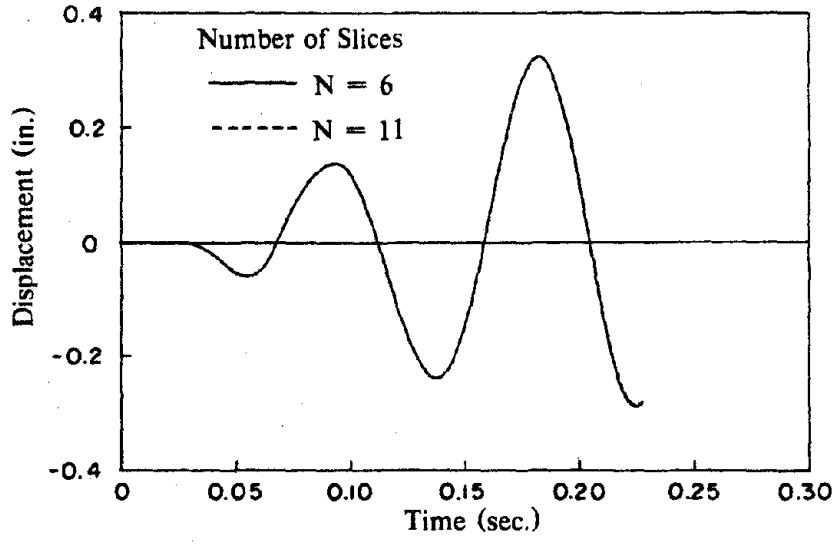

(a) Tip Displacement History

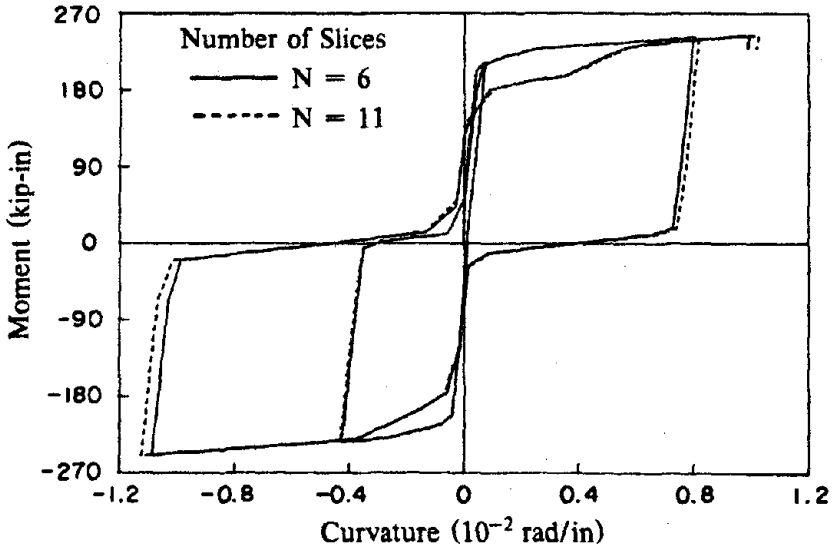

(b) Base moment-curvature history

Fig. 4.4 Analysis of reinforced concrete column using 6 and 11 slices

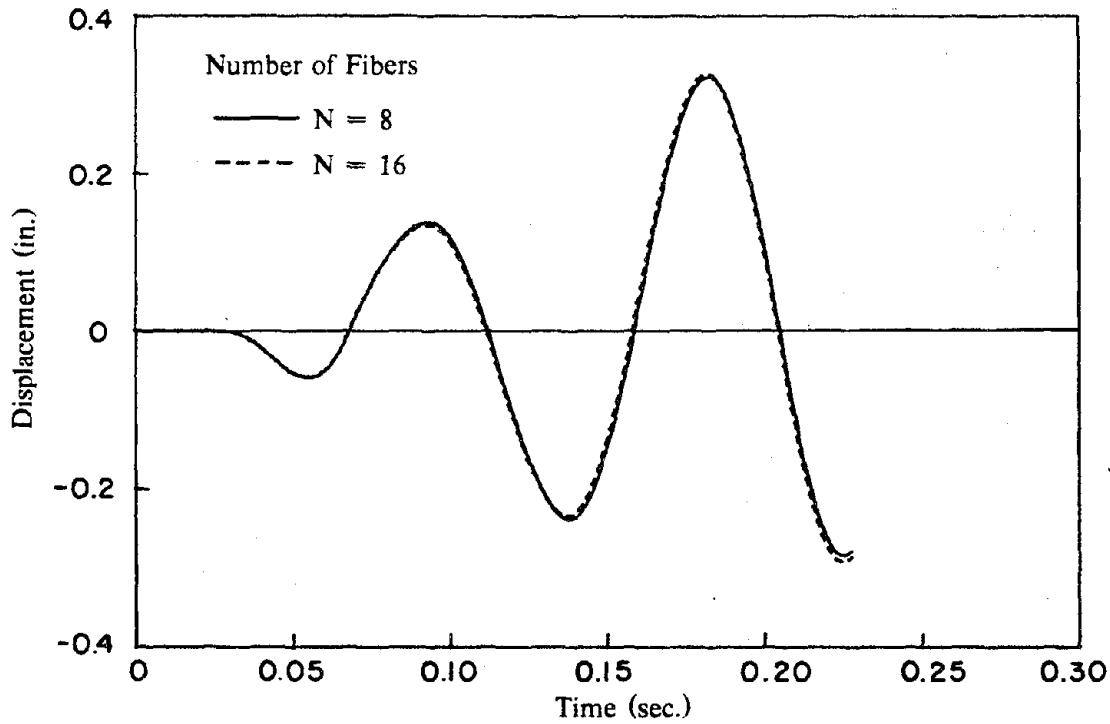

(a) Tip Displacement History

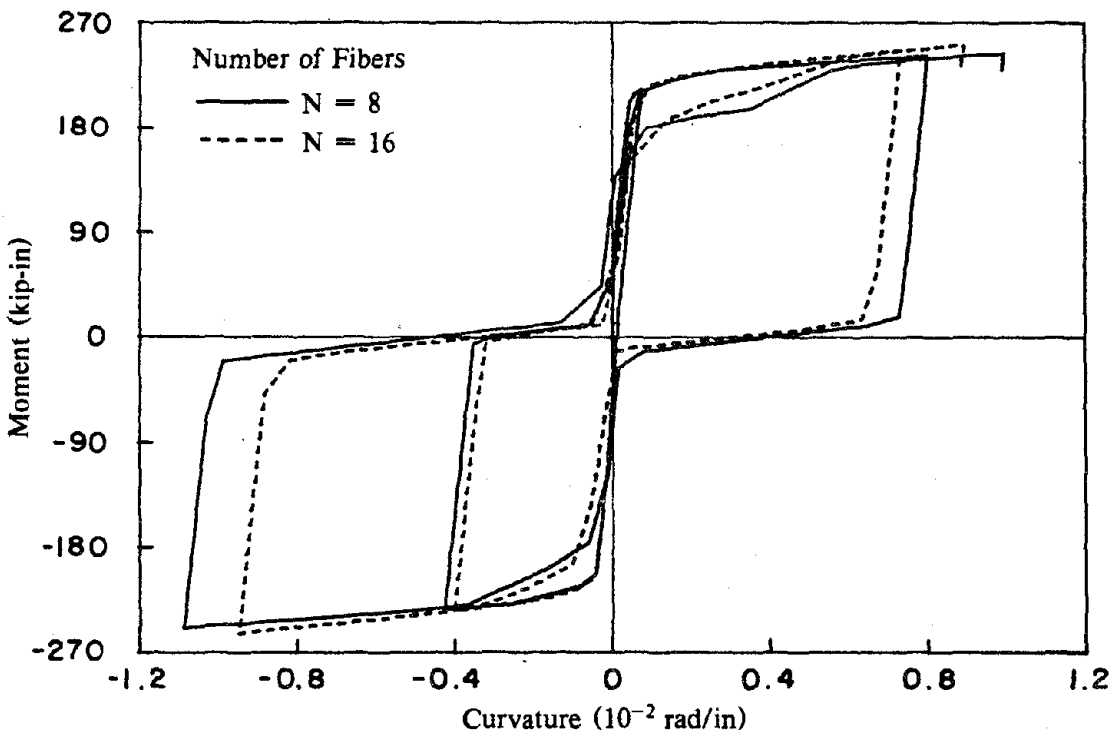

(b) Base moment-curvature history

Fig. 4.5 Analysis of reinforced concrete column using 8 and 16 fibers per slice

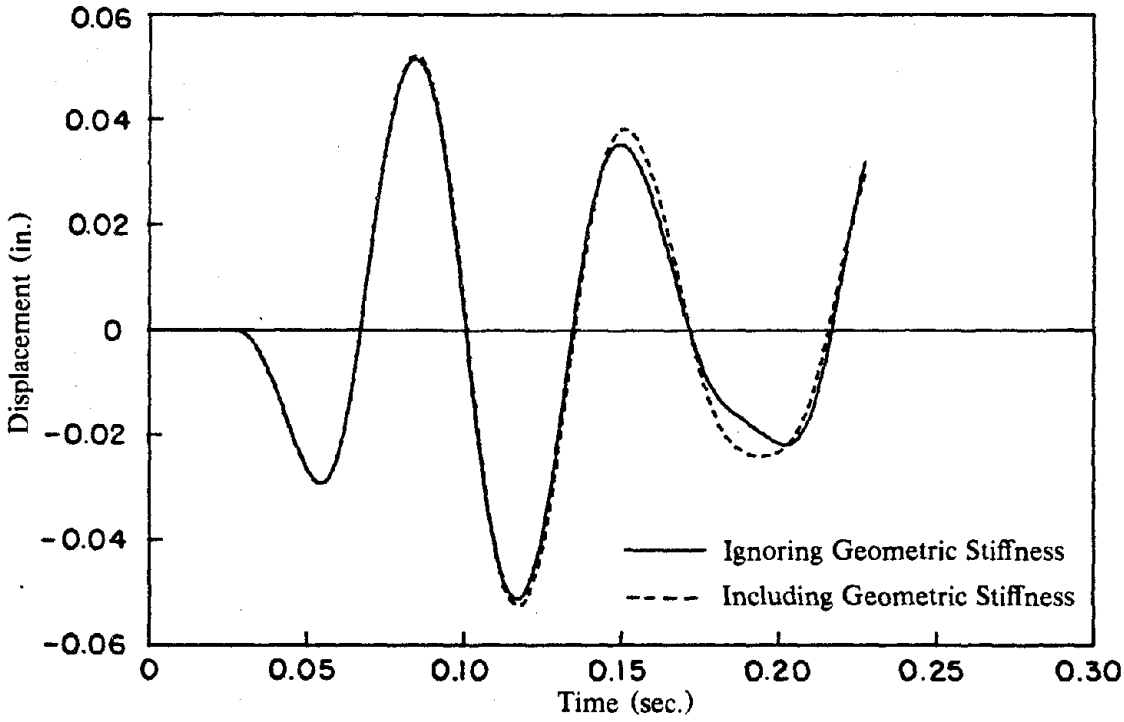

Fig. 4.6 Including geometric stiffness in the analysis of a reinforced concrete column

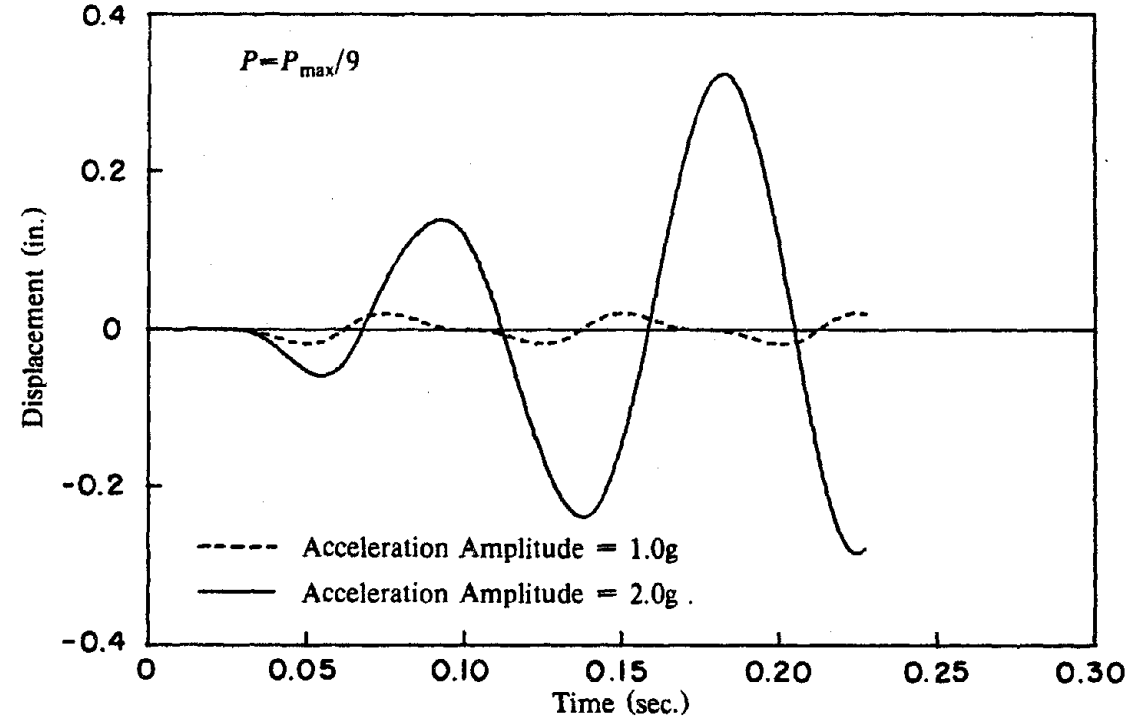

Fig. 4.7 Analysis of reinforced concrete column using different acceleration amplitudes

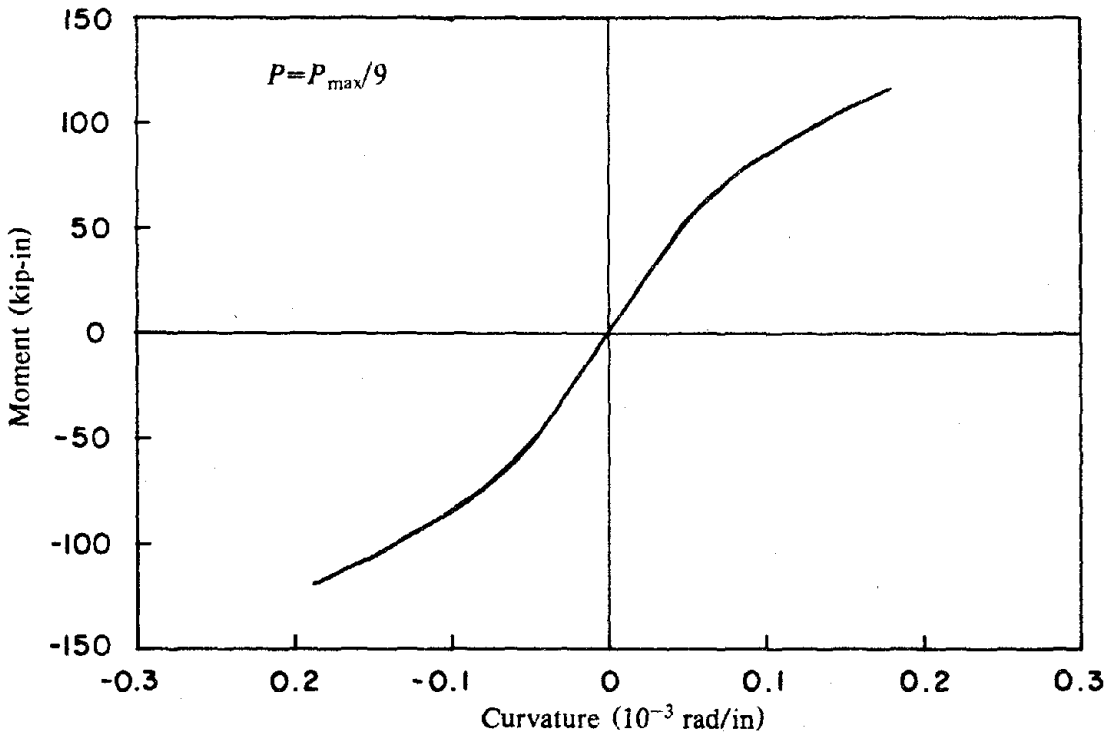

(a) Acceleration Amplitude = 1.0g

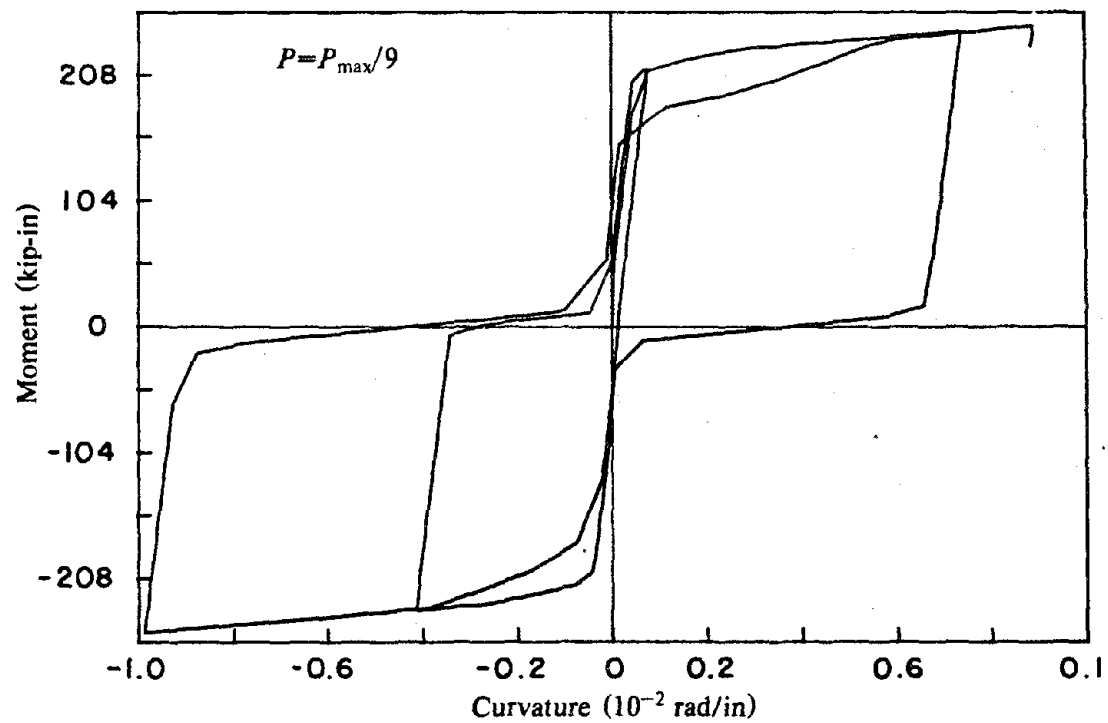

(b) Acceleration Amplitude = 2.0g

Fig. 4.8 Moment-curvature history using different acceleration amplitudes

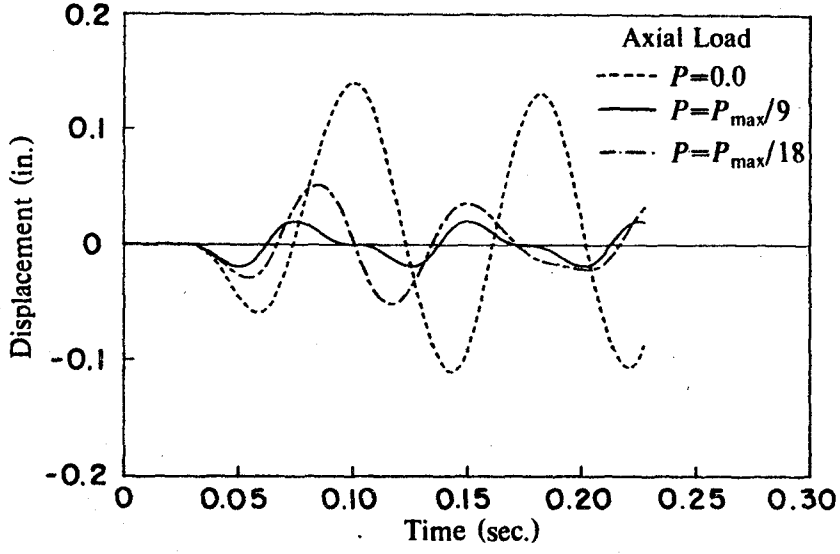

(a) Displacement histories for various axial loads

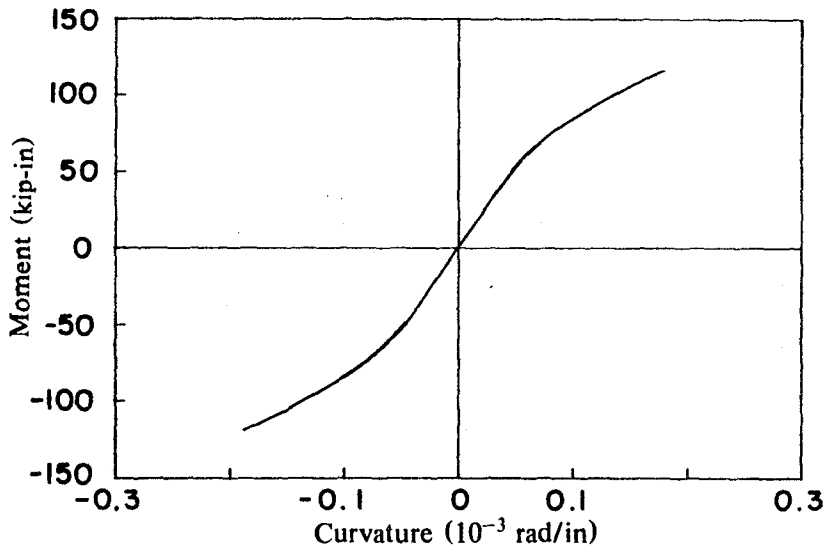

(b) Moment-curvature history for axial load = $P_{max}/9$

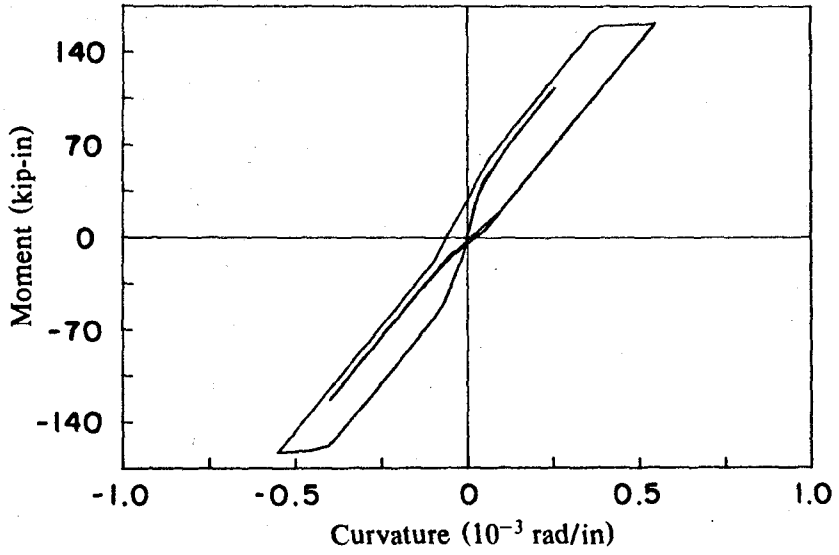

(c) Moment-curvature history for axial load = $P_{max}/18$

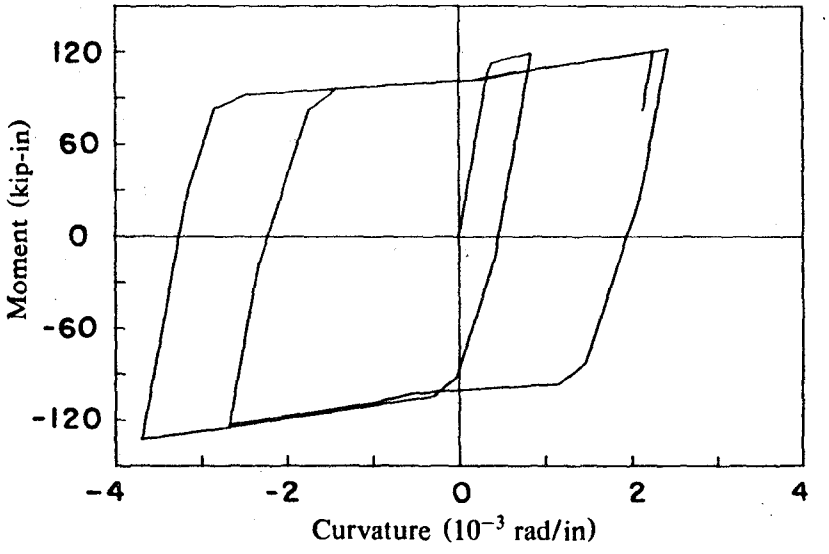

(d) Moment-curvature history for axial load = 0.0

Fig. 4.9 Analysis of reinforced concrete column subjected to different axial loads

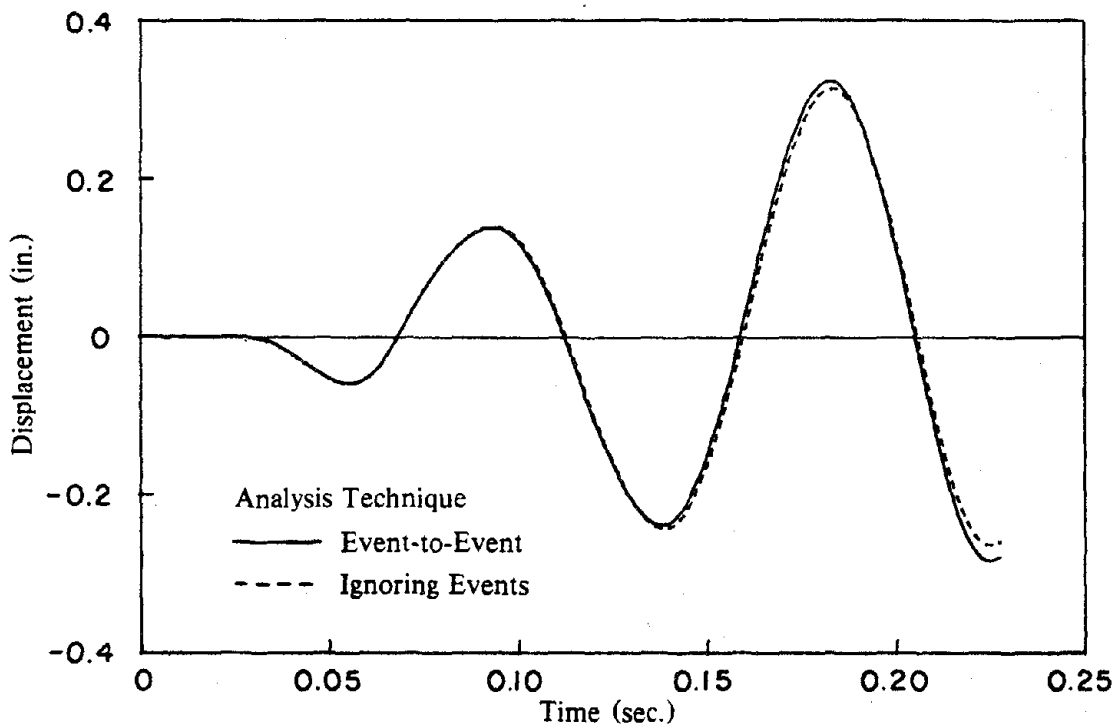

(a) Tip displacement history

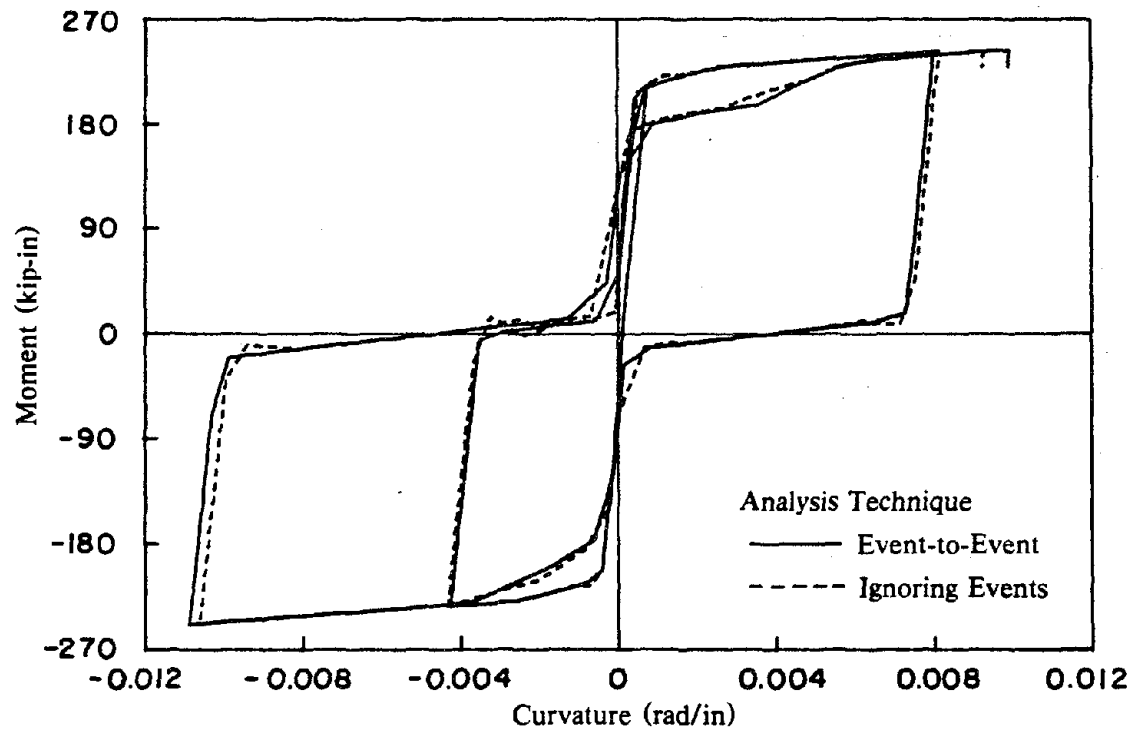

(b) Base moment-curvature history .

Fig. 4.10 Effect of ignoring all changes in fiber stiffness between steps

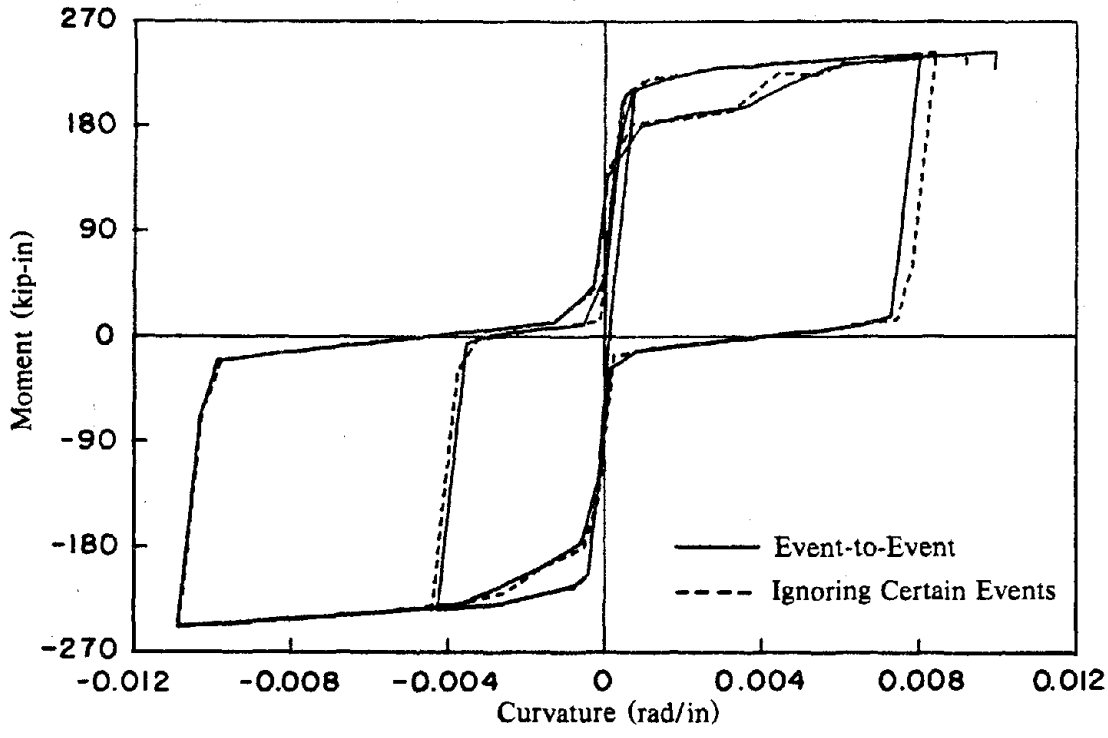

(a) Base moment-curvature history

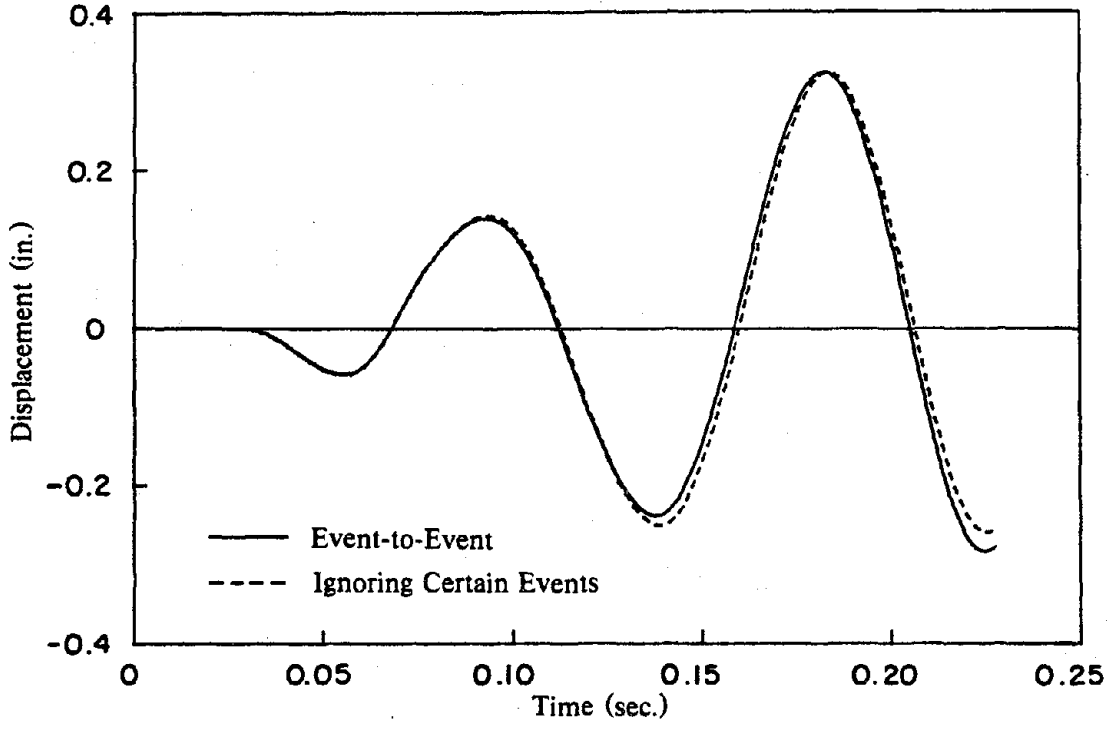

(b) Tip displacement history

Fig. 4.11 Effect of ignoring certain changes in fiber stiffness between steps

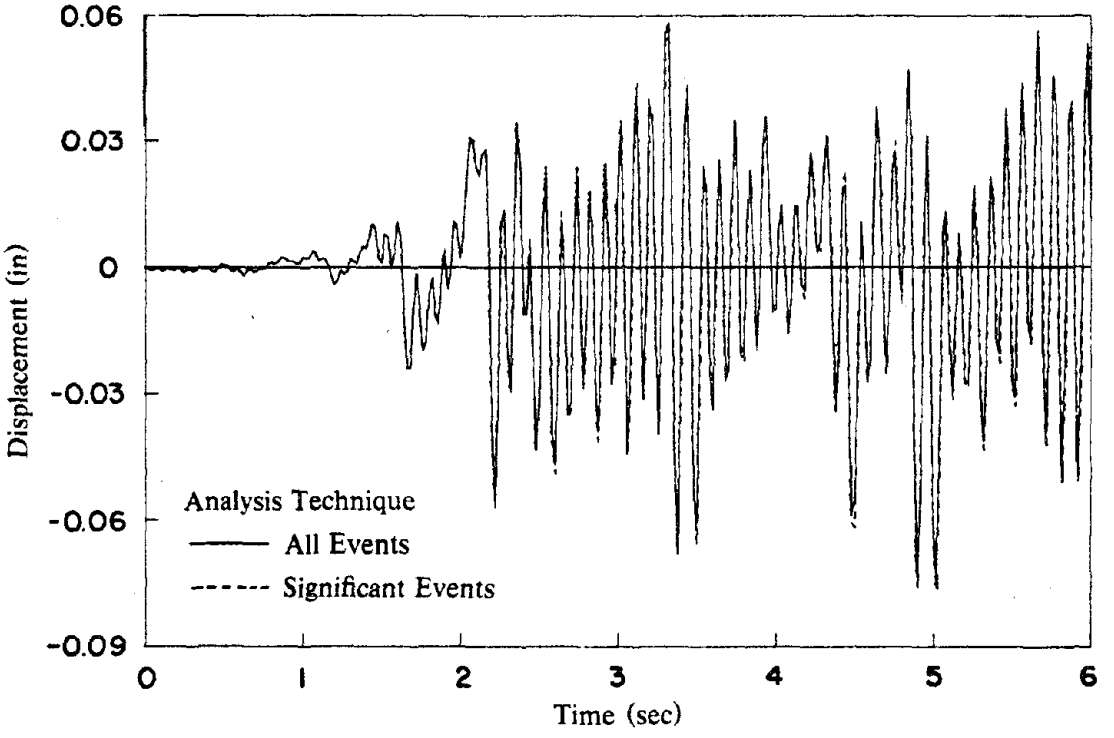

Fig. 4.12 Response to El-Centro considering all events and significant events

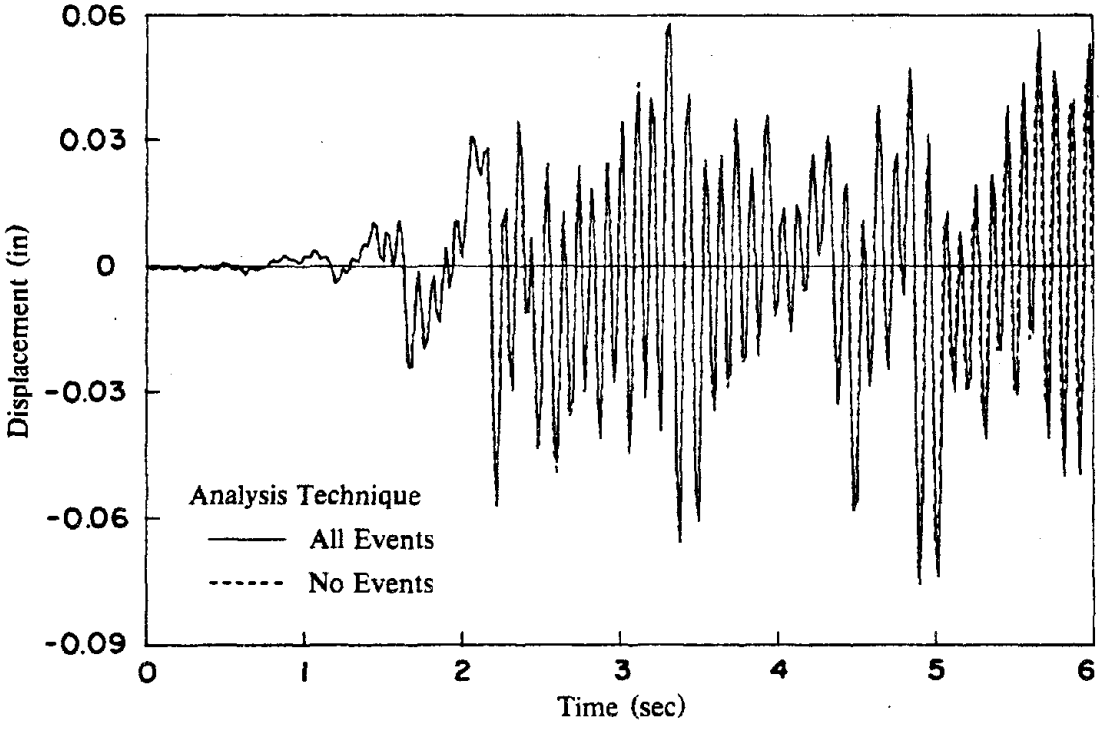

Fig. 4.13 Response to El-Centro considering all events and no events

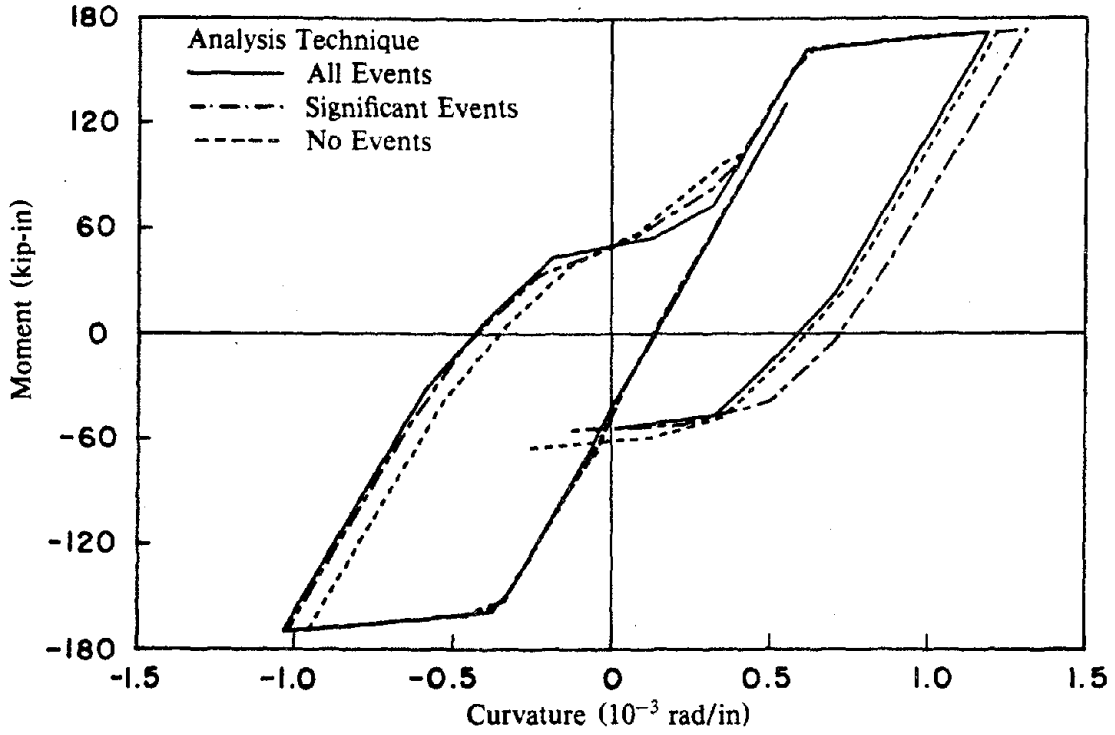

Fig. 4.14 Hysteretic loop from response to El Centro using various techniques

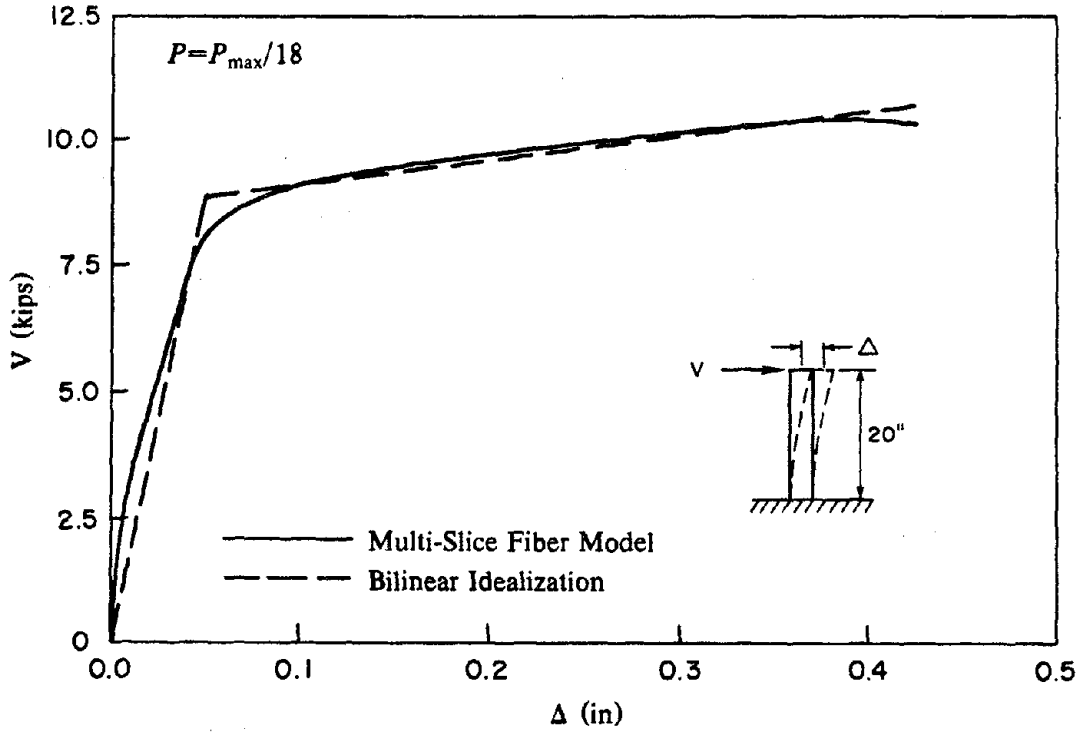

Fig. 4.15 Load-displacement relation and corresponding bilinear idealization

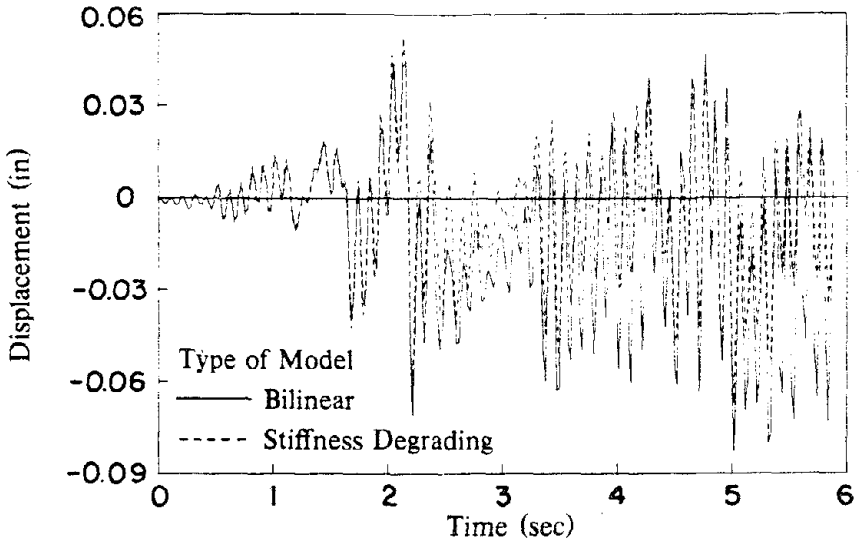

Fig. 4.16 Response to El Centro using bilinear and stiffness degrading models

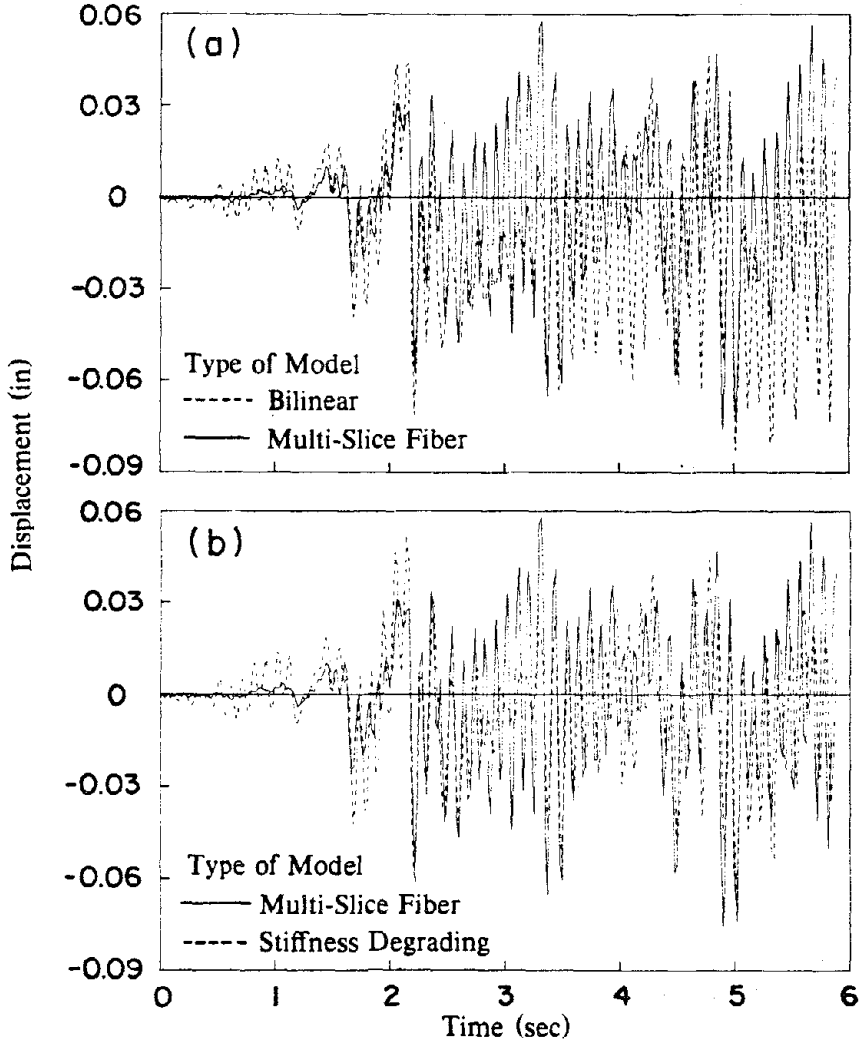

Fig. 4.17 Response to El Centro using simple models and multi-slice fiber model

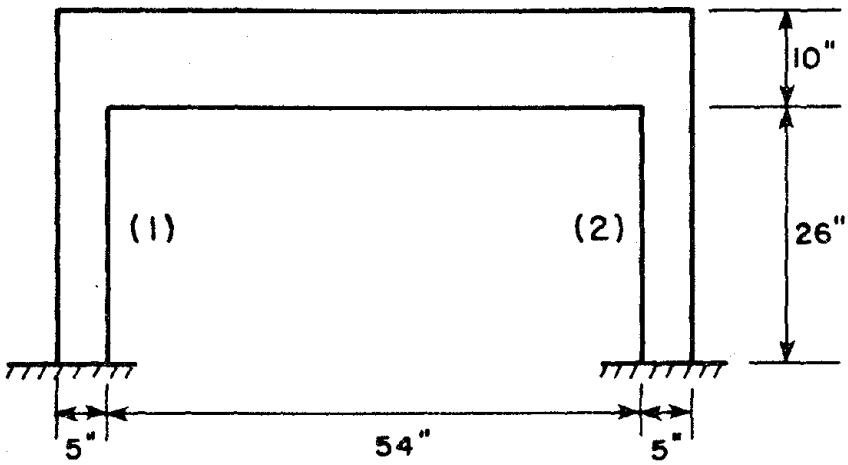

(a) Frame dimensions

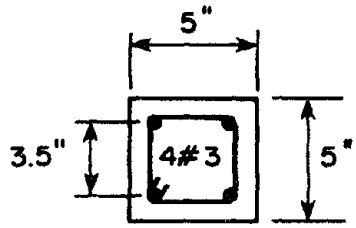

(b) Column section

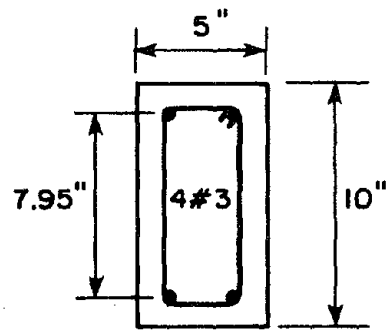

(c) Beam section

Fig. 4.18 Geometry of Gulkan frame - series F

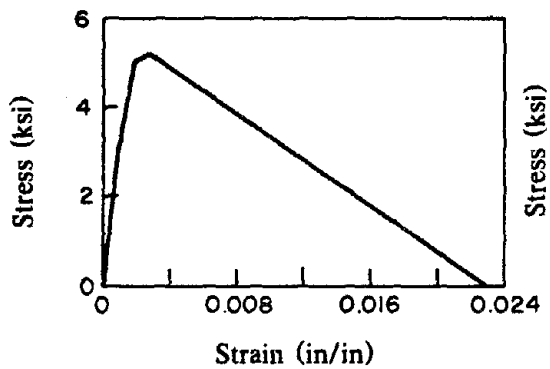

(a) Steel stress-strain relation

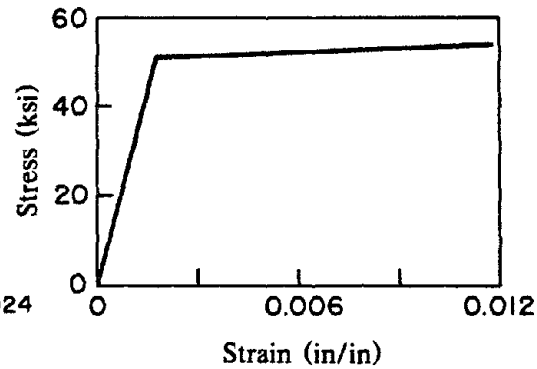

(b) Concrete stress-strain relation

Fig. 4.19 Idealized material properties for analysis of Gulkan's frame

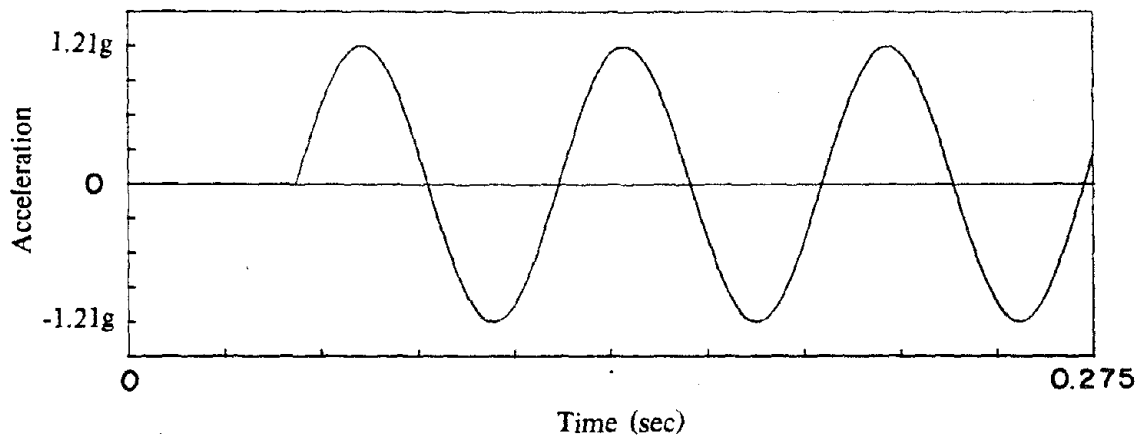

Fig. 4.20 Sinusoidal record used to analyze Gulkan's frame

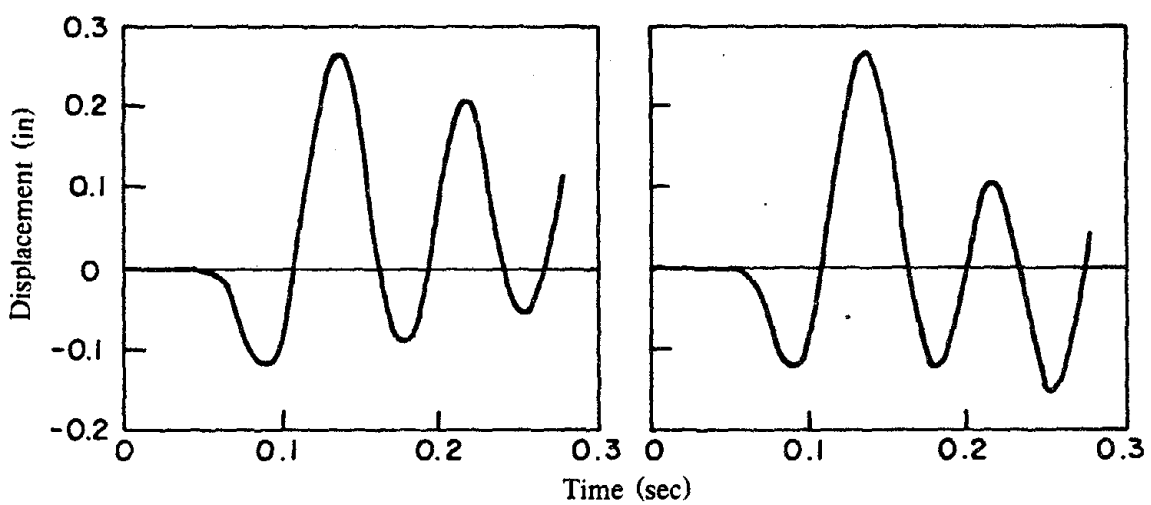

(a) Δ t = 0.001 seconds (b) Δ t = 0.0005 seconds

Fig. 4.21 Mark's analyses of Gulkan's frame using two different time steps

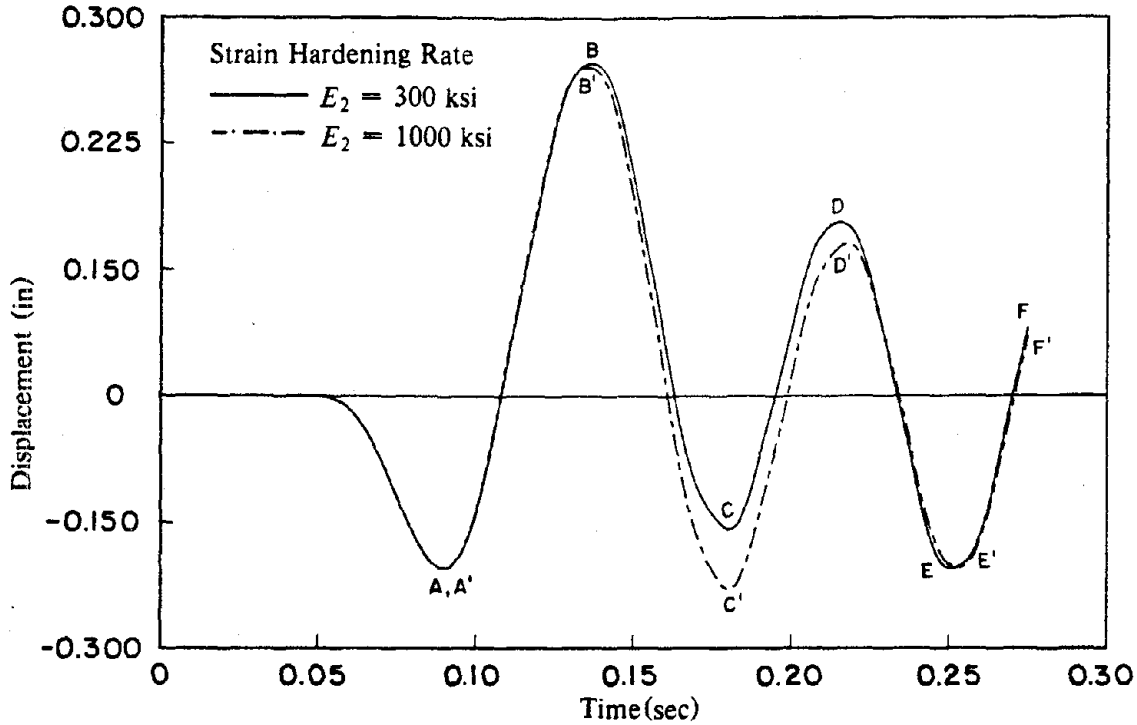

(a) Tip displacement history

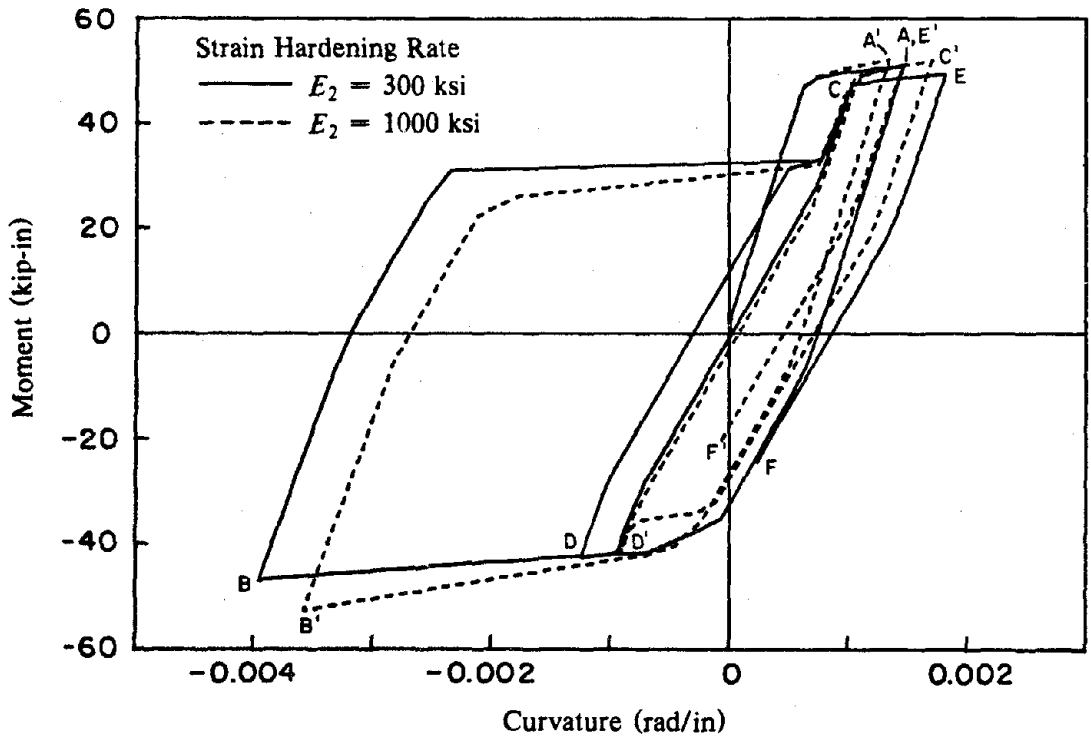

(b) Moment-curvature history

Fig. 4.22 Influence of steel strain hardening rate on calculated response

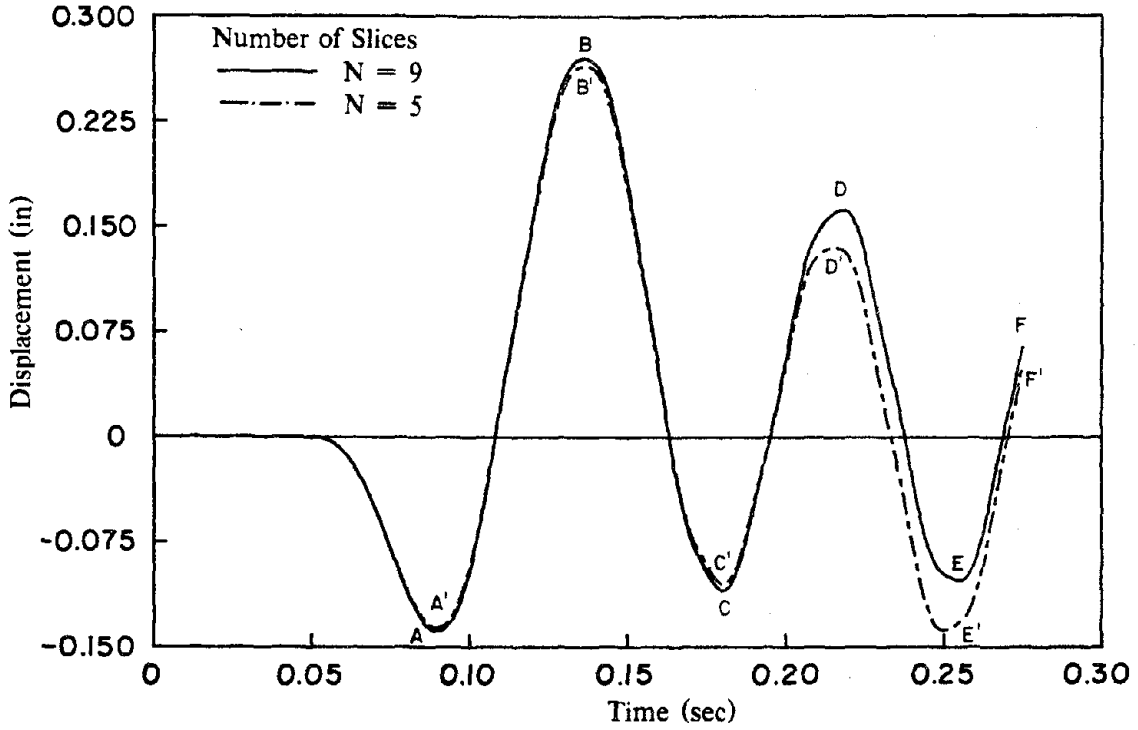

(a) Tip displacement history

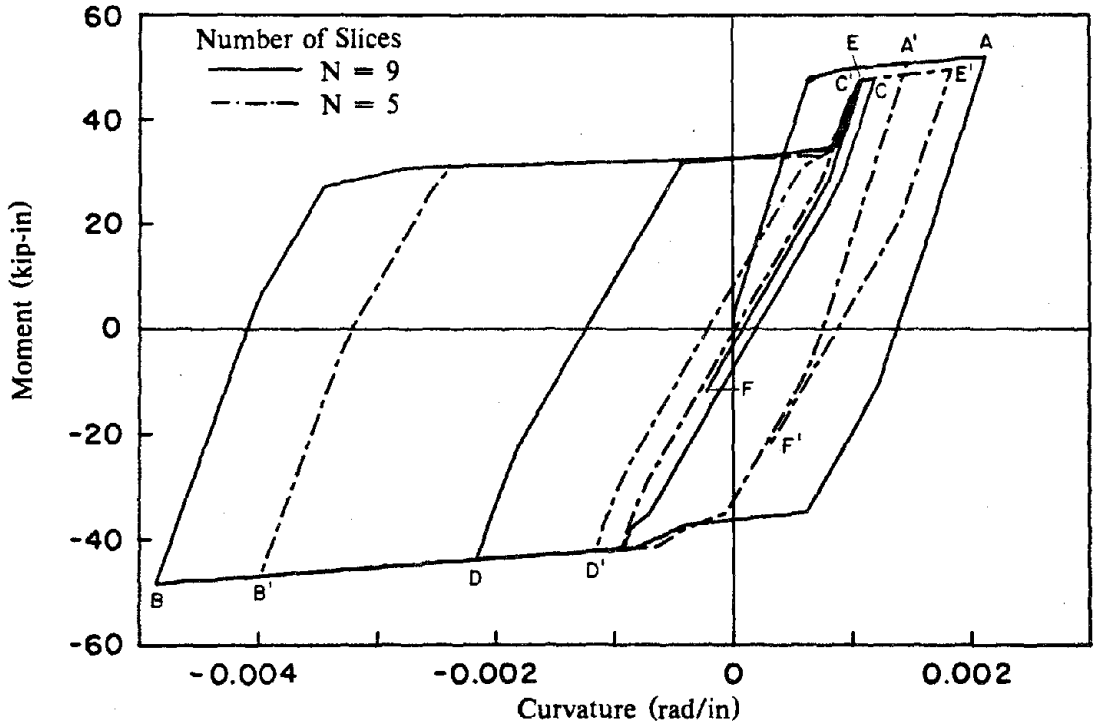

(b) Moment-curvature history

Fig. 4.23 Influence of number of slices used on calculated response

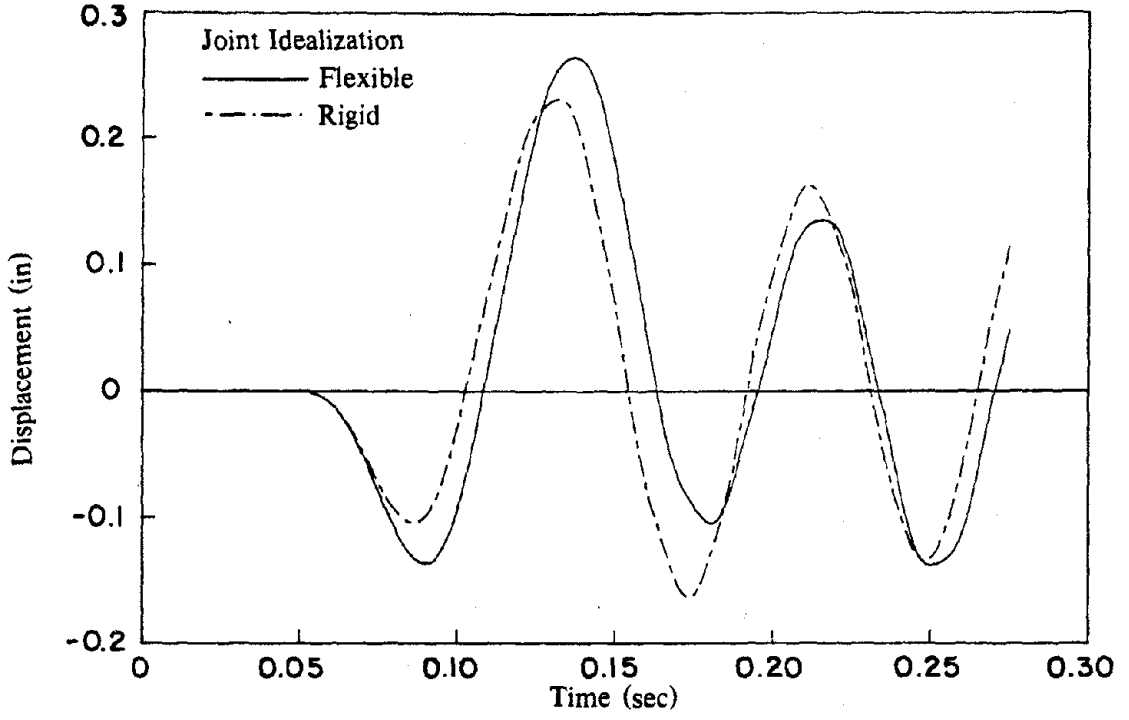

Fig. 4.24 Influence of joint idealization on calculated response

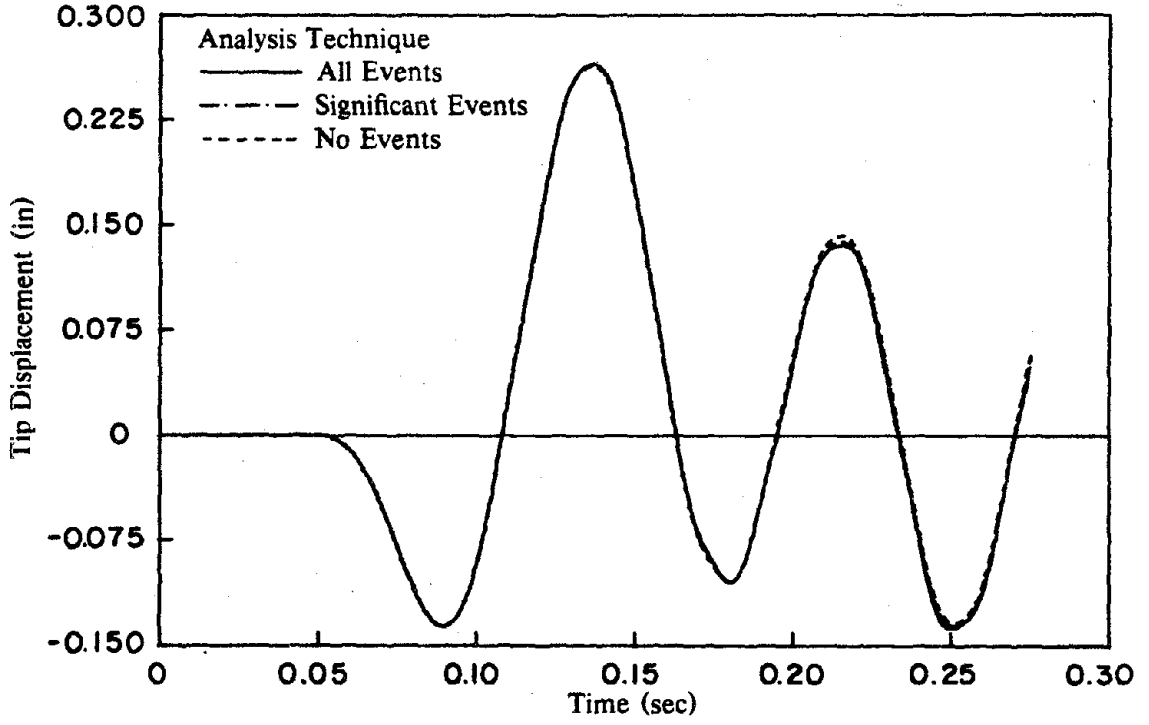

Fig. 4.25 Influence of analysis technique on displacement response (Δ t = .00125 sec)

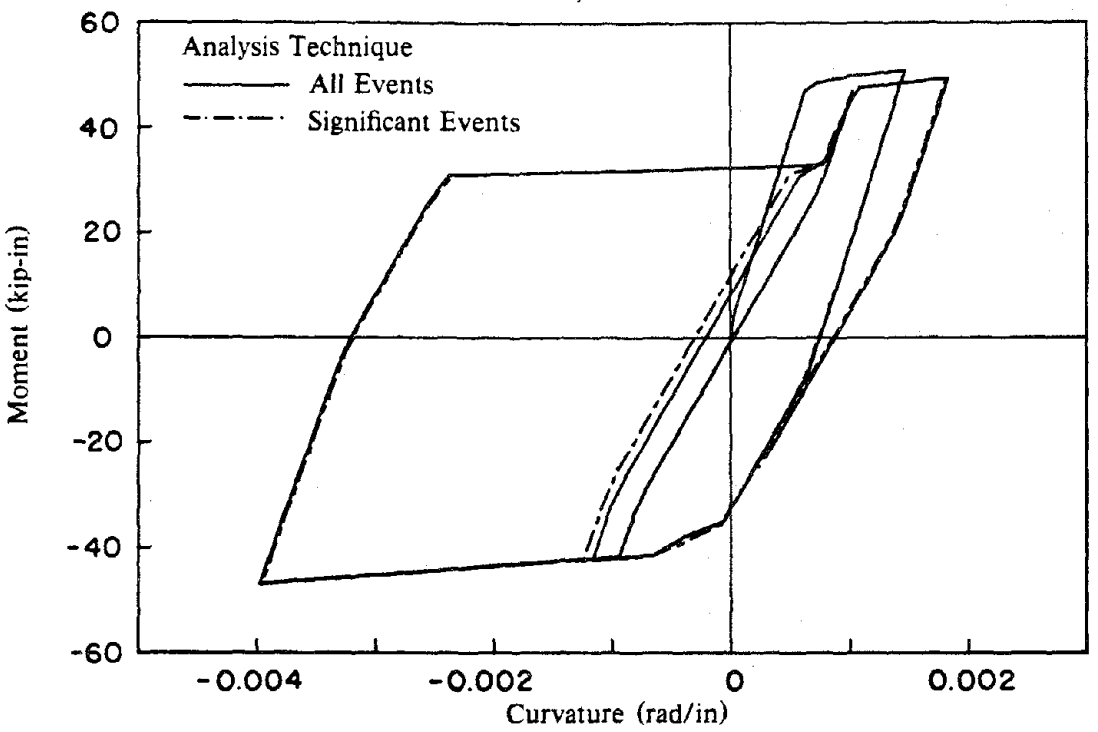

(a) Considering all events vs. only significant events

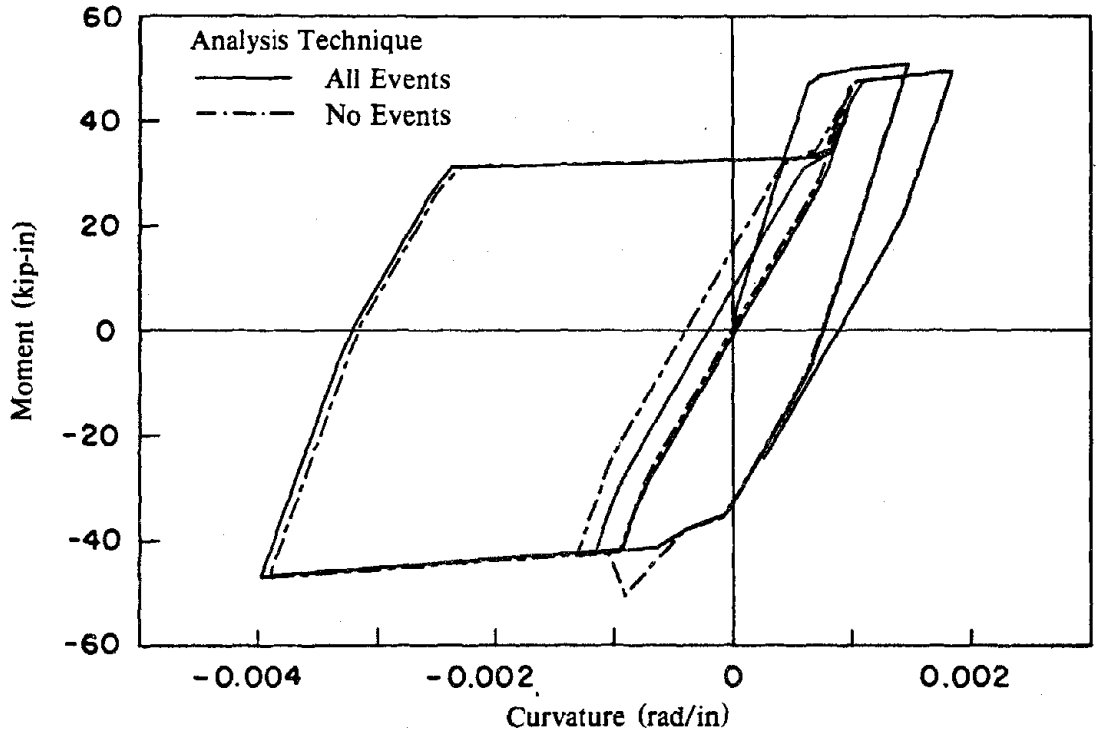

(b) Considering all events vs. no events

Fig. 4.26 Influence of analysis technique on calculated moment-curvature response

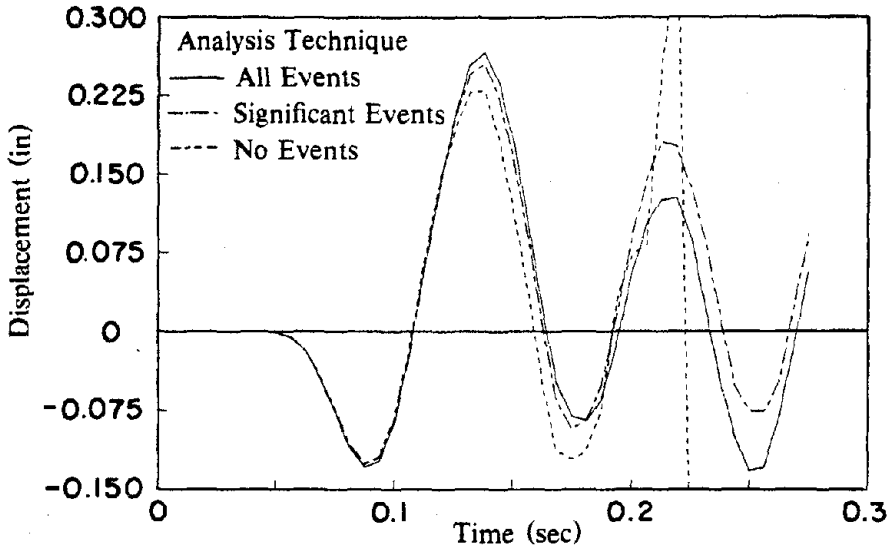

Fig. 4.27 Influence of large time step size on calculated response

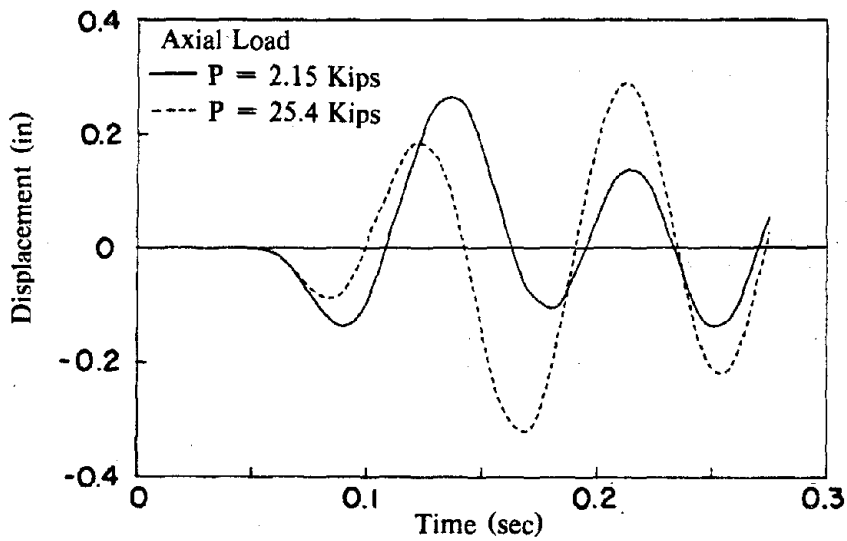

(a) Displacement History

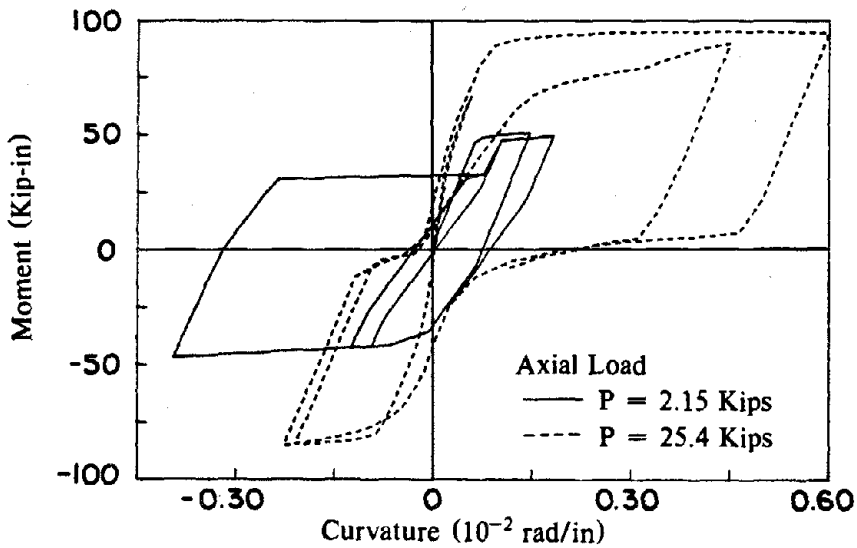

(b) Moment-curvature history

Fig. 4.28 Dynamic response of Gulkan frame for two values of axial loads

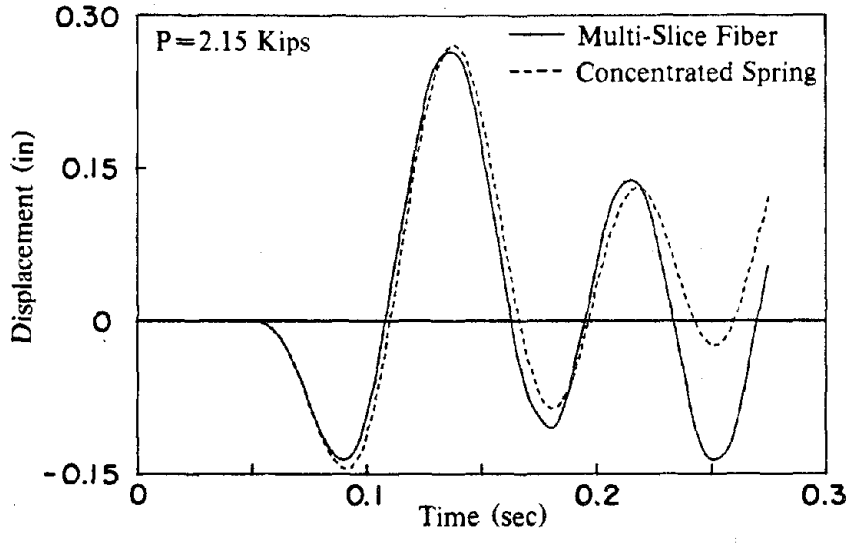

Fig. 4.29 Response using multi-slice fiber model and concentrated spring model

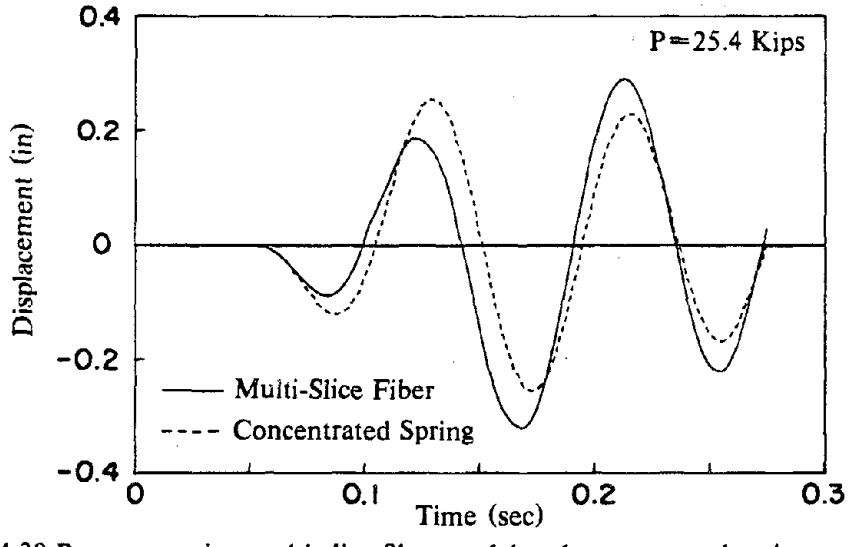

Fig. 4.30 Response using multi-slice fiber model and concentrated spring model

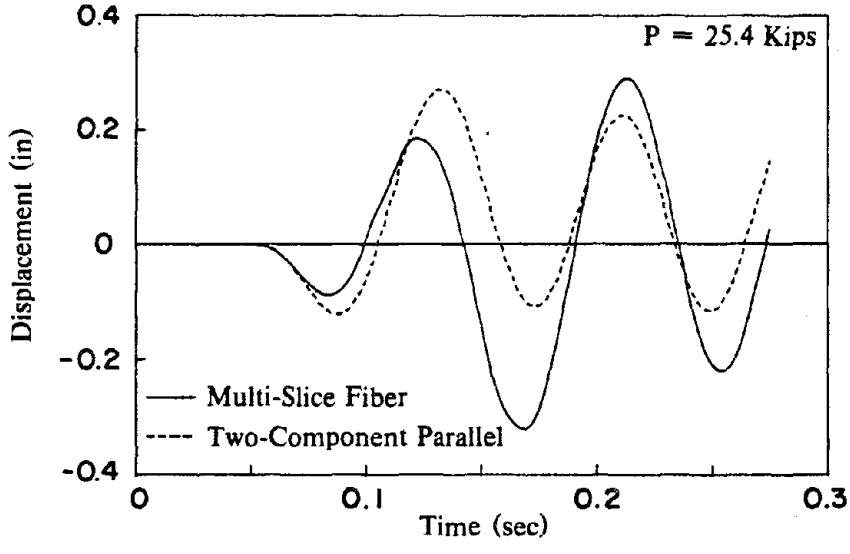

Fig. 4.31 Response using multi-slice fiber model and two-component parallel model

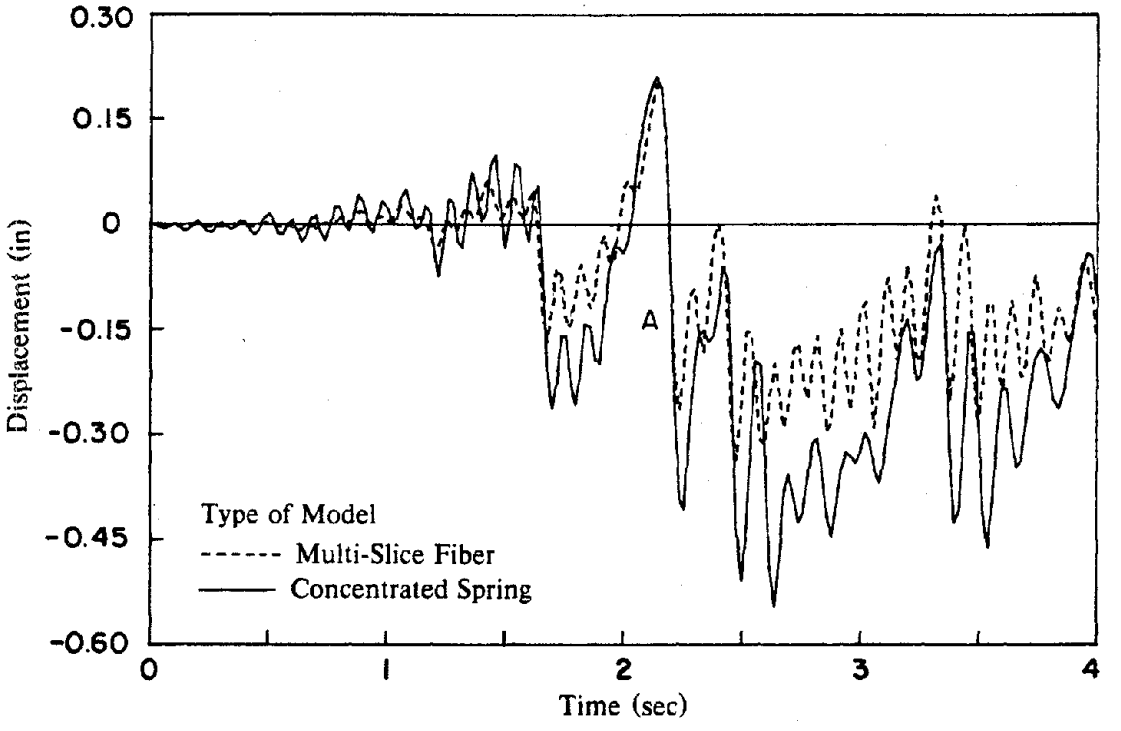

(a) Displacement History

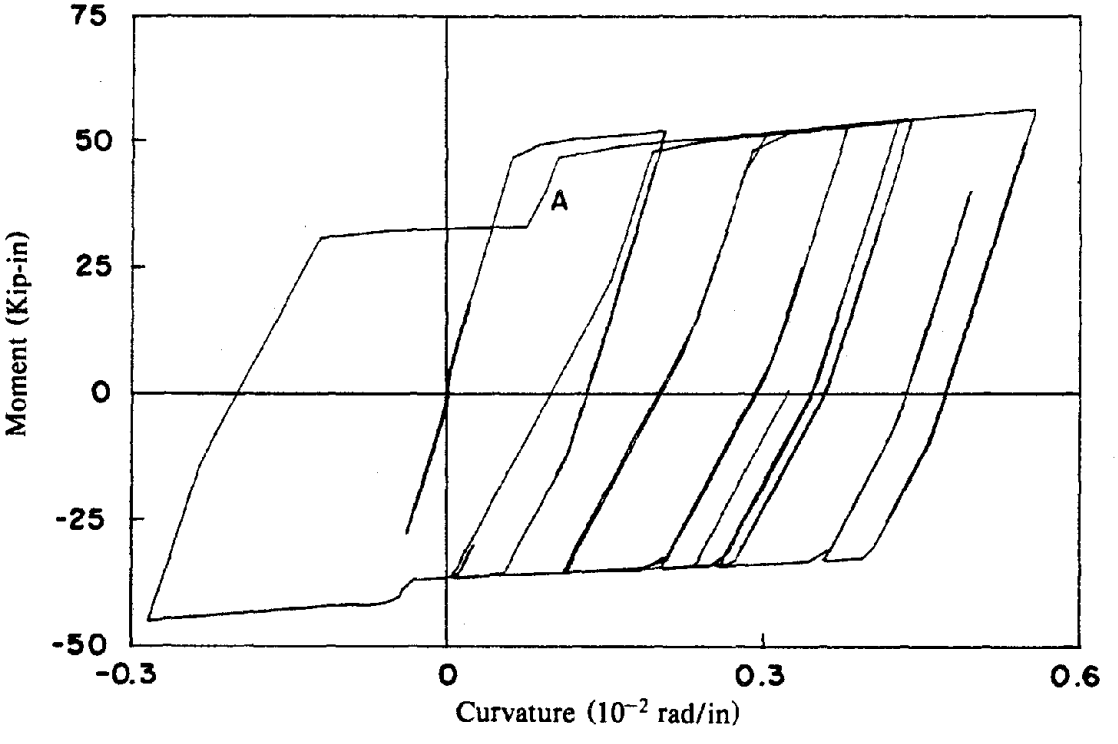

(b) Moment-curvature history

Fig. 4.32 Response to El-Centro using multi-slice fiber and concentrated spring models

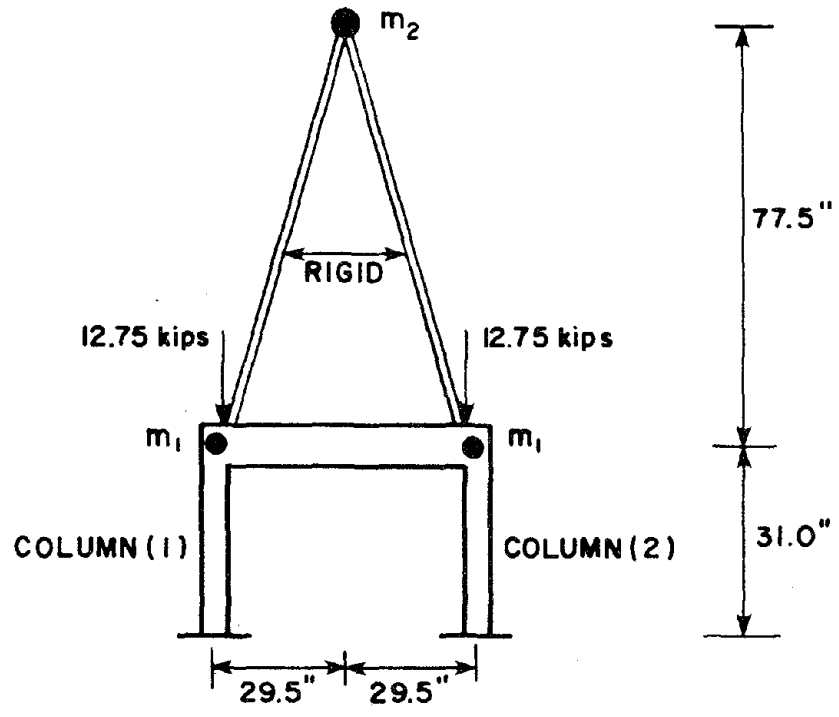

Fig. 4.33 Example frame with concentrated mass to simulate additional stories

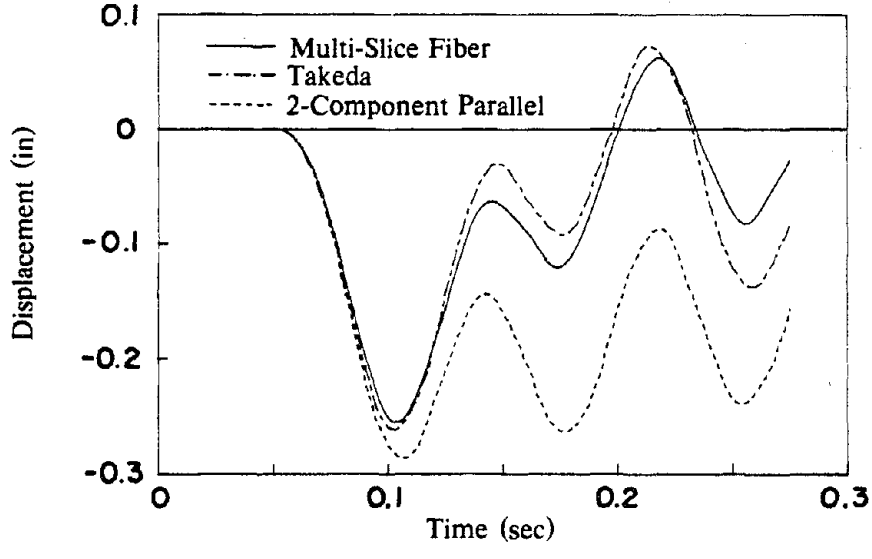

Fig. 4.34 Displacement history of frame shown in Fig. 4.33

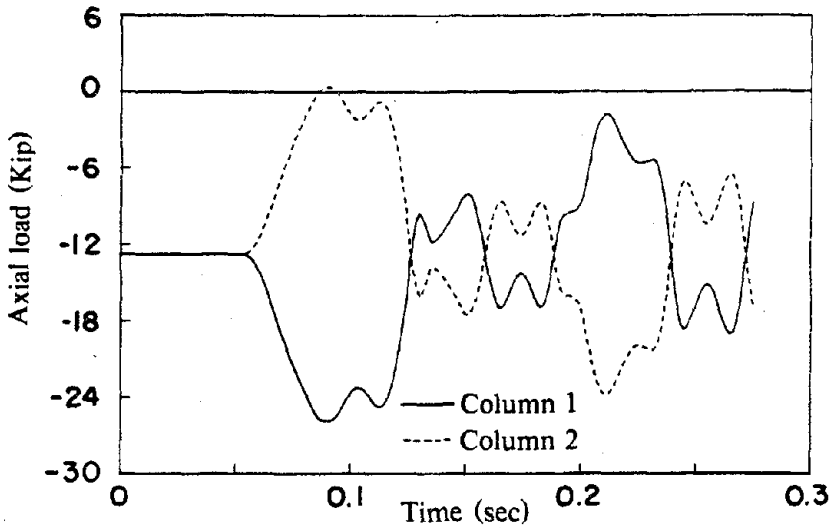

Fig. 4.35 Axial load history in the two columns

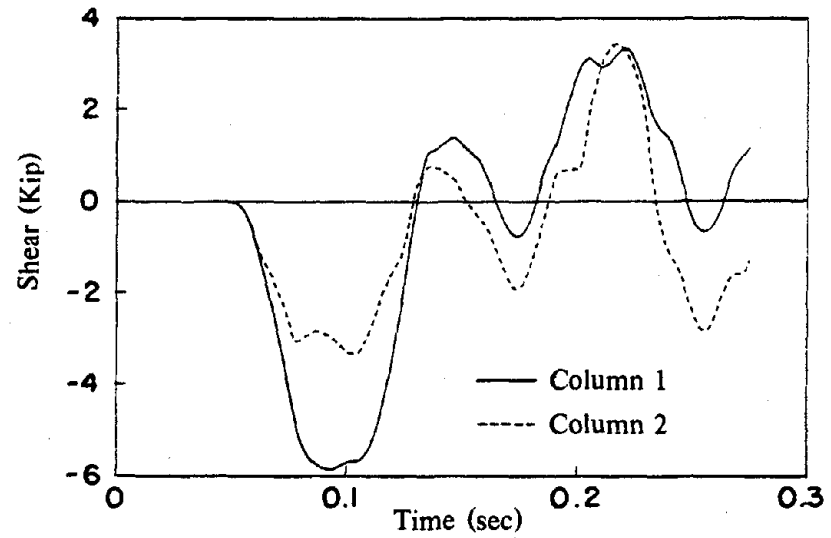

Fig. 4.36 History of shear variation in the two columns

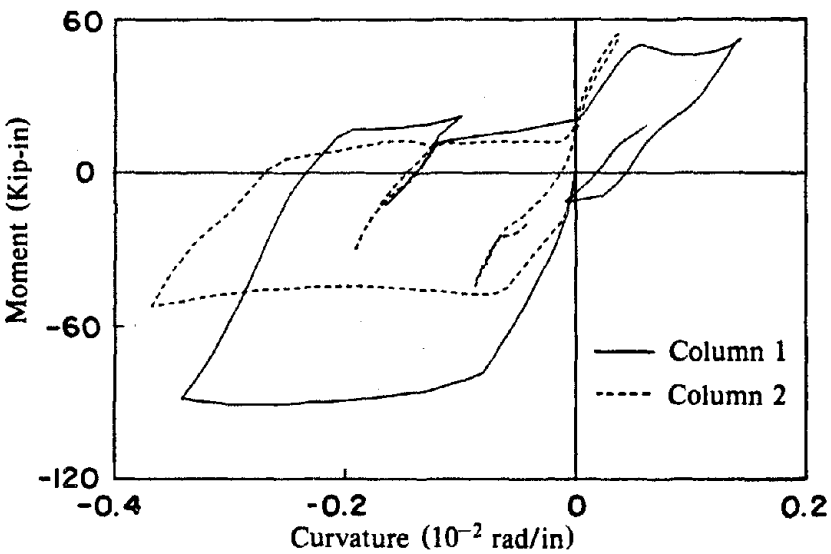

Fig. 4.37 Moment-curvature history at the base of the two columns

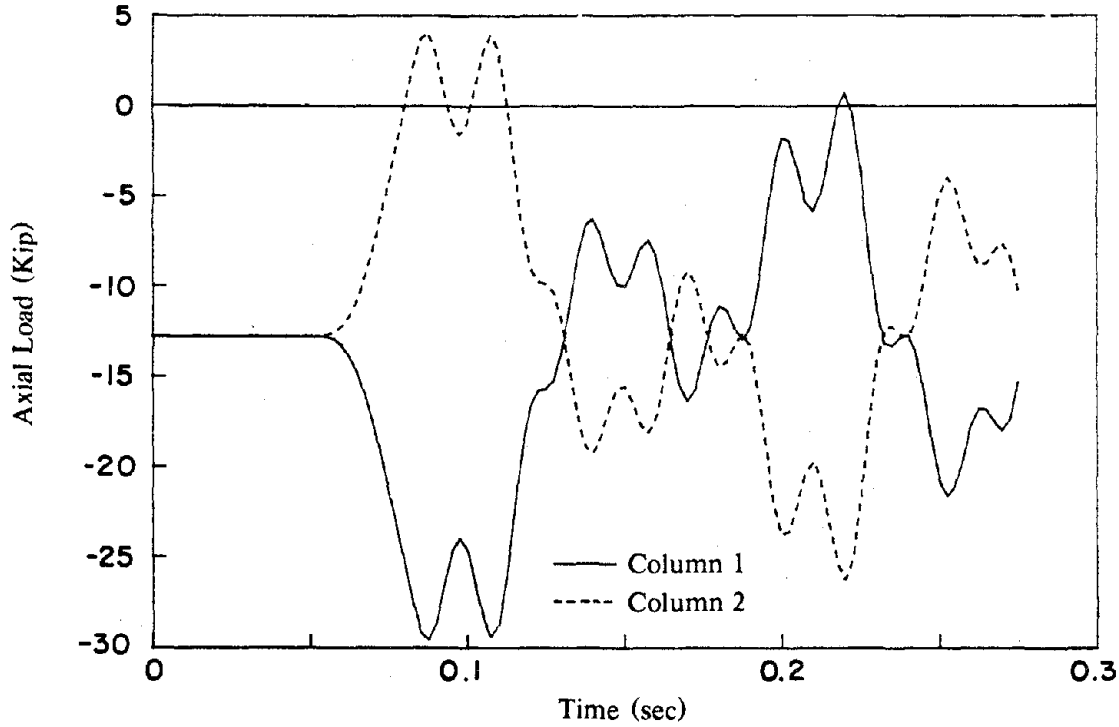

(a) History of axial load variation in the two columns

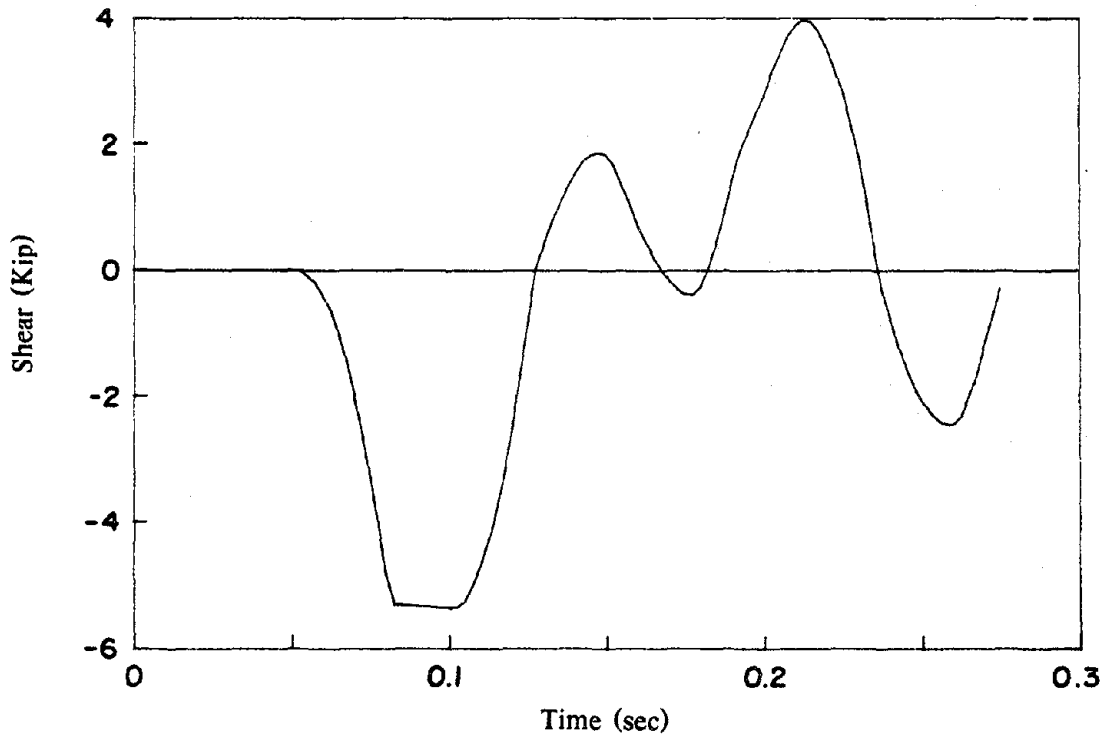

(b) History of shear variation in the two columns

Fig. 4.38 Analysis results of frame of Fig. 4.33 using Takeda model

Appendix A

Use of the Multi-Slice Fiber Model for Dynamic Analysis

The multi-slice fiber model has been adapted to work as part of DRAIN-2D2 - a program for the analysis of two-dimensional frames subjected to base acceleration for which input data is described in [4]. The following is a description of the part of the input data relating to the multi-slice fiber element. The numbers in parenthesis refer to the notes at the end of the appendix. The limits on the size of the various arrays and parameters are given in Appendix B.

A. Group control card (3I5,1X,16A4):

Element type identification number (= 3), number of elements, event code for the group (KGREP) (1), analysis title.

B. Group material data

1. Group control card (2I5): number of concrete types (2), number of steel types (2)

2. Concrete description; two cards for every type (delete if there aren't any concrete fibers): The first card (5F10.0) contains five strain values and the second (5F10.0) the corresponding five stress values. Note that an initial point is assumed to be (0.,0.). The six pairs of values describe the multi-linear concrete stress-strain relationship - see Fig. A.1. (3)

3. Steel description (3F10.0); one card for every type (delete if there aren't any steel fibers): Initial or elastic slope, second or strain hardening slope, and the yield stress (f_y).

C. Element data : for each element in the group data should be prepared conforming to the following specifications:

1. Element control card (7I5)

I-node number, J-node number, number of slices, geometric stiffness indicator (KGEOM) (4), output printout control (KOUT) (5), event type indicator (KVNT) (6), detailed output file number (KOUT3) (7), maximum allowed number of events per time step (IND3), default=50. If this number is exceeded the analysis moves on to the next time step.

2. Slice spacings (8F10.0): One or two cards to accommodate the number of spacings starting from the one closest to node I (one less than number of slices specified). (8)

3. Rigid end zones' lengths (2F10.0): respectively) to be considered perfectly rigid - e.g. parts of the element within the joints. (2)(8)

4. Slice description; the following date should be included for every slice (unless automatic slice generation is used):

4.1 Slice control card (2I5): NGC = number of concrete groups of fibers (2)(9), NGS = number of steel groups of fibers (2)(9). Note if slice is identical to the previous one then set NGC = -1 and delete rest of slice description.

4.2 Concrete configuration (delete if NGC = 0): the following for every group of concrete fibers:

4.2.1 Concrete group control card (2I5, F10.0, I5):

Number of fibers in group, concrete material type associated with group, area of concrete fiber in group, coordinate generation index (IY) = 0 to generate fiber coordinates and = 1 if coordinates are to be explicitly specified.

4.2.2 Fiber coordinates (8F10.0)(10): If IY = 0, give coordinates of centroids of first and last fibers. If IY = 1, list coordinates of all fibers in the group.

4.3 Steel configuration (delete if NGS = 0): the following for every group of steel fibers:

4.3.1 Steel group control card (2I5, F10.0, I5):

Number of layers in group, steel material type associated with group, area of steel fiber in group, coordinate generation index (IY) = 0 to generate fiber coordinates and = 1 if coordinates are to be explicitly specified.

4.3.2 Fiber coordinates (8F10.0)(10): If IY = 0, give coordinates of centroids of first and last fibers. If IY = 1, list coordinates of all fibers in the group.

NOTES

(1) If any type of midstep event is to be considered for any of the elements in the group, KGREP should be set equal to one. If midstep events are to be ignored for all elements in the group, KGREP should be set equal to zero - see 6 below.

(2) Can be zero.

(3) Note that abrupt breaks in the concrete stress-strain relation as well as too steep a descending branch might result in equilibrium errors and/or numerical instabilities. For strain values larger than the last specified strain (the sixth), the concrete is assumed crushed and a zero stress is assigned to the fiber henceforth. Note that computational savings can be achieved if the concrete stress-strain relationship can be adequately described in fewer than six points - in this case specify appropriate strains and zero stress for the superfluous points as shown in Fig. A.2.

(4) Set KGEOM = 1, if geometric $(P-\Delta)$ stiffness based on static analysis is to be included; set equal to 0 to ignore geometric stiffness.

(5) KOUT is used to control element output as follows :

Set = -1 for no output and no element description

0 for no output

1 to print only

2 to print and save

3 to save only

4 to save and print 'reorganized' time history

Note that this output, along with other program output, is written to file IOU, and is independent of the individual element output files referred to in (7) below.

(6) To include event-to-event calculations, KGREP (see 1 above) must be set equal to one. KVNT should be set equal to zero to include all events. It should be set equal to one to include steel fiber events and concrete fiber unloading events only. Note that if KGREP is set equal to zero (i.e., ignore midstep events), KVNT should be set equal to one to calculate and correct for unbalanced forces - see Section 2.3(e).

(7) Set KOUT3 = 0, if no detailed output for the element is required, otherwise indicate number of file in which the output is to be written. These files are opened and named in the MAIN program. Detailed output consists of the history of element forces and deformations written in 10 columns which include : time, curvature(i), rotation(i), moment(i), curvature(j), rotation(j), moment(j), axial displacement (Δ), axial load, and shear force. Note that curvatures and moments are those of the slice at or closest to the indicated node.

(8) A warning is given by the program if the sum of the slice spacings and the two rigid end zones' lengths is not equal to the distance between the nodes which the element connects.

(9) Fibers in the same group should have the same material type and area.

(10) The coordinates with respect to an axis chosen by the user, usually at the section's midheight or at its plastic centroid. Note that this is the axis around which the moments are calculated.

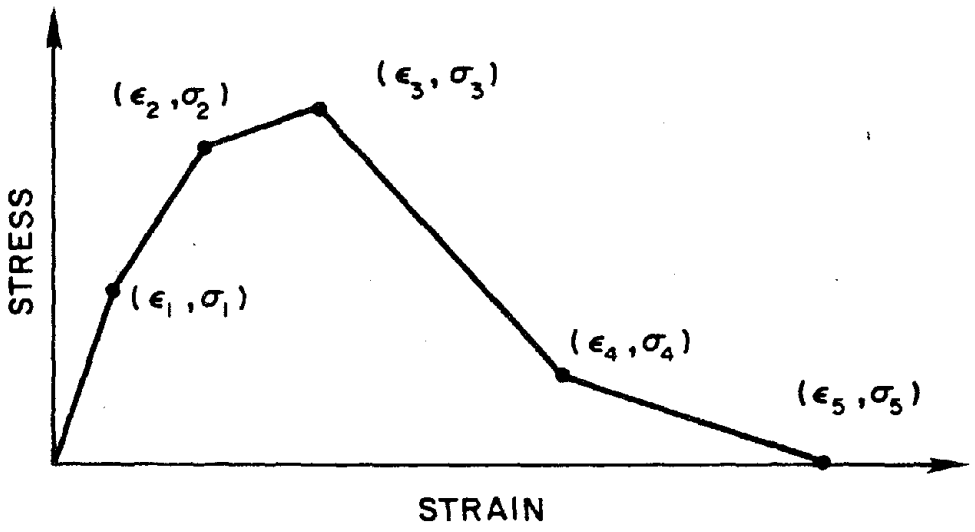

Fig. A.1 Concrete stress-strain envelope showing required input parameters

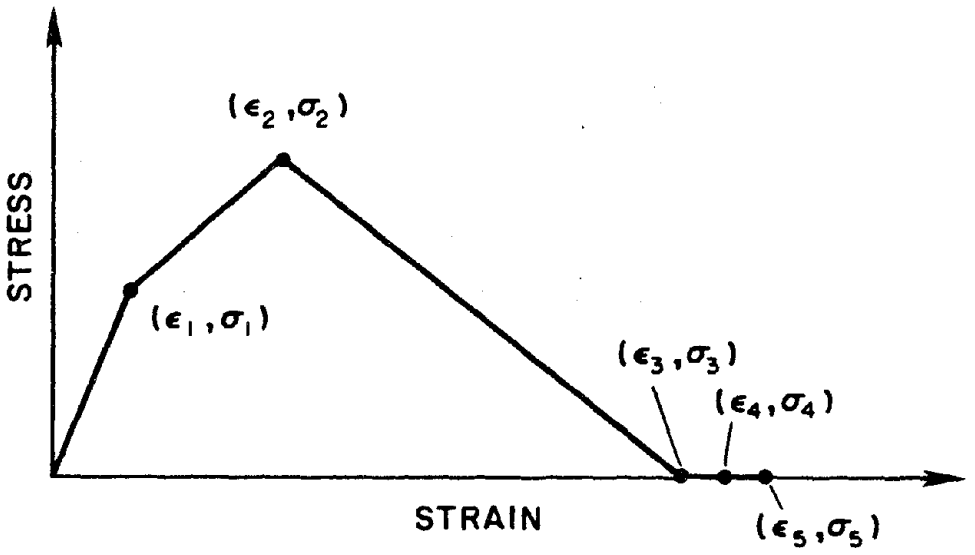

Fig. A.2 Simplified concrete stress-strain curve

Appendix B

Current Array Size Limitations

The array sizes as currently implemented in the program are given below. The limits can be relaxed by modifying the array sizes found in the various COMMON blocks in the multi-slice fiber element subroutines. Note, however, that such modifications must be relayed to the main program by updating the values of variables NINFG and/or NINFE see [4].

B.1 Limitations on Size of Group Arrays

Total Number of Concrete Types	=	12
Total Number of Steel Types	=	9

B.2 Limitations on Size of Element Arrays

NSLIC	=	Number of Slices	=	15
NFC	=	Number of Concrete Groups of Fibers	=	30
NFS	=	Number of Steel Groups of Fibers	=	15
Number of Concrete Fibers per Element			=	150
Number of Steel Fibers per Element			=	50

EARTHQUAKE ENGINEERING RESEARCH CENTER REPORTS

NOTE: Numbers in parentheses are Accession Numbers assigned by the National Technical Information Service; these are followed by a price code. Copies of the reports may be ordered from the National Technical Information Service, 5285 Port Royal Road, Springfield, Virginia, 22161. Accession Numbers should be quoted on orders for reports (PB --- ---) and remittance must accompany each order. Reports without this information were not available at time of printing. The complete list of EERC reports (from EERC 67-1) is available upon request from the Earthquake Engineering Research Center, University of California, Berkeley, 47th Street and Hoffman Boulevard, Richmond, California 94804.

UCB/EERC-77/01 "PLUSH - A Computer Program for Probabilistic Finite Element Analysis of Seismic Soil-Structure Interaction," by M.P. Romo Organista, J. Lysmer and H.B. Seed - 1977 (PB81 177 651)A05

UCB/EERC-77/02 "Soil-Structure Interaction Effects at the Humboldt Bay Power Plant in the Ferndale Earthquake of June 7, 1975," by J.E. Valera, H.B. Seed, C.F. Tsai and J. Lysmer - 1977 (PB 265 795)A04

UCB/EERC-77/03 "Influence of Sample Disturbance on Sand Response to Cyclic Loading," by K. Mori, H.B. Seed and C.K. Chan - 1977 (PB 267 352)A04

UCB/EERC-77/04 "Seismological Studies of Strong Motion Records," by J. Shoja-Taheri - 1977 (PB 269 655)A10

UCB/EERC-77/05 Unassigned

UCB/EERC-77/06 "Developing Methodologies for Evaluating the Earthquake Safety of Existing Buildings," by No. 1 - B. Bresler; No. 2 - B. Bresler, T. Okada and D. Zisling; No. 3 - T. Okada and B. Bresler; No. 4 - V.V. Bertero and B. Bresler - 1977 (PB 267 354)A08

UCB/EERC-77/07 "A Literature Survey - Transverse Strength of Masonry Walls," by Y. Omote, R.L. Mayes, S.W. Chen and R.W. Clough - 1977 (PB 277 933)A07

UCB/EERC-77/08 "DRAIN-TABS: A Computer Program for Inelastic Earthquake Response of Three Dimensional Buildings," by R. Guendelman-Israel and G.H. Powell - 1977 (PB 270 693)A07

UCB/EERC-77/09 "SUBWALL: A Special Purpose Finite Element Computer Program for Practical Elastic Analysis and Design of Structural Walls with Substructure Option," by D.Q. Le, H. Peterson and E.P. Popov - 1977 (PB 270 567)A05

UCB/EERC-77/10 "Experimental Evaluation of Seismic Design Methods for Broad Cylindrical Tanks," by D.P. Clough (PB 272 280)A13

UCB/EERC-77/11 "Earthquake Engineering Research at Berkeley - 1976," - 1977 (PB 273 507)A09

UCB/EERC-77/12 "Automated Design of Earthquake Resistant Multistory Steel Building Frames," by N.D. Walker, Jr. - 1977 (PB 276 526)A09

UCB/EERC-77/13 "Concrete Confined by Rectangular Hoops Subjected to Axial Loads," by J. Vallenas, V.V. Bertero and E.P. Popov - 1977 (PB 275 165)A06

UCB/EERC-77/14 "Seismic Strain Induced in the Ground During Earthquakes," by Y. Sugimura - 1977 (PB 284 201)A04

UCB/EERC-77/15 Unassigned

UCB/EERC-77/16 "Computer Aided Optimum Design of Ductile Reinforced Concrete Moment Resisting Frames," by S.W. Zagajeski and V.V. Bertero - 1977 (PB 280 137)A07

UCB/EERC-77/17 "Earthquake Simulation Testing of a Stepping Frame with Energy-Absorbing Devices," by J.M. Kelly and D.F. Tsztoo - 1977 (PB 273 506)A04

UCB/EERC-77/18 "Inelastic Behavior of Eccentrically Braced Steel Frames under Cyclic Loadings," by C.W. Roeder and E.P. Popov - 1977 (PB 275 526)A15

UCB/EERC-77/19 "A Simplified Procedure for Estimating Earthquake-Induced Deformations in Dams and Embankments," by F.I. Makdisi and H.B. Seed - 1977 (PB 276 820)A04

UCB/EERC-77/20 "The Performance of Earth Dams during Earthquakes," by H.B. Seed, F.I. Makdisi and P. de Alba - 1977 (PB 276 821)A04

UCB/EERC-77/21 "Dynamic Plastic Analysis Using Stress Resultant Finite Element Formulation," by P. Lukkunapvasit and J.M. Kelly - 1977 (PB 275 453)A04

UCB/EERC-77/22 "Preliminary Experimental Study of Seismic Uplift of a Steel Frame," by R.W. Clough and A.A. Huckelbridge 1977 (PB 278 769)A08

UCB/EERC-77/23 "Earthquake Simulator Tests of a Nine-Story Steel Frame with Columns Allowed to Uplift," by A.A. Huckelbridge - 1977 (PB 277 944)A09

UCB/EERC-77/24 "Nonlinear Soil-Structure Interaction of Skew Highway Bridges," by M.-C. Chen and J. Penzien - 1977 (PB 276 176)A07

UCB/EERC-77/25 "Seismic Analysis of an Offshore Structure Supported on Pile Foundations," by D.D.-N. Liou and J. Penzien 1977 (PB 283 180)A06

UCB/EERC-77/26 "Dynamic Stiffness Matrices for Homogeneous Viscoelastic Half-Planes," by G. Dasgupta and A.K. Chopra - 1977 (PB 279 654)A06

UCB/EERC-77/27 "A Practical Soft Story Earthquake Isolation System," by J.M. Kelly, J.M. Eidinger and C.J. Derham - 1977 (PB 276 814)A07

UCB/EERC-77/28 "Seismic Safety of Existing Buildings and Incentives for Hazard Mitigation in San Francisco: An Exploratory Study," by A.J. Meltsner - 1977 (PB 281 970)A05

UCB/EERC-77/29 "Dynamic Analysis of Electrohydraulic Shaking Tables," by D. Rea, S. Abedi-Hayati and Y. Takahashi 1977 (PB 282 569)A04

UCB/EERC-77/30 "An Approach for Improving Seismic - Resistant Behavior of Reinforced Concrete Interior Joints," by B. Galunic, V.V. Bertero and E.P. Popov - 1977 (PB 290 870)A06

UCB/EERC-78/01 "The Development of Energy-Absorbing Devices for Aseismic Base Isolation Systems," by J.M. Kelly and D.F. Tsztoo - 1978 (PB 284 978)A04

UCB/EERC-78/02 "Effect of Tensile Prestrain on the Cyclic Response of Structural Steel Connections, by J.G. Bouwkamp and A. Mukhopadhyay - 1978

UCB/EERC-78/03 "Experimental Results of an Earthquake Isolation System using Natural Rubber Bearings," by J.M. Eidinger and J.M. Kelly - 1978 (PB 281 686)A04

UCB/EERC-78/04 "Seismic Behavior of Tall Liquid Storage Tanks," by A. Niwa - 1978 (PB 284 017)A14

UCB/EERC-78/05 "Hysteretic Behavior of Reinforced Concrete Columns Subjected to High Axial and Cyclic Shear Forces," by S.W. Zagajeski, V.V. Bertero and J.G. Bouwkamp - 1978 (PB 283 858)A13

UCB/EERC-78/06 "Three Dimensional Inelastic Frame Elements for the ANSR-I Program," by A. Riahi, D.G. Row and G.H. Powell - 1978 (PB 295 755)A04

UCB/EERC-78/07 "Studies of Structural Response to Earthquake Ground Motion," by O.A. Lopez and A.K. Chopra - 1978 (PB 282 790)A05

UCB/EERC-78/08 "A Laboratory Study of the Fluid-Structure Interaction of Submerged Tanks and Caissons in Earthquakes," by R.C. Byrd - 1978 (PB 284 957)A08

UCB/EERC-78/09 Unassigned

UCB/EERC-78/10 "Seismic Performance of Nonstructural and Secondary Structural Elements," by I. Sakamoto - 1978 (PB81 154 593)A05

UCB/EERC-78/11 "Mathematical Modelling of Hysteresis Loops for Reinforced Concrete Columns," by S. Nakata, T. Sproul and J. Penzien - 1978 (PB 298 274)A05

UCB/EERC-78/12 "Damageability in Existing Buildings," by T. Blejwas and B. Bresler - 1978 (PB 80 166 978)A05

UCB/EERC-78/13 "Dynamic Behavior of a Pedestal Base Multistory Building," by R.M. Stephen, E.L. Wilson, J.G. Bouwkamp and M. Button - 1978 (PB 286 650)A08

UCB/EERC-78/14 "Seismic Response of Bridges - Case Studies," by R.A. Imbsen, V. Nutt and J. Penzien - 1978 (PB 286 503)A10

UCB/EERC-78/15 "A Substructure Technique for Nonlinear Static and Dynamic Analysis," by D.G. Row and G.H. Powell - 1978 (PB 288 077)A10

UCB/EERC-78/16 "Seismic Risk Studies for San Francisco and for the Greater San Francisco Bay Area," by C.S. Oliveira - 1978 (PB 81 120 115)A07

UCB/EERC-78/17 "Strength of Timber Roof Connections Subjected to Cyclic Loads," by P. Gülkan, R.L. Mayes and R.W. Clough - 1978 (HUD-000 1491)A07

UCB/EERC-78/18 "Response of K-Braced Steel Frame Models to Lateral Loads," by J.G. Bouwkamp, R.M. Stephen and E.P. Popov - 1978

UCB/EERC-78/19 "Rational Design Methods for Light Equipment in Structures Subjected to Ground Motion," by J.L. Sackman and J.M. Kelly - 1978 (PB 292 357)A04

UCB/EERC-78/20 "Testing of a Wind Restraint for Aseismic Base Isolation," by J.M. Kelly and D.E. Chitty - 1978 (PB 292 833)A03

UCB/EERC-78/21 "APOLLO - A Computer Program for the Analysis of Pore Pressure Generation and Dissipation in Horizontal Sand Layers During Cyclic or Earthquake Loading," by P.P. Martin and H.B. Seed - 1978 (PB 292 835)A04

UCB/EERC-78/22 "Optimal Design of an Earthquake Isolation System," by M.A. Bhatti, K.S. Pister and E. Polak - 1978 (PB 294 735)A06

UCB/EERC-78/23 "MASH - A Computer Program for the Non-Linear Analysis of Vertically Propagating Shear Waves in Horizontally Layered Deposits," by P.P. Martin and H.B. Seed - 1978 (PB 293 101)A05

UCB/EERC-78/24 "Investigation of the Elastic Characteristics of a Three Story Steel Frame Using System Identification," by I. Kaya and H.D. McNiven - 1978 (PB 296 225)A06

UCB/EERC-78/25 "Investigation of the Nonlinear Characteristics of a Three-Story Steel Frame Using System Identification," by I. Kaya and H.D. McNiven - 1978 (PB 301 363)A05

UCB/EERC-78/26 "Studies of Strong Ground Motion in Taiwan," by Y.M. Hsiung, B.A. Bolt and J. Penzien - 1978 (PB 298 436)A06

UCB/EERC-78/27 "Cyclic Loading Tests of Masonry Single Piers: Volume 1 - Height to Width Ratio of 2," by P.A. Hidalgo, R.L. Mayes, H.D. McNiven and R.W. Clough - 1978 (PB 296 211)A07

UCB/EERC-78/28 "Cyclic Loading Tests of Masonry Single Piers: Volume 2 - Height to Width Ratio of 1," by S.-W.J. Chen, P.A. Hidalgo, R.L. Mayes, R.W. Clough and H.D. McNiven - 1978 (PB 296 212)A09

UCB/EERC-78/29 "Analytical Procedures in Soil Dynamics," by J. Lysmer - 1978 (PB 298 445)A06

UCB/EERC-79/01 "Hysteretic Behavior of Lightweight Reinforced Concrete Beam-Column Subassemblages," by B. Forzani, E.P. Popov and V.V. Bertero - April 1979(PB 298 267)A06

UCB/EERC-79/02 "The Development of a Mathematical Model to Predict the Flexural Response of Reinforced Concrete Beams to Cyclic Loads, Using System Identification," by J. Stanton & H. McNiven - Jan. 1979(PB 295 875)A10

UCB/EERC-79/03 "Linear and Nonlinear Earthquake Response of Simple Torsionally Coupled Systems," by C.L. Kan and A.K. Chopra - Feb. 1979(PB 298 262)A06

UCB/EERC-79/04 "A Mathematical Model of Masonry for Predicting its Linear Seismic Response Characteristics," by Y. Mengi and H.D. McNiven - Feb. 1979(PB 298 266)A06

UCB/EERC-79/05 "Mechanical Behavior of Lightweight Concrete Confined by Different Types of Lateral Reinforcement," by M.A. Manrique, V.V. Bertero and E.P. Popov - May 1979(PB 301 114)A06

UCB/EERC-79/06 "Static Tilt Tests of a Tall Cylindrical Liquid Storage Tank," by R.W. Clough and A. Niwa - Feb. 1979 (PB 301 167)A06

UCB/EERC-79/07 "The Design of Steel Energy Absorbing Restrainers and Their Incorporation into Nuclear Power Plants for Enhanced Safety: Volume 1 - Summary Report," by P.N. Spencer, V.F. Zackay, and E.R. Parker - Feb. 1979(UCB/EERC-79/07)A09

UCB/EERC-79/08 "The Design of Steel Energy Absorbing Restrainers and Their Incorporation into Nuclear Power Plants for Enhanced Safety: Volume 2 - The Development of Analyses for Reactor System Piping,""Simple Systems" by M.C. Lee, J. Penzien, A.K. Chopra and K. Suzuki "Complex Systems" by G.H. Powell, E.L. Wilson, R.W. Clough and D.G. Row - Feb. 1979(UCB/EERC-79/08)A10

UCB/EERC-79/09 "The Design of Steel Energy Absorbing Restrainers and Their Incorporation into Nuclear Power Plants for Enhanced Safety: Volume 3 - Evaluation of Commercial Steels," by W.S. Owen, R.M.N. Pelloux, R.O. Ritchie, M. Faral, T. Ohhashi, J. Toplosky, S.J. Hartman, V.F. Zackay and E.R. Parker - Feb. 1979(UCB/EERC-79/09)A04

UCB/EERC-79/10 "The Design of Steel Energy Absorbing Restrainers and Their Incorporation into Nuclear Power Plants for Enhanced Safety: Volume 4 - A Review of Energy-Absorbing Devices," by J.M. Kelly and M.S. Skinner - Feb. 1979(UCB/EERC-79/10)A04

UCB/EERC-79/11 "Conservatism In Summation Rules for Closely Spaced Modes," by J.M. Kelly and J.L. Sackman - May 1979(PB 301 328)A03

UCB/EERC-79/12 "Cyclic Loading Tests of Masonry Single Piers; Volume 3 - Height to Width Ratio of 0.5," by P.A. Hidalgo, R.L. Mayes, H.D. McNiven and R.W. Clough - May 1979(PB 301 321)A08

UCB/EERC-79/13 "Cyclic Behavior of Dense Course-Grained Materials in Relation to the Seismic Stability of Dams," by N.G. Banerjee, H.B. Seed and C.K. Chan - June 1979(PB 301 373)A13

UCB/EERC-79/14 "Seismic Behavior of Reinforced Concrete Interior Beam-Column Subassemblages," by S. Viwathanatepa, E.P. Popov and V.V. Bertero - June 1979(PB 301 326)A10

UCB/EERC-79/15 "Optimal Design of Localized Nonlinear Systems with Dual Performance Criteria Under Earthquake Excitations," by M.A. Bhatti - July 1979(PB 80 167 109)A06

UCB/EERC-79/16 "OPTDYN - A General Purpose Optimization Program for Problems with or without Dynamic Constraints," by M.A. Bhatti, E. Polak and K.S. Pister - July 1979(PB 80 167 091)A05

UCB/EERC-79/17 "ANSR-II, Analysis of Nonlinear Structural Response, Users Manual," by D.P. Mondkar and G.H. Powell July 1979(PB 80 113 301)A05

UCB/EERC-79/18 "Soil Structure Interaction in Different Seismic Environments," A. Gomez-Masso, J. Lysmer, J.-C. Chen and H.B. Seed - August 1979(PB 80 101 520)A04

UCB/EERC-79/19 "ARMA Models for Earthquake Ground Motions," by M.K. Chang, J.W. Kwiatkowski, R.F. Nau, R.M. Oliver and K.S. Pister - July 1979(PB 301 166)A05

UCB/EERC-79/20 "Hysteretic Behavior of Reinforced Concrete Structural Walls," by J.M. Vallenas, V.V. Bertero and E.P. Popov - August 1979(PB 80 165 905)A12

UCB/EERC-79/21 "Studies on High-Frequency Vibrations of Buildings - 1: The Column Effect," by J. Lubliner - August 1979 (PB 80 158 553)A03

UCB/EERC-79/22 "Effects of Generalized Loadings on Bond Reinforcing Bars Embedded in Confined Concrete Blocks," by S. Viwathanatepa, E.P. Popov and V.V. Bertero - August 1979(PB 81 124 018)A14

UCB/EERC-79/23 "Shaking Table Study of Single-Story Masonry Houses, Volume 1: Test Structures 1 and 2," by P. Gülkan, R.L. Mayes and R.W. Clough - Sept. 1979 (HUD-000 1763)A12

UCB/EERC-79/24 "Shaking Table Study of Single-Story Masonry Houses, Volume 2: Test Structures 3 and 4," by P. Gülkan, R.L. Mayes and R.W. Clough - Sept. 1979 (HUD-000 1836)A12

UCB/EERC-79/25 "Shaking Table Study of Single-Story Masonry Houses, Volume 3: Summary, Conclusions and Recommendations," by R.W. Clough, R.L. Mayes and P. Gülkan - Sept. 1979 (HUD-000 1837)A06

UCB/EERC-79/26 "Recommendations for a U.S.-Japan Cooperative Research Program Utilizing Large-Scale Testing Facilities," by U.S.-Japan Planning Group - Sept. 1979(PB 301 407)A06

UCB/EERC-79/27 "Earthquake-Induced Liquefaction Near Lake Amatitlan, Guatemala," by H.B. Seed, I. Arango, C.K. Chan, A. Gomez-Masso and R. Grant de Ascoli - Sept. 1979(NUREG-CR1341)A03

UCB/EERC-79/28 "Infill Panels: Their Influence on Seismic Response of Buildings," by J.W. Axley and V.V. Bertero Sept. 1979(PB 80 163 371)A10

UCB/EERC-79/29 "3D Truss Bar Element (Type 1) for the ANSR-II Program," by D.P. Mondkar and G.H. Powell - Nov. 1979 (PB 80 169 709)A02

UCB/EERC-79/30 "2D Beam-Column Element (Type 5 - Parallel Element Theory) for the ANSR-II Program," by D.G. Row, G.H. Powell and D.P. Mondkar - Dec. 1979(PB 80 167 224)A03

UCB/EERC-79/31 "3D Beam-Column Element (Type 2 - Parallel Element Theory) for the ANSR-II Program," by A. Riahi, G.H. Powell and D.P. Mondkar - Dec. 1979(PB 80 167 216)A03

UCB/EERC-79/32 "On Response of Structures to Stationary Excitation," by A. Der Kiureghian - Dec. 1979(PB 80166 929)A03

UCB/EERC-79/33 "Undisturbed Sampling and Cyclic Load Testing of Sands," by S. Singh, H.B. Seed and C.K. Chan Dec. 1979(ADA 087 298)A07

UCB/EERC-79/34 "Interaction Effects of Simultaneous Torsional and Compressional Cyclic Loading of Sand," by P.M. Griffin and W.N. Houston - Dec. 1979(ADA 092 352)A15

UCB/EERC-80/01 "Earthquake Response of Concrete Gravity Dams Including Hydrodynamic and Foundation Interaction Effects," by A.K. Chopra, P. Chakrabarti and S. Gupta - Jan. 1980(AD-A087297)A10

UCB/EERC-80/02 "Rocking Response of Rigid Blocks to Earthquakes," by C.S. Yim, A.K. Chopra and J. Penzien - Jan. 1980 (PB80 166 002)A04

UCB/EERC-80/03 "Optimum Inelastic Design of Seismic-Resistant Reinforced Concrete Frame Structures," by S.W. Zagajeski and V.V. Bertero - Jan. 1980(PB80 164 635)A06

UCB/EERC-80/04 "Effects of Amount and Arrangement of Wall-Panel Reinforcement on Hysteretic Behavior of Reinforced Concrete Walls," by R. Iliya and V.V. Bertero - Feb. 1980(PB81 122 525)A09

UCB/EERC-80/05 "Shaking Table Research on Concrete Dam Models," by A. Niwa and R.W. Clough - Sept. 1980(PB81 122 368)A06

UCB/EERC-80/06 "The Design of Steel Energy-Absorbing Restrainers and their Incorporation into Nuclear Power Plants for Enhanced Safety (Vol 1A): Piping with Energy Absorbing Restrainers: Parameter Study on Small Systems," by G.H. Powell, C. Oughourlian and J. Simons - June 1980

UCB/EERC-80/07 "Inelastic Torsional Response of Structures Subjected to Earthquake Ground Motions," by Y. Yamazaki April 1980(PB81 122 327)A08

UCB/EERC-80/08 "Study of X-Braced Steel Frame Structures Under Earthquake Simulation," by Y. Ghanaat - April 1980 (PB81 122 335)A11

UCB/EERC-80/09 "Hybrid Modelling of Soil-Structure Interaction," by S. Gupta, T.W. Lin, J. Penzien and C.S. Yeh May 1980(PB81 122 319)A07

UCB/EERC-80/10 "General Applicability of a Nonlinear Model of a One Story Steel Frame," by B.I. Sveinsson and H.D. McNiven - May 1980(PB81 124 877)A06

UCB/EERC-80/11 "A Green-Function Method for Wave Interaction with a Submerged Body," by W. Kioka - April 1980 (PB81 122 269)A07

UCB/EERC-80/12 "Hydrodynamic Pressure and Added Mass for Axisymmetric Bodies," by F. Nilrat - May 1980(PB81 122 343)A08

UCB/EERC-80/13 "Treatment of Non-Linear Drag Forces Acting on Offshore Platforms," by B.V. Dao and J. Penzien May 1980(PB81 153 413)A07

UCB/EERC-80/14 "2D Plane/Axisymmetric Solid Element (Type 3 - Elastic or Elastic-Perfectly Plastic) for the ANSR-II Program," by D.P. Mondkar and G.H. Powell - July 1980(PB81 122 350)A03

UCB/EERC-80/15 "A Response Spectrum Method for Random Vibrations," by A. Der Kiureghian - June 1980(PB81 122 301)A03

UCB/EERC-80/16 "Cyclic Inelastic Buckling of Tubular Steel Braces," by V.A. Zayas, E.P. Popov and S.A. Mahin June 1980(PB81 124 885)A10

UCB/EERC-80/17 "Dynamic Response of Simple Arch Dams Including Hydrodynamic Interaction," by C.S. Porter and A.K. Chopra - July 1980(PB81 124 000)A13

UCB/EERC-80/18 "Experimental Testing of a Friction Damped Aseismic Base Isolation System with Fail-Safe Characteristics," by J.M. Kelly, K.E. Beucke and M.S. Skinner - July 1980(PB81 148 595)A04

UCB/EERC-80/19 "The Design of Steel Energy-Absorbing Restrainers and their Incorporation into Nuclear Power Plants for Enhanced Safety (Vol 1B): Stochastic Seismic Analyses of Nuclear Power Plant Structures and Piping Systems Subjected to Multiple Support Excitations," by M.C. Lee and J. Penzien - June 1980

UCB/EERC-80/20 "The Design of Steel Energy-Absorbing Restrainers and their Incorporation into Nuclear Power Plants for Enhanced Safety (Vol 1C): Numerical Method for Dynamic Substructure Analysis," by J.M. Dickens and E.L. Wilson - June 1980

UCB/EERC-80/21 "The Design of Steel Energy-Absorbing Restrainers and their Incorporation into Nuclear Power Plants for Enhanced Safety (Vol 2): Development and Testing of Restraints for Nuclear Piping Systems," by J.M. Kelly and M.S. Skinner - June 1980

UCB/EERC-80/22 "3D Solid Element (Type 4-Elastic or Elastic-Perfectly-Plastic) for the ANSR-II Program," by D.P. Mondkar and G.H. Powell - July 1980(PB81 123 242)A03

UCB/EERC-80/23 "Gap-Friction Element (Type 5) for the ANSR-II Program," by D.P. Mondkar and G.H. Powell - July 1980 (PB81 122 285)A03

UCB/EERC-80/24 "U-Bar Restraint Element (Type 11) for the ANSR-II Program," by C. Oughourlian and G.H. Powell July 1980(PB81 122 293)A03

UCB/EERC-80/25 "Testing of a Natural Rubber Base Isolation System by an Explosively Simulated Earthquake," by J.M. Kelly - August 1980(PB81 201 360)A04

UCB/EERC-80/26 "Input Identification from Structural Vibrational Response," by Y. Hu - August 1980(PB81 152 308)A05

UCB/EERC-80/27 "Cyclic Inelastic Behavior of Steel Offshore Structures," by V.A. Zayas, S.A. Mahin and E.P. Popov August 1980(PB81 196 180)A15

UCB/EERC-80/28 "Shaking Table Testing of a Reinforced Concrete Frame with Biaxial Response," by M.G. Oliva October 1980(PB81 154 304)A10

UCB/EERC-80/29 "Dynamic Properties of a Twelve-Story Prefabricated Panel Building," by J.G. Bouwkamp, J.P. Kollegger and R.M. Stephen - October 1980(PB82 117 128)A06

UCB/EERC-80/30 "Dynamic Properties of an Eight-Story Prefabricated Panel Building," by J.G. Bouwkamp, J.P. Kollegger and R.M. Stephen - October 1980(PB81 200 313)A05

UCB/EERC-80/31 "Predictive Dynamic Response of Panel Type Structures Under Earthquakes," by J.P. Kollegger and J.G. Bouwkamp - October 1980(PB81 152 316)A04

UCB/EERC-80/32 "The Design of Steel Energy-Absorbing Restrainers and their Incorporation into Nuclear Power Plants for Enhanced Safety (Vol 3): Testing of Commercial Steels in Low-Cycle Torsional Fatigue," by P. Spencer, E.R. Parker, E. Jongewaard and M. Drory

UCB/EERC-80/33 "The Design of Steel Energy-Absorbing Restrainers and their Incorporation into Nuclear Power Plants for Enhanced Safety (Vol 4): Shaking Table Tests of Piping Systems with Energy-Absorbing Restrainers," by S.F. Stiemer and W.G. Godden - Sept. 1980

UCB/EERC-80/34 "The Design of Steel Energy-Absorbing Restrainers and their Incorporation into Nuclear Power Plants for Enhanced Safety (Vol 5): Summary Report," by P. Spencer

UCB/EERC-80/35 "Experimental Testing of an Energy-Absorbing Base Isolation System," by J.M. Kelly, M.S. Skinner and K.E. Beucke - October 1980(PB81 154 072)A04

UCB/EERC-80/36 "Simulating and Analyzing Artificial Non-Stationary Earthquake Ground Motions," by R.F. Nau, R.M. Oliver and K.S. Pister - October 1980(PB81 153 397)A04

UCB/EERC-80/37 "Earthquake Engineering at Berkeley - 1980," - Sept. 1980(PB81 205 874)A09

UCB/EERC-80/38 "Inelastic Seismic Analysis of Large Panel Buildings," by V. Schricker and G.H. Powell - Sept. 1980 (PB81 154 338)A13

UCB/EERC-80/39 "Dynamic Response of Embankment, Concrete-Gravity and Arch Dams Including Hydrodynamic Interaction," by J.F. Hall and A.K. Chopra - October 1980(PB81 152 324)A11

UCB/EERC-80/40 "Inelastic Buckling of Steel Struts Under Cyclic Load Reversal," by R.G. Black, W.A. Wenger and E.P. Popov - October 1980(PB81 154 312)A08

UCB/EERC-80/41 "Influence of Site Characteristics on Building Damage During the October 3, 1974 Lima Earthquake," by P. Repetto, I. Arango and H.B. Seed - Sept. 1980(PB81 161 739)A05

UCB/EERC-80/42 "Evaluation of a Shaking Table Test Program on Response Behavior of a Two Story Reinforced Concrete Frame," by J.M. Blondet, R.W. Clough and S.A. Mahin

UCB/EERC-80/43 "Modelling of Soil-Structure Interaction by Finite and Infinite Elements," by F. Medina - December 1980(PB81 229 270)A04

UCB/EERC-81/01 "Control of Seismic Response of Piping Systems and Other Structures by Base Isolation," edited by J.M. Kelly - January 1981 (PB81 200 735)A05

UCB/EERC-81/02 "OPTNSR - An Interactive Software System for Optimal Design of Statically and Dynamically Loaded Structures with Nonlinear Response," by M.A. Bhatti, V. Ciampi and K.S. Pister - January 1981 (PB81 218 851)A09

UCB/EERC-81/03 "Analysis of Local Variations in Free Field Seismic Ground Motions," by J.-C. Chen, J. Lysmer and H.B. Seed - January 1981 (AD-A099508)A13

UCB/EERC-81/04 "Inelastic Structural Modeling of Braced Offshore Platforms for Seismic Loading," by V.A. Zayas, P.-S.B. Shing, S.A. Mahin and E.P. Popov - January 1981(PB82 138 777)A07

UCB/EERC-81/05 "Dynamic Response of Light Equipment in Structures," by A. Der Kiureghian, J.L. Sackman and B. Nour-Omid - April 1981 (PB81 218 497)A04

UCB/EERC-81/06 "Preliminary Experimental Investigation of a Broad Base Liquid Storage Tank," by J.G. Bouwkamp, J.P. Kollegger and R.M. Stephen - May 1981(PB82 140 385)A03

UCB/EERC-81/07 "The Seismic Resistant Design of Reinforced Concrete Coupled Structural Walls," by A.E. Aktan and V.V. Bertero - June 1981(PB82 113 358)A11

UCB/EERC-81/08 "The Undrained Shearing Resistance of Cohesive Soils at Large Deformations," by M.R. Pyles and H.B. Seed - August 1981

UCB/EERC-81/09 "Experimental Behavior of a Spatial Piping System with Steel Energy Absorbers Subjected to a Simulated Differential Seismic Input," by S.F. Stiemer, W.G. Godden and J.M. Kelly - July 1981

UCB/EERC-81/10 "Evaluation of Seismic Design Provisions for Masonry in the United States," by B.I. Sveinsson, R.L. Mayes and H.D. McNiven - August 1981 (PB82 166 075)A08

UCB/EERC-81/11 "Two-Dimensional Hybrid Modelling of Soil-Structure Interaction," by T.-J. Tzong, S. Gupta and J. Penzien - August 1981(PB82 142 118)A04

UCB/EERC-81/12 "Studies on Effects of Infills in Seismic Resistant R/C Construction," by S. Brokken and V.V. Bertero - September 1981 (PB82 166 190)A09

UCB/EERC-81/13 "Linear Models to Predict the Nonlinear Seismic Behavior of a One-Story Steel Frame," by H. Valdimarsson, A.H. Shah and H.D. McNiven - September 1981(PB82 138 793)A07

UCB/EERC-81/14 "TLUSH: A Computer Program for the Three-Dimensional Dynamic Analysis of Earth Dams," by T. Kagawa, L.H. Mejia, H.B. Seed and J. Lysmer - September 1981(PB82 139 940)A06

UCB/EERC-81/15 "Three Dimensional Dynamic Response Analysis of Earth Dams," by L.H. Mejia and H.B. Seed - September 1981 (PB82 137 274)A12

UCB/EERC-81/16 "Experimental Study of Lead and Elastomeric Dampers for Base Isolation Systems," by J.M. Kelly and S.B. Hodder - October 1981 (PB82 166 182)A05

UCB/EERC-81/17 "The Influence of Base Isolation on the Seismic Response of Light Secondary Equipment," by J.M. Kelly - April 1981 (PB82 255 266)A04

UCB/EERC-81/18 "Studies on Evaluation of Shaking Table Response Analysis Procedures," by J. Marcial Blondet - November 1981 (PB82 197 278)A10

UCB/EERC-81/19 "DELIGHT.STRUCT: A Computer-Aided Design Environment for Structural Engineering," by R.J. Balling, K.S. Pister and E. Polak - December 1981 (PB82 218 496)A07

UCB/EERC-81/20 "Optimal Design of Seismic-Resistant Planar Steel Frames," by R.J. Balling, V. Ciampi, K.S. Pister and E. Polak - December 1981 (PB82 220 179)A07

UCB/EERC-82/01 "Dynamic Behavior of Ground for Seismic Analysis of Lifeline Systems," by T. Sato and A. Der Kiureghian - January 1982 (PB82 218 926)A05

UCB/EERC-82/02 "Shaking Table Tests of a Tubular Steel Frame Model," by Y. Ghanaat and R. W. Clough - January 1982 (PB82 220 161)A07

UCB/EERC-82/03 "Behavior of a Piping System under Seismic Excitation: Experimental Investigations of a Spatial Piping System supported by Mechanical Shock Arrestors and Steel Energy Absorbing Devices under Seismic Excitation," by S. Schneider, H.-M. Lee and W. G. Godden - May 1982 (PB83 172 544)A09

UCB/EERC-82/04 "New Approaches for the Dynamic Analysis of Large Structural Systems," by E. L. Wilson - June 1982 (PB83 148 080)A05

UCB/EERC-82/05 "Model Study of Effects of Damage on the Vibration Properties of Steel Offshore Platforms," by F. Shahrivar and J. G. Bouwkamp - June 1982 (PB83 148 742)A10

UCB/EERC-82/06 "States of the Art and Practice in the Optimum Seismic Design and Analytical Response Prediction of R/C Frame-Wall Structures," by A. E. Aktan and V. V. Bertero - July 1982 (PB83 147 736)A05

UCB/EERC-82/07 "Further Study of the Earthquake Response of a Broad Cylindrical Liquid-Storage Tank Model," by G. C. Manos and R. W. Clough - July 1982 (PB83 147 744)A11

UCB/EERC-82/08 "An Evaluation of the Design and Analytical Seismic Response of a Seven Story Reinforced Concrete Frame - Wall Structure," by F. A. Charney and V. V. Bertero - July 1982(PB83 157 628)A09

UCB/EERC-82/09 "Fluid-Structure Interactions: Added Mass Computations for Incompressible Fluid," by J. S.-H. Kuo - August 1982 (PB83 156 281)A07

UCB/EERC-82/10 "Joint-Opening Nonlinear Mechanism: Interface Smeared Crack Model," by J. S.-H. Kuo - August 1982 (PB83 149 195)A05

UCB/EERC-82/11 "Dynamic Response Analysis of Techi Dam," by R. W. Clough, R. M. Stephen and J. S.-H. Kuo - August 1982 (PB83 147 496)A06

UCB/EERC-82/12 "Prediction of the Seismic Responses of R/C Frame-Coupled Wall Structures," by A. E. Aktan, V. V. Bertero and M. Piazza - August 1982 (PB83 149 203)A09

UCB/EERC-82/13 "Preliminary Report on the SMART 1 Strong Motion Array in Taiwan," by B. A. Bolt, C. H. Loh, J. Penzien, Y. B. Tsai and Y. T. Yeh - August 1982 (PB83 159 400)A10

UCB/EERC-82/14 "Shaking-Table Studies of an Eccentrically X-Braced Steel Structure," by M. S. Yang - September 1982 (PB83 260 778)A12

UCB/EERC-82/15 "The Performance of Stairways in Earthquakes," by C. Roha, J. W. Axley and V. V. Bertero - September 1982 (PB83 157 693)A07

UCB/EERC-82/16 "The Behavior of Submerged Multiple Bodies in Earthquakes," by W.-G. Liao - Sept. 1982 (PB83 158

UCB/EERC-82/17 "Effects of Concrete Types and Loading Conditions on Local Bond-Slip Relationships," by A. D. Cowell, E. P. Popov and V. V. Bertero - September 1982 (PB83 153 577)A04

UCB/EERC-82/18 "Mechanical Behavior of Shear Wall Vertical Boundary Members: An Experimental Investigation," by M. T. Wagner and V. V. Bertero - October 1982 (PB83 159 764)A05

UCB/EERC-82/19 "Experimental Studies of Multi-support Seismic Loading on Piping Systems," by J. M. Kelly and A. D. Cowell - November 1982

UCB/EERC-82/20 "Generalized Plastic Hinge Concepts for 3D Beam-Column Elements," by P. F.-S. Chen and G. H. Powell - November 1982 (PB83 247 981)A13

UCB/EERC-82/21 "ANSR-III: General Purpose Computer Program for Nonlinear Structural Analysis," by C. V. Oughourlian and G. H. Powell - November 1982 (PB83 251 330)A12

UCB/EERC-82/22 "Solution Strategies for Statically Loaded Nonlinear Structures," by J. W. Simons and G. H. Powell - November 1982 (PB83 197 970)A06

UCB/EERC-82/23 "Analytical Model of Deformed Bar Anchorages under Generalized Excitations," by V. Ciampi, R. Eligehausen, V. V. Bertero and E. P. Popov - November 1982 (PB83 169 532)A06

UCB/EERC-82/24 "A Mathematical Model for the Response of Masonry Walls to Dynamic Excitations," by H. Sucuoğlu, Y. Mengi and H. D. McNiven - November 1982 (PB83 169 011)A07

UCB/EERC-82/25 "Earthquake Response Considerations of Broad Liquid Storage Tanks," by F. J. Cambra - November 1982 (PB83 251 215)A09

UCB/EERC-82/26 "Computational Models for Cyclic Plasticity, Rate Dependence and Creep," by B. Mosaddad and G. H. Powell - November 1982 (PB83 245 829)A08

UCB/EERC-82/27 "Inelastic Analysis of Piping and Tubular Structures," by M. Mahasuverachai and G. H. Powell - November 1982 (PB83 249 987)A07

UCB/EERC-83/01 "The Economic Feasibility of Seismic Rehabilitation of Buildings by Base Isolation," by J. M. Kelly - January 1983 (PB83 197 988)A05

UCB/EERC-83/02 "Seismic Moment Connections for Moment-Resisting Steel Frames," by E. P. Popov - January 1983 (PB83 195 412)A04

UCB/EERC-83/03 "Design of Links and Beam-to-Column Connections for Eccentrically Braced Steel Frames," by E. P. Popov and J. O. Malley - January 1983 (PB83 194 811)A04

UCB/EERC-83/04 "Numerical Techniques for the Evaluation of Soil-Structure Interaction Effects in the Time Domain," by E. Bayo and E. L. Wilson - February 1983 (PB83 245 605)A09

UCB/EERC-83/05 "A Transducer for Measuring the Internal Forces in the Columns of a Frame-Wall Reinforced Concrete Structure," by R. Sause and V. V. Bertero - May 1983 (PB84 119 494)A06

UCB/EERC-83/06 "Dynamic Interactions between Floating Ice and Offshore Structures," by P. Croteau - May 1983 (PB84 119 486)A16

UCB/EERC-83/07 "Dynamic Analysis of Multiply Tuned and Arbitrarily Supported Secondary Systems," by T. Igusa and A. Der Kiureghian - June 1983 (PB84 118 272)A11

UCB/EERC-83/08 "A Laboratory Study of Submerged Multi-body Systems in Earthquakes," by G. R. Ansari - June 1983 (PB83 261 842)A17

UCB/EERC-83/09 "Effects of Transient Foundation Uplift on Earthquake Response of Structures," by C.-S. Yim and A. K. Chopra - June 1983 (PB83 261 396)A07

UCB/EERC-83/10 "Optimal Design of Friction-Braced Frames under Seismic Loading," by M. A. Austin and K. S. Pister - June 1983 (PB84 119 288)A06

UCB/EERC-83/11 "Shaking Table Study of Single-Story Masonry Houses: Dynamic Performance under Three Component Seismic Input and Recommendations," by G. C. Manos, R. W. Clough and R. L. Mayes - June 1983

UCB/EERC-83/12 "Experimental Error Propagation in Pseudodynamic Testing," by P. B. Shing and S. A. Mahin - June 1983 (PB84 119 270)A09

UCB/EERC-83/13 "Experimental and Analytical Predictions of the Mechanical Characteristics of a 1/5-scale Model of a 7-story R/C Frame-Wall Building Structure," by A. E. Aktan, V. V. Bertero, A. A. Chowdhury and T. Nagashima - August 1983 (PB84 119 213)A07

UCB/EERC-83/14 "Shaking Table Tests of Large-Panel Precast Concrete Building System Assemblages," by M. G. Oliva and R. W. Clough - August 1983

UCB/EERC-83/15 "Seismic Behavior of Active Beam Links in Eccentrically Braced Frames," by K. D. Hjelmstad and E. P. Popov - July 1983 (PB84 119 676)A09

UCB/EERC-83/16 "System Identification of Structures with Joint Rotation," by J. S. Dimsdale and H. D. McNiven - July 1983

UCB/EERC-83/17 "Construction of Inelastic Response Spectra for Single-Degree-of-Freedom Systems," by S. Mahin and J. Lin - July 1983

UCB/EERC-83/18 "Interactive Computer Analysis Methods for Predicting the Inelastic Cyclic Behaviour of Structural Sections," by S. Kaba and S. Mahin - July 1983

UCB/EERC-83/19 "Effects of Bond Deterioration on Hysteretic Behavior of Reinforced Concrete Joints," by F.C. Filippou, E.P. Popov and V.V. Bertero - August 1983

UCB/EERC-83/20 "Analytical and Experimental Correlation of Large-Panel Precast Building System Performance," by M.G. Oliva, R.W. Clough, M. Velkov, P. Gavrilovic and J. Petrovski - November 1983

UCB/EERC-83/21 "Mechanical Characteristics of Materials Used in a 1/5 Scale Model of a 7-Story Reinforced Concrete Test Structure," by V.V. Bertero, A.E. Aktan, H.G. Harris and A.A. Chowdhury - September 1983

UCB/EERC-83/22 "Hybrid Modelling of Soil-Structure Interaction in Layered Media," by T.-J. Tzong and J. Penzien - October 1983

UCB/EERC-83/23 "Local Bond Stress-Slip Relationships of Deformed Bars under Generalized Excitations," by R. Eligehausen, E.P. Popov and V.V. Bertero - October 1983

UCB/EERC-83/24 "Design Considerations for Shear Links in Eccentrically Braced Frames," by J.O. Malley and E.P. Popov - November 1983

UCB/EERC-84/01 "Pseudodynamic Test Method for Seismic Performance Evaluation: Theory and Implementation," by P.-S. B. Shing and S. A. Mahin - January 1984 (PB84 190 644) A08

UCB/EERC-84/02 "Dynamic Response Behavior of Xiang Hong Dian Dam," by R. W. Clough, K.-T. Chang, H.-Q. Chen, R. M. Stephen, G.-L. Wang, and Y. Ghanaat - April 1984

UCB/EERC-84/03 "Refined Modelling of Reinforced Concrete Columns for Seismic Analysis," by S.A. Kaba and S.A. Mahin - April, 1984